

Scuola di Scienze
Dipartimento di Fisica e Astronomia
Corso di Laurea Magistrale in Fisica

Testing electroweak baryogenesis at the LHC in a
minimal extension of the standard model

Relatore:
Prof. Fabio Maltoni

Presentata da:
Antonio Del Donno

Correlatore:
Prof. Alberto Mariotti
(VRIJE UNIVERSITEIT BRUSSEL)

Anno Accademico 2018/2019

SOMMARIO

Il modello standard è la teoria che descrive con spettacolare accuratezza le interazioni fra i costituenti fondamentali della materia come oggi ci sono noti. Nonostante il successo nel confronto fra teoria ed esperimenti, diverse questioni rimangono insolute. Indicazioni esistono riguardo l'esistenza di una fisica oltre il modello standard, anche se ancora ignoriamo la sua natura. L'obiettivo principale di questo lavoro è di caratterizzare una delle più semplici estensioni del modello standard che prevede un singoletto scalare interagente con il solo bosone di Higgs. Questo nuovo stato potrebbe avere un'influenza sulla fenomenologia del bosone di Higgs ai collider e dare luogo al meccanismo della bariogenesi elettrodebole. Una volta classificate le differenti possibilità, concentriamo la nostra attenzione su un modello semplificato caratterizzato da una simmetria \mathbb{Z}_2 , nel quale le modifiche al self-coupling del bosone di Higgs possono apparire solo ad un loop. Il calcolo dei contributi corrispondenti permette di identificare la regione dello spazio dei parametri dove è possibile ottenere una transizione di fase elettrodebole del primo ordine, e di verificare se le deviazioni dalle previsioni del modello standard possano essere rilevabili ad LHC. Consideriamo sia il modello completo che la corrispondente approssimazione effettiva, studiandone il regime di applicabilità. Infine, otteniamo le previsioni per la produzione di una coppia di bosoni di Higgs. I nostri risultati preliminari mostrano come nelle regioni dello spazio dei parametri nelle quali è possibile avere la transizione del primo ordine un approccio effettivo sia sufficiente a riprodurre il modello completo. Inoltre, le differenze di shape e sezione d'urto fra la estensione con un singoletto ed il modello standard sono visibili per valori della massa del singoletto potenzialmente rilevabili a LHC.

ABSTRACT

The Standard Model (SM) is the theory that describes with an astonishing accuracy the interactions among the fundamental constituents of matter as we know them today. Notwithstanding the successful comparison between theory and experiment, a number of unanswered questions remain. Many indications exist that some physics Beyond the SM (BSM) must exist, even though we do not know its nature. The main goal of this work is to characterise one of the simplest extension of the SM featuring an extra scalar state interacting with the SM via the Higgs boson, in terms of the effects that it might have on the Higgs phenomenology at colliders and the realisation of Electroweak baryogenesis (EWBG). After classifying various possibilities, we focus our attention on a simplified model featuring an unbroken \mathbb{Z}_2 symmetry. In this case modifications of the self-coupling of the Higgs boson can only happen at one loop and we compute the corresponding contributions. We identify the regions of parameter space where a first-order transition for the EW symmetry breaking can be realised and then check whether deviations from the SM expectations could be detectable at the LHC. We perform these studies both in the full model and in the corresponding EFT approximation studying in particular its range of applicability. We compare the singlet extension and the standard model in the double Higgs production at the LHC, in which the trilinear Higgs self-coupling is involved. Our preliminary results show that in the regions of parameter space which lead to a first-order phase transition, an EFT approach is sufficient to reproduce the full theory behaviour. Moreover, the shape and cross section differences between the singlet extension and the standard model are noticeable for values of the singlet mass which are potentially accessible at the LHC.

ACKNOWLEDGEMENTS

To the University of Bologna, the Université Catholique de Louvain and the Vrije Universiteit Brussel. Three wonderful places where I met just as wonderful people. A special thanks to Prof. Roberto Soldati, Prof. Fabio Maltoni, and Prof. Alberto Mariotti, which were and are a huge source of inspiration for me.

To my relatives and friends, to my band, to anyone who has supported, endured and loved me.

This thesis is still dedicated to Olimpia, who accompanied me on the beautiful and ugly days of these months of growth.

La festa dell'insignificanza

Una sera Dio malinconico e mesto
disse che l'uomo stava scoprendo tutte le Sue sorprese troppo presto.
Sondava l'universo
e poco ci mancò che non scoprì il Suo rifugio in questo mio verso.
Dissezionava il cielo
e
-questo non ci sta scritto nel vangelo-
per paura Dio
creò l'amore, i desideri, la rabbia e l'oblio
e tutti gli altri passi di danza
che balla in vita l'uomo nella festa dell'insignificanza.

Olimpia Peroni

1	Introduction	8
1.1	The current status of high energy physics	8
1.1.1	Beyond standard model physics with effective theories	9
1.1.2	Outline	10
2	A brief review of the standard model	11
2.1	Gauge symmetry breaking via the BEH mechanism	11
2.1.1	Quantisation and Feynman rules	14
2.2	The BEH mechanism in the standard model	16
2.2.1	Gauge fields and fermions masses	19
2.2.2	Introducing quarks and gluons	20
2.3	\mathcal{CP} -violation in the standard model	22
2.4	Shortcomings of the standard model	24
2.4.1	Electroweak baryogenesis	25
3	Effective field theory approach	27
3.1	Physics and philosophy behind	27
3.1.1	On mass and energy scales	28
3.2	Illustrating the process	31
3.2.1	Mathematical formulation and tree-level matching	32
3.2.2	1-loop corrections and renormalisation group running	35
3.2.3	1-loop matching	39
3.2.4	Heavy fermion/light Scalar: Sketch of The calculations	44
3.3	The SM as an effective field theory	45
3.3.1	Operator bases and reduction	46
3.3.2	Phenomenological lagrangians	47

4	Minimally extending the standard model	49
4.1	The real scalar singlet portal	50
4.1.1	The effective theory	52
4.2	\mathbb{Z}_2 preserving potential: spontaneous symmetry breaking	54
4.2.1	Integrating out the singlet via E.O.M.	57
4.2.2	Matching to the EFT with amplitudes	58
4.3	\mathbb{Z}_2 explicit breaking potential	62
4.3.1	Integrating out the singlet via E.O.M.	64
4.4	\mathbb{Z}_2 preserving potential : 1-loop matching	66
4.4.1	Matching by scattering amplitudes	67
4.5	Singlet models showdown	72
5	Electroweak baryogenesis via singlet portals	74
5.1	Introduction	74
5.2	Sakharov conditions in the standard model	75
5.2.1	Baryon number violation	75
5.2.2	\mathcal{CP} -violation from the Quark sector	78
5.2.3	Departure from Thermal Equilibrium: Strong First Order Phase Transition	79
5.3	The Effective Potential	80
5.3.1	Symmetry breaking via radiative corrections: the Coleman-Weinberg potential	80
5.4	Finite Temperature Effective potential	85
5.4.1	Daisy Resummation	87
5.5	A \mathbb{Z}_2 singlet portal for electroweak baryogenesis	88
5.5.1	Phase Transition in the Full Theory	88
6	Singlet Phenomenology at Colliders	92
6.1	Full Theory Analysis	93
6.2	Effective Theory Analysis	94
6.3	Benchmarks	95
6.3.1	Full-theory and EFT comparison	95
6.3.2	BSM theory and SM comparison	97
7	Conclusions	100
A	Covariant Derivative Expansion	102
A.1	Exemplifying with the \mathbb{Z}_2 -preserving singlet extension	103
B	Constraints in the Singlet Extension	104
B.1	Perturbative unitarity at tree-level	104
B.2	Couplings and boundedness from below	108
B.2.1	\mathbb{Z}_2 Symmetric Model	108

B.2.2 The General Case	108
----------------------------------	-----

1.1 The current status of high energy physics

The outstanding predictive power behind the Standard Model (SM) of fundamental particles and interactions has led to a rich phenomenology which has been studied in the last few decades. Up to now the SM has been capable of describing all data collected at LHC up to 13 TeV energy, with every particle known included into this glorious picture. In other words, the lack of additional new states observation at colliders can be simply explained by the SM, and the discovery of any new particle being postponed to a later (unknown) date/energy scale.

It seems that the SM as we have defined it, is just as good as it is in describing basically all particle physics phenomenology. About one hundred inverse femtobarn of data has been collected by CMS and ATLAS collaborations, pushing towards a precision measurements era.

On the contrary, the main evidence concerning the existence of some kind of Beyond Standard Model (BSM) physics mostly comes from astrophysical and cosmological observations. Neutrino oscillations have shown beyond any doubt that neutrinos have a (tiny) finite mass (and therefore right-handed states need to be added to the SM). While the identification of Dark Matter/Energy, and the observed baryon/antibaryon asymmetry of the universe (BAU) remain a mystery. None of the particles and interactions in the SM seems to be capable to give a complete understanding/description and particle interpretation of Dark Matter. On the BAU, the SM seem to be containing all the necessary ingredients to explain Electroweak Baryogenesis (EWBG) yet with the actual measured parameters today, such a transition is too weak (and CP violation too) to generate the observed asymmetry.

Motivated by these evidences, for most of the HEP community the SM is far from being a complete theory. Thus, the search for a more complete theory continues. If

the scale of new physics higher than the energies directly accessible at LHC, one can still detect the imprints of such a complete theory in the interactions among the SM particles. This approach builds upon an effective description. Among the many proposals been presented through the years, the STANDARD MODEL EFFECTIVE FIELD THEORY (SMEFT) is among the most promising ones. Assuming a linear realisation of the gauge symmetry and that the scale of new physics is higher than about one TeV, fixes all the degrees of freedom at each order in powers of the inverse powers of the new physics scale. In this formulation, non-renormalisable, yet fully gauge invariant, interactions between SM particles are taken into account as the low energy behavior of more complicated interactions between SM and a BSM/hidden sector.

1.1.1 Beyond standard model physics with effective theories

The main goal of this work is to classify how one among the simplest extensions of the SM, i.e. adding a real scalar singlet under all the gauge interactions of the SM, is capable of affecting the Higgs sector. In particular, we focus on how to extend the Higgs potential in order to modify the early universe EW phase transition making it *strongly* of first order, and to consequently achieve the electroweak baryogenesis¹.

The idea is to minimally deform the SM by introducing a massive scalar particle s which does not interact with the SM particles at the tree- and renormalisable level, except for the Higgs boson, through the $|\Phi|^2$ portal term:

$$\mathcal{L} = \mathcal{L}_{\text{SM}} + \frac{1}{2} (\partial^\mu s)^2 - \frac{\mu_s^2}{2} s^2 - \frac{\lambda_m}{2} |\Phi|^2 s^2 - \frac{\mu_3}{3} s^3 - \frac{\lambda_s}{4} s^4 + \mu_4 |\Phi|^2 s . \quad (1.1)$$

This is the most general Lagrangian of the well-known Singlet Higgs Portal (SHP), which has been widely discussed in the literature in recent years.

As we will see, this simple extension is capable of significantly modifying the self Higgs couplings, if different orders of perturbation theory are considered depending on if the extended potential is equipped with a \mathbb{Z}_2 explicit symmetry or not. As this trilinear shift also enters in the main process of production of the Higgs boson at LHC, the interesting question is whether modifications which are sufficient to explain EWBG can be detected in collider observables. Moreover, this new s scalar state turns out to also be a possible component of the dark matter, anyhow, even though in a strongly constrained region of its parameter space.

One can also consider model-independent modifications of the Higgs boson potential using the SMEFT approach, i.e. understanding the SM as non-renormalisable Lagrangian,

$$\mathcal{L}_{\text{eff}} = \mathcal{L}_{\text{SM}} + \frac{c_h}{2\Lambda^2} \partial^\mu \left(\Phi^\dagger \Phi - \frac{v^2}{2} \right) \partial_\mu \left(\Phi^\dagger \Phi - \frac{v^2}{2} \right) + \sum_{n=3}^{\infty} \frac{c_{2n}}{\Lambda^{2n-4}} \left(\Phi^\dagger \Phi - \frac{v^2}{2} \right)^n , \quad (1.2)$$

and then determine the c_n coefficients in the case of (heavy) scalar singlet model, by matching the full theory to the effective one.

¹For the moment, we set aside the \mathcal{CP} -violation problem and leave it for future investigations.

We will investigate this matching in details for the singlet scalar extension of the SM, re-deriving existing results and performing novel computations. Moreover, we will investigate the phenomenology of the \mathbb{Z}_2 symmetric case at the LHC, focusing on the double Higgs production. For this purpose, we will first implement in MadGraph the one-loop corrections to the Higgs potential induced by the \mathbb{Z}_2 symmetric singlet. Then, we will analyse the differential distributions to compare the full BSM model and the EFT description, and also to highlight their differences with respect to the SM. This phenomenological analysis constitutes an original contribution of this thesis.

1.1.2 Outline

In chapter 2 we briefly review the main features of SM, discussing in particular those that will be important for our analysis later, such as the scalar sector (Yukawa and potential) and the source(s) of \mathcal{CP} -violation. Chapter 3 is dedicated to the introduction of EFT techniques. A methodological argument is given to motivate the approach and then a specific case is explained in detailed taking a toy model as example, and eventually the SMEFT is introduced.

The following chapter 4 introduces the SM minimal extensions, primarily discussing the singlet portals. Full matching calculation to the up-to-8-dimensional effective Higgs potential are performed in three different cases, endorsing two different matching procedures.

In chapter 5 we select one of the main models studied in the previous chapter to analyse how the singlet is capable to trigger the strong first order EWPT. A brief review of the Sakharov conditions in the SM is made, then the singlet is introduced considering its one loop and thermal corrections in the effective potential to finally perform a detailed analysis of the parameters space region where the transition is allowed.

Finally, in chapter 6 we simulate how the double Higgs production at LHC gets modified by considering the new scalar state, both in the full and effective theory frameworks.

A brief review of the standard model

We start reviewing the Brout-Englert-Higgs (BEH) mechanism for the mass generation of an abelian gauge field, then we proceed with phenomenologically constructing the standard model, discussing non-abelian gauge symmetries, boson/fermion mass generation, flavor changing interactions and \mathcal{CP} violation, ending with a brief discussion about the Higgs potential.

In passing, some of the standard model shortcomings are highlighted, with particular reference to baryogenesis and how a modification of the potential as generated by an effective field theory scenario can explain the phenomenon. The main review references used in the chapter are [1, 2, 3].

2.1 Gauge symmetry breaking via the BEH mechanism

Let us consider a scalar QED theory in which a charged scalar field interacts with a massless abelian vector field, as described by the Lagrangian

$$\mathcal{L} = (D_\mu \phi)^* D^\mu \phi + \mu^2 \phi^* \phi - \lambda (\phi^* \phi)^2 - \frac{1}{4} F^{\mu\nu} F_{\mu\nu}, \quad (2.1)$$

where $D^\mu \phi = (\partial^\mu - ieA^\mu)\phi$ is the covariant derivative, λ and e are positive, and where we took the crucial positive sign on the scalar field mass term. Expanding the field strength tensor as well as the covariant derivative, we can rewrite the Lagrangian explicitly as

$$\begin{aligned} \mathcal{L} = & \partial^\mu \phi^* \partial_\mu \phi + \mu^2 \phi^* \phi - \frac{1}{2} \partial^\mu A^\nu (\partial_\mu A_\nu - \partial_\nu A_\mu) \\ & - \lambda (\phi^* \phi)^2 + A^\mu \phi^* ie \overleftrightarrow{\partial}_\mu \phi + e^2 A^\mu A_\mu \phi^* \phi. \end{aligned} \quad (2.2)$$

Using the Euler-Lagrange equations for each field leads us to

$$D_\mu^* (D^\mu \phi)^* - \mu^2 \phi^* + 2\lambda (\phi^*)^2 \phi = 0, \quad (2.3)$$

with the related complex conjugate equation, and

$$\partial^\nu F_{\mu\nu} + \phi^* i e \overleftrightarrow{D}_\mu \phi = 0. \quad (2.4)$$

Taking the divergence of the last equation we arrive to

$$\partial^\mu \partial^\nu F_{\mu\nu} + \underbrace{\partial^\mu (i e \phi^* \overleftrightarrow{D}_\mu \phi)}_{J^\mu} = 0 \rightarrow \partial_\mu J^\mu = 0. \quad (2.5)$$

The Lagrangian defined above turns out to be invariant under full non-homogeneous Lorentz group and the U(1) group of the local phase transformations, which acts on the field variables as

$$\phi(x) \rightarrow \phi'(x) = e^{ie\theta(x)} \phi(x), \quad (2.6)$$

$$A_\mu(x) \rightarrow A'_\mu(x) = A_\mu(x) + \partial_\mu \theta(x). \quad (2.7)$$

In particular, (2.5) expresses the continuity equation for the abelian U(1) current J^μ , which also defines the U(1) charge conservation

$$Q = -e \int d\mathbf{r} \phi^* i \overleftrightarrow{D}_0 \phi. \quad (2.8)$$

We also see the covariant derivative to transform homogeneously under these field transformations

$$(D_\mu \phi(x))' = e^{ie\theta(x)} D_\mu \phi(x). \quad (2.9)$$

Owing to the Poincaré symmetry of the Lagrangian, we can define the energy-momentum tensor as

$$T_{\mu\nu} = D_\mu \phi (D_\nu \phi)^* + (D_\mu \phi)^* D_\nu \phi - F_{\mu\lambda} \partial_\nu A^\lambda - g_{\mu\nu} \mathcal{L}, \quad (2.10)$$

from which we can write down the energy of the system¹:

$$P_0 = E = \int d\mathbf{r} \left\{ \dot{\phi}(\mathbf{r}, t) (D_0 \phi)^*(\mathbf{r}, t) + D_0 \phi(\mathbf{r}, t) \dot{\phi}^*(\mathbf{r}, t) - \mathbf{E}(\mathbf{r}, t) \cdot \dot{\mathbf{A}}(\mathbf{r}, t) - \mathcal{L}(\mathbf{r}, t) \right\}. \quad (2.11)$$

Then, writing the conjugated momenta of the field variables

$$\begin{aligned} \frac{\delta \mathcal{L}}{\delta \dot{\phi}(\mathbf{r}, t)} &\equiv \Pi^*(\mathbf{r}, t) = (D_0 \phi(\mathbf{r}, t))^* & \frac{\delta \mathcal{L}}{\delta \dot{\mathbf{A}}(\mathbf{r}, t)} &\equiv -\mathbf{E}(\mathbf{r}, t) \\ \frac{\delta \mathcal{L}}{\delta \dot{\phi}^*(\mathbf{r}, t)} &= 0 & \frac{\delta \mathcal{L}}{\delta \dot{\phi}^*(\mathbf{r}, t)} &\equiv \Pi(\mathbf{r}, t) = D_0 \phi(\mathbf{r}, t), \end{aligned} \quad (2.12)$$

we substitute

$$\dot{\phi} = \Pi + i e \varphi \phi, \quad \dot{\mathbf{A}} = -\mathbf{E} - \nabla \varphi, \quad (2.13)$$

¹Here we explicitly set $A^\mu = (\varphi, \mathbf{A})$.

in the energy functional obtained above, arriving to the classical Hamiltonian functional, namely

$$H = \int d\mathbf{r} \left\{ \Pi(\mathbf{r}, t) \Pi^*(\mathbf{r}, t) + D_k \phi(\mathbf{r}, t) (D_k \phi)^*(\mathbf{r}, t) + V(\phi \phi^*) + \frac{1}{2} \mathbf{E}^2(\mathbf{r}, t) + \frac{1}{2} \mathbf{B}^2(\mathbf{r}, t) + \mathbf{E}(\mathbf{r}, t) \cdot \nabla \varphi(\mathbf{r}, t) + \varphi(\mathbf{r}, t) J_0(\mathbf{r}, t) \right\}, \quad (2.14)$$

where we defined

$$V(\phi^* \phi) = -\mu^2 \phi^* \phi + \lambda (\phi^* \phi)^2. \quad (2.15)$$

Now, as

$$\partial^\mu F_{\mu\nu} + ie \phi^* \overleftrightarrow{D}_\nu \phi = 0 \quad (2.16)$$

$$\partial^k F_{k0} + ie \phi^* \overleftrightarrow{D}_0 \phi = 0 \quad (2.17)$$

and so

$$\nabla \cdot \mathbf{E}(\mathbf{r}, t) = J_0(\mathbf{r}, t), \quad (2.18)$$

we can transform the last two terms in (2.14) and let them vanish according to the fact that

$$\mathbf{E}(\mathbf{r}, t) \cdot \nabla \varphi(\mathbf{r}, t) + \varphi(\mathbf{r}, t) J_0(\mathbf{r}, t) = \nabla \cdot (\mathbf{E}(\mathbf{r}, t) \varphi(\mathbf{r}, t)). \quad (2.19)$$

Eventually, we are left with

$$H = \int d\mathbf{r} \left(\Pi \Pi^* + D_k \phi (D_k \phi)^* + \frac{1}{2} \mathbf{E}^2 + \frac{1}{2} \mathbf{B}^2 - \mu^2 \phi \phi^* + \lambda (\phi \phi^*)^2 \right),$$

which turns out to be non positive semi-definite, owing to the negative mass sign of the scalar field.

We find the stationary points of this Hamiltonian by letting

$$\phi(\mathbf{r}, t) = \phi_0 \quad , \quad A_\mu^0(\mathbf{r}, t) = 0 \quad ,$$

so that we reduce to

$$H = \int d\mathbf{r} V(\phi_0^* \phi_0) \quad (2.20)$$

and we can directly analyse the scalar potential to find the extremes.

It follows

$$\frac{\delta V(\phi_0^* \phi_0)}{\delta \phi_0} = \phi_0^* (2\lambda \phi_0 \phi_0^* - \mu^2) = 0 \iff \boxed{\phi_0 = 0 \quad , \quad \phi_0 \phi_0^* = \frac{\mu^2}{2\lambda}} \quad (2.21)$$

$$H_0(0) = 0 \quad H_0(\phi \phi^*) = -\frac{\mu^4}{4\lambda}, \quad (2.22)$$

with the minimal constant field configuration describing an U(1) symmetric circle of ray $\mu/\sqrt{2\lambda}$ in the complex ϕ_0 plane.

2.1.1 Quantisation and Feynman rules

The quantisation of the Higgs abelian gauge invariant model follows after a redefinition of the field functions and the inclusion of supplementary gauge fixing terms.

Essentially, we identify the vacuum expectation value of the Higgs field as the constant field minima derived upon

$$|\langle 0 | \phi(x) | 0 \rangle| = \frac{\mu}{\sqrt{2\lambda}} = \frac{v}{\sqrt{2}}, \quad (2.23)$$

and then we expand the scalar field over the vacuum as

$$\phi(x) = \frac{1}{\sqrt{2}} (v + \eta(x)) \exp\{i\chi(x)/v\}. \quad (2.24)$$

Moreover, owing to the gauge invariance of the vector field, we have

$$A_\mu(x) = V_\mu(x) + \partial_\mu \chi(x)/ve. \quad (2.25)$$

where $\chi(x)$ is the so called Goldstone field, and where we identify $\eta(x)$ and $V^\mu(x)$ as the new dynamic fields.

Now we proceed to add the gauge fixing Lagrangian

$$\mathcal{L}_{\mathbf{g.f.}} = V^\nu \partial_\nu B + \frac{\xi}{2} B^2 = \frac{\xi}{2} B^2 + \left(A^\nu - \frac{1}{ve} \partial^\nu \chi \right) \partial_\nu B, \quad (2.26)$$

with $B(x)$ a real scalar auxiliary field.

Definitely, we obtain

$$\begin{aligned} \mathcal{L} = & \partial^\mu \phi^* \partial_\mu \phi + \mu^2 \phi^* \phi - \frac{1}{2} \partial^\mu A^\nu (\partial_\mu A_\nu - \partial_\nu A_\mu) - \lambda (\phi^* \phi)^2 \\ & + A^\mu \phi^* ie \overleftrightarrow{\partial}_\mu \phi + e^2 A^\mu A_\mu \phi^* \phi + \frac{\xi}{2} B^2 + \left(A^\mu - \frac{1}{ve} \partial^\mu \chi \right) \partial_\mu B. \end{aligned} \quad (2.27)$$

As can be easily checked, the fields redefinitions in equations (2.24), (2.25) translates in

$$D_\mu \phi(x) = \frac{e^{\frac{i\chi(x)}{v}}}{\sqrt{2}} (\partial_\mu \eta(x) - ieV_\mu(x)\eta(x) - iveV_\mu(x)), \quad (2.28)$$

and

$$\begin{aligned} D^\mu \phi (D_\mu \phi)^* = & \frac{1}{2} (\partial^\mu \eta)^2 + \frac{e^2}{2} V^2 \eta^2 \\ & + ve^2 V^2 \eta + \underbrace{\frac{e^2 v^2}{2}}_{m^2/2} V^2, \end{aligned} \quad (2.29)$$

$$V(\phi\phi^*) = -\frac{\mu^4}{4\lambda} + \mu^2 \eta^2 + \mu\sqrt{\lambda} \eta^3 + \frac{\lambda}{4} \eta^4, \quad (2.30)$$

$$\frac{1}{4} F^{\mu\nu} F_{\mu\nu} = \frac{1}{2} \partial^\mu V^\nu (\partial_\mu V_\nu - \partial_\nu V_\mu). \quad (2.31)$$

Thus, employing the transformations in (2.24),(2.25) as well as the relations derived here above, equation (2.27) becomes

$$\begin{aligned}\mathcal{L} = & \frac{1}{2}\partial^\mu\eta\partial_\mu\eta - \mu^2\eta^2 - \frac{1}{4}F^{\mu\nu}F_{\mu\nu} + \frac{m^2}{2}V^\mu V_\mu \\ & + \frac{e^2}{2}V^\mu V_\mu\eta^2 + \frac{\mu e^2}{\sqrt{\lambda}}V^\mu V_\mu\eta - \mu\sqrt{\lambda}\eta^3 - \frac{\lambda}{4}\eta^4 \\ & + V^\mu\partial_\mu B + \frac{\xi}{2}B^2 + \frac{\mu^4}{4\lambda} .\end{aligned}\tag{2.32}$$

We notice that:

- the Goldstone field $\chi(x)$ has completely disappeared from the gauge fixed Lagrangian;
- the abelian vector field $V_\mu(x)$ is now suited with a Proca mass term which can be directly read in equation (2.29).

These two facts are the essence of the Higgs mechanism. We started from a gauge invariant Lagrangian, and then, by expanding the fields over the minimal constant field configurations, we spontaneously broke the $U(1)$ symmetry, generating the two consequences described above.

To derive the Feynman rules we calculate the equations of motion from the new Lagrangian, obtaining

$$(\square + m^2)V^\nu = (\xi - 1)\partial^\nu B - e^2\eta\left(\frac{2\mu}{\sqrt{\lambda}} + \eta\right)V^\nu ,\tag{2.33}$$

$$(\square + 2\mu^2)\eta = e^2V^2\left(\frac{\mu}{\sqrt{\lambda}} + \eta\right) - 3\mu\sqrt{\lambda}\eta^2 - \lambda\eta^3 ,\tag{2.34}$$

$$(\square + \xi m^2)B = 0 \quad , \quad \partial^\mu V_\mu = \xi B .\tag{2.35}$$

Then, substituting the second equation of (2.35) into the gauge fixing Lagrangian (2.26), we find

$$\mathcal{L}_{\mathbf{g.f.}} = \frac{1}{2\xi}V^\rho(x)\partial_\rho\partial_\nu V^\nu(x) .\tag{2.36}$$

Therefore, we can rewrite the full Lagrangian in a form that makes the kinetic terms for the vector and scalar fields explicit. We have

$$\begin{aligned}\mathcal{L} = & -\frac{1}{2}(\square + 2\mu^2)\eta(x) + \frac{1}{2}V^\mu(x)\left[\left(\square + \frac{e^2\mu^2}{\lambda}\right)g_{\mu\nu} - \partial_\mu\partial_\nu(1 - \xi^{-1})\right]V^\nu(x) \\ & + \frac{e^2}{2}V^2(x)\eta^2(x) + \frac{\mu e^2}{\sqrt{\lambda}}\eta(x)V^2(x) - \mu\sqrt{\lambda}\eta^3(x) - \frac{\lambda}{4}\eta^4(x) ,\end{aligned}\tag{2.37}$$

which leads to the momentum space Feynman rules:

- scalar Higgs boson propagator:

$$D_s(p) = \frac{i}{p^2 - 2\mu^2};$$

- massive abelian vector particles:

$$\frac{i\lambda}{\lambda k^2 - e^2 \mu^2} \left(-g_{\mu\nu} + \frac{\lambda(1-\xi)k_\mu k_\nu}{\lambda k^2 - \xi e^2 \mu^2} \right);$$

- three points scalar vertex: $-6i\mu\sqrt{\lambda}$;
- four points scalar vertex: $-6i\lambda$;
- three points vertex with one scalar and two massive vectors: $i2\mu e^2 g^{\mu\nu} / \sqrt{\lambda}$;
- four points vertex with two scalars and two massive vectors $2ie^2 g^{\mu\nu}$.

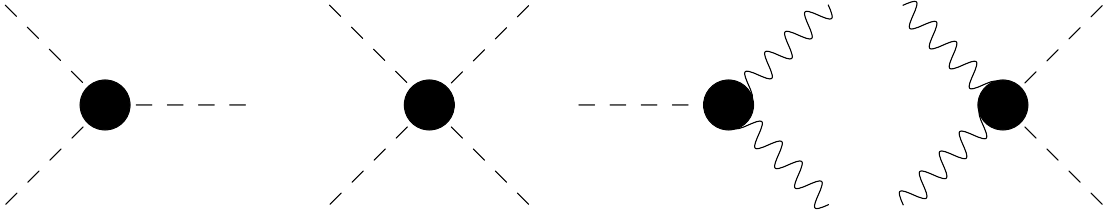


Figure 2.1: Feynman rules for the gauge fixed spontaneously broken abelian Higgs Lagrangian. The dashed lines representing massive scalar bosons, and the wavy lines representing massive vectors.

Finally, we recall that the Hilbert subspace of the physical states is recovered by removing unphysical ghost-Stückelberg states with the subsidiary condition

$$B^-(x) |\text{phys}\rangle = 0 , \quad (2.38)$$

and in the $\xi \rightarrow \infty$ limit we turn to the unitary gauge with the non-renormalisable massive vector boson propagator.

In this section we saw how a massless vector field acquires mass via the Higgs mechanism. In the next section we will extend this discussion to the non-abelian case and to fermions, with the goal of a complete phenomenological building of the standard model.

2.2 The BEH mechanism in the standard model

The standard model for the weak and electromagnetic interactions is empirically based upon the non-semi-simple and unitary gauge group $\mathbb{G} = \text{SU}(2) \times \text{U}(1) \sim \text{U}(2)$, in which the corresponding gauge bosons exchange the associated elementary interactions. Inside this picture, we have to arrange the known matter and the interaction fields. In practice, we proceed bottom-up, by phenomenological considerations and experimental evidence.

We choose to take the left-handed matter fields as doublets of the fundamental representations of $\text{SU}(2)$:

$$\Psi_i(x) = \begin{pmatrix} \nu_i(x) \\ \ell_i^-(x) \end{pmatrix} \quad \ell_i^-(x) = \frac{(\mathbb{I} - \gamma^5)}{2} \ell_i(x) \quad ,$$

where i is understood to run over the 3 different families of leptons (e, μ, τ). The right-handed ones are singlets of $\text{SU}(2)$, and are defined by

$$\ell_i^+(x) = \frac{(\mathbb{I} + \gamma^5)}{2} \ell_i(x) ,$$

where $\gamma^5 = i\gamma^0\gamma^1\gamma^2\gamma^3$.

At this point, we are left with the choice of the Higgs scalar field, and following the Occam's razor argument, we base our choice on simplicity, choosing the *parametrisation* containing the minimal number of degrees of freedom possible. Once again, experimental data tell us that is necessary to give mass to 3 vectors, i.e. the non-abelian gauge bosons, and to keep the photon massless. So, owing to the Goldstone theorem and to the spontaneous symmetry breaking pattern $\text{SU}(2) \times \text{U}(1)_Y \rightarrow \text{U}(1)_{\text{em}}$, we choose to arrange the Higgs and the Goldstone bosons into a complex $\text{SU}(2)$ doublet into one of the fundamental representations of the gauge group, namely

$$\Phi(x) = \begin{pmatrix} \phi^+(x) \\ \phi^0(x) \end{pmatrix} .$$

Essentially, everything that concerns the standard model follows from these basic assumptions/arrangements made above.

As a consequence of the spontaneous symmetry breaking, the electric charge turns out to be a linear combination of both $\text{SU}(2)$ and $\text{U}(1)$ generators, namely

$$Q = \mathbb{T}_3 + \frac{1}{2}\mathbb{Y}. \quad (2.39)$$

Now we can proceed to write down the most general, renormalisable, gauge invariant Lagrangian involving the fields considered above. Owing to the constraining criterion of renormalisability, every term in \mathcal{L} MUST be a **local monomial of the fields and their derivatives of canonical engineering dimension D in natural units $D \leq 4$** . Thus, the *famous*, unique and necessary result is

$$\begin{aligned} \mathcal{L} = & -\frac{1}{4} W_I^{\mu\nu} W_{\mu\nu}^I - \frac{1}{4} B^{\mu\nu} B_{\mu\nu} + (D^\mu \Phi)^\dagger D_\mu \Phi - \mathbb{V}(\Phi) \\ & + i\bar{\Psi}_i \not{D} \Psi_i + i\bar{\ell}_i^+ \not{D} \ell_i^+ - y_i (\bar{\Psi}_i \cdot \Phi \ell_i^+ + \text{h.c.}) . \end{aligned} \quad (2.40)$$

Where $W_I^{\mu\nu}$ and $B^{\mu\nu}$ are respectively the non-abelian and abelian field strength tensors, and where D^μ is the $\text{SU}(2) \times \text{U}(1)$ covariant derivative. Moreover, the Higgs potential which respects the gauge symmetry of the Lagrangian and the renormalisability criterion is the generalisation of the Higgs potential introduced in the former section, i.e.

$$\mathbb{V}(\Phi^\dagger \Phi) = -\mu^2 \Phi^\dagger \Phi + \lambda (\Phi^\dagger \Phi)^2 . \quad (2.41)$$

It turns out that all the vector gauge bosons, as well as all the lepton fields, appear to be MASS-LESS. In fact:

- The assumed transformation laws for the left and right-handed components forbid the introduction of an $SU(2)$ invariant Dirac or Majorana mass for leptons.
- It is not possible to include a Proca-like mass term for the non-abelian gauge vector bosons, as this inevitably leads to a both non-renormalisable/non-unitary theory at the quantum level.
- It could be possible to introduce a Proca mass term for the abelian gauge vector boson, and so to recover a renormalisable and unitary theory at the quantum level², but the experimental limit on the photon mass is extremely low, being fixed around 10^{-18} eV.

The obvious consequence is that every particle mass in the standard model is expected to be proportional to the absolute value of the only mass scale of the theory, *i.e.* the Higgs mass.

In the following section we will see how via the spontaneous symmetry breaking mechanism both non-abelian gauge bosons, the fermions and the Higgs field itself do acquire mass. It turns out that the classical Hamiltonian which follows from the (2.40) reaches its minimum for vanishing lepton and gauge vector fields values, but for non-zero, constant values of the $SU(2)$ Higgs scalar doublet:

$$\Phi_0^\dagger \Phi_0 = \frac{\mu^2}{2\lambda},$$

in the same fashion of the already discussed Higgs abelian gauge invariant model.

Then, the electroweak symmetry breaking follows assuming a non-zero vacuum expectation value of the Higgs doublet

$$\langle 0 | \Phi(x) | 0 \rangle = \frac{1}{\sqrt{2}} \begin{pmatrix} 0 \\ v \end{pmatrix}, \quad v^2 = \frac{\mu^2}{\lambda}, \quad v \simeq 246 \text{ GeV}. \quad (2.42)$$

Using the polar decomposition as

$$\Phi(x) = \frac{1}{\sqrt{2}} U_\chi(x) [v + h(x)] \begin{pmatrix} 0 \\ 1 \end{pmatrix}, \quad (2.43)$$

$$U_\chi(x) = \exp\{i\chi_a(x)\tau_a/v\}, \quad (2.44)$$

one can identify h as the neutral scalar Higgs field, while χ_a is a matrix containing the anticipated Goldstone scalar fields which will decouple from the dynamics in order to let the gauge boson acquire a mass.

²via the Stueckelberg trick

2.2.1 Gauge fields and fermions masses

Let us start by considering the transformation law for the covariant derivative acting on the scalar Higgs field. We have

$$(D^\mu \Phi)(x) = \left(\partial^\mu - igV^\mu - \frac{ig'}{2} B^\mu \right) \Phi(x) , \quad (2.45)$$

where g and g' are respectively the SU(2) and U(1) couplings, and where V^μ and B^μ are the corresponding fields.

Defining

$$V_\mu(x) = U_\chi W_\mu(x) U_\chi^{-1} - \frac{i}{g} (\partial_\mu U_\chi) U_\chi^{-1} , \quad (2.46)$$

with

$$W_\mu(x) = \frac{1}{2} \begin{pmatrix} W_\mu^3(x) & W_\mu^+(x)/\sqrt{2} \\ W_\mu^-(x)/\sqrt{2} & W_\mu^3(x) \end{pmatrix} , \quad (2.47)$$

$$W_\mu^\pm(x) = \frac{W_\mu^1(x) \mp iW_\mu^2(x)}{\sqrt{2}} , \quad (2.48)$$

$$W_\mu(x) W^\mu(x) = \frac{1}{4} g^{\mu\nu} \sum_{a=1}^3 W_\mu^a(x) W_\nu^a(x) \begin{pmatrix} 1 & 0 \\ 0 & 1 \end{pmatrix} , \quad (2.49)$$

it follows that

$$\begin{aligned} (D^\mu \Phi)^\dagger D_\mu \Phi &= \frac{1}{2} \partial_\mu h \partial^\mu h + \frac{g^2}{2} [v + h]^2 W_\mu^+ W_\mu^- \\ &+ \frac{1}{8} (gW_3^\mu - g'B^\mu)(gW_\mu^3 - g'B_\mu) [v + h]^2 . \end{aligned} \quad (2.50)$$

The term in W_μ^\pm is easily understood to be the mass term leading to $m_W = vg/2$. The new feature here is that we are still not able to guess the abelian field and the W_μ^3 masses, as they share a non-diagonal mass matrix.

To find a correct identification, we have to move to the mass eigenstates. We reach this goal by setting

$$\begin{pmatrix} W_\mu^3 \\ B_\mu \end{pmatrix} = \begin{pmatrix} \cos \theta_W & \sin \theta_W \\ -\sin \theta_W & \cos \theta_W \end{pmatrix} \begin{pmatrix} Z_\mu^0 \\ A_\mu \end{pmatrix} , \quad (2.51)$$

which makes the mass matrix diagonal if and only if $\tan \theta_W = g'/g$. This choice corresponds to $m_A = 0$ and $m_Z = m_W / \cos \theta_W$, which are respectively identified with the photon and Z boson masses.

For what concerns the fermions, we find that their mass can be generated by Yukawa terms. Then, defining the Higgs doublet into the conjugate SU(2) representation as

$$\tilde{\Phi}(x) = i\sigma_2 \Phi^*(x) , \quad (2.52)$$

and substituting the same Higgs field parametrisation made before, we obtain

$$y_i \left(\bar{\Psi}_i \cdot \Phi \ell_i^+ + \tilde{\Phi} \cdot \bar{\ell}_i^+ \Psi_i \right) = \frac{y_i v}{\sqrt{2}} \left(\frac{h}{v} + 1 \right) (\bar{\ell}_i^- \ell_i^+ + \bar{\ell}_i^+ \ell_i^-) . \quad (2.53)$$

Finally, considering the covariant derivative acting on a fermion as

$$iD_\mu \Psi'_i(x) = \left(i\partial_\mu + gV_\mu - \frac{g'}{2} B_\mu \right) U_\chi \Psi_i(x), \quad (2.54)$$

and employing once again (2.51), it is possible to show that the positron charge is identified as $e = g \sin \theta_W$.

Eventually, we arrive to the leptons Lagrangian of the electroweak standard model³

$$\begin{aligned} \mathcal{L}_{leptons} = \sum_{i=1}^3 & \left[i \bar{\Psi}_i \not{\partial} \Psi_i + i \bar{\ell}_i^+ \not{\partial} \ell_i^+ - m_i (1 + h/v) \bar{\ell}_i \ell_i \right] \\ & + g \left(W_\mu^+ J_\mu^+ + W_\mu^- J_\mu^- + Z_\mu^0 J_\mu^0 \right) - e A_\mu J^\mu . \end{aligned} \quad (2.55)$$

2.2.2 Introducing quarks and gluons

As far as we know, the elementary constituents of matter can be organised in six leptons and six quarks, with the latter being also subject to the STRONG INTERACTIONS described by QUANTUM CHROMO DYNAMICS (QCD). As in this work we will focus on the EW interactions, will not discuss the details of QCD, but limit ourselves to introducing how the strong interactions are incorporated in the standard model Lagrangian.

The introduction of quarks and gluons shares some common features with the leptonic sector of the standard model. The quarks Lagrangian is understood to be the same as (2.40), but with quark fields replacing leptons:

$$\mathcal{L}_{quarks} = \sum_{\text{colors}} \left[i \bar{u}_i \not{D} u_i + i \bar{d}_i \not{D} d_i - \left(y_d (\bar{q}_i^- \cdot \Phi) d_i^+ + y_u (\bar{q}_i^- \cdot \tilde{\Phi}) u_i^+ + \text{h.c.} \right) \right] . \quad (2.56)$$

Here, an interesting feature related to the presence of three experimentally seen families of quarks needs to be discussed. In fact, the Lagrangian for the quark families might not simply be the sum of the corresponding Lagrangians, and mixing can take place.

This is what experimentally one observes in EW interactions among quarks, i.e. that quark families numbers are not conserved. Moreover, in principle, there is no compelling reason to pair the quarks doublets as done in (2.56).

In fact, one is completely free to choose any basis in the quarks families space. This leads to the anticipated feature that in order to have the Yukawa interaction terms into a diagonal form, the weak interactions will contain off-diagonal terms mixing different families.

³a complete form of the currents will be specified in the next subsection after introducing quarks and gluons.

It turns out that the most general quarks action must contain two non-diagonal matrices that correspond to families mixing in arbitrary bases. After the introduction of the $SU(3)$ non-abelian vector fields and the related strength tensor, corresponding to **gluons**, *i.e.* the carriers of strong interactions, we are ready to write down the full standard model Lagrangian

$$\begin{aligned}
\mathcal{L}_{SM} = & -\frac{1}{4} G_{\mu\nu}^A G_A^{\mu\nu} - \frac{1}{4} W_{\mu\nu}^I W_I^{\mu\nu} - \frac{1}{4} B^{\mu\nu} B_{\mu\nu} + (D^\mu \Phi)^\dagger D_\mu \Phi - \mathbf{v}(\Phi) \\
& + \sum_{i=1}^3 \left[i \bar{\Psi}_i \not{D} \Psi_i + i \bar{\ell}_i^+ \not{D} \ell_i^+ - y_i (\bar{\Psi}_i \cdot \Phi \ell_i^+ + \text{h.c.}) \right] \\
& + \sum_{\text{colors}} \sum_{i=1}^3 \left[i \bar{u}_i \not{D} u_i + i \bar{d}_i \not{D} d_i \right. \\
& \left. - \left(\sum_{j=1}^3 \mathbf{y}_{ij}^d (\bar{q}_i \cdot \Phi) d_j^+ + \mathbf{y}_{ij}^u (\bar{q}_i \cdot \tilde{\Phi}) u_j^+ + \text{h.c.} \right) \right].
\end{aligned} \tag{2.57}$$

Then, moving to the eigenstate basis in which the mass matrix is diagonal by employing the unitary matrices $V_{\mp}^{u,d}$, as defined by

$$u^\mp(x) = V_{\mp}^u \mathbf{u}^\mp(x) \quad , \quad d^\mp(x) = V_{\mp}^d \mathbf{d}^\mp(x) \quad , \tag{2.58}$$

and considering spontaneous breaking of the electroweak symmetry as done earlier, we come to the broken phase Lagrangian⁴

$$\begin{aligned}
\mathcal{L}_{SM} = & -\frac{1}{4} G_{\mu\nu}^A G_A^{\mu\nu} - \frac{1}{4} W_{\mu\nu}^I W_I^{\mu\nu} - \frac{1}{4} B^{\mu\nu} B_{\mu\nu} \\
& + \frac{1}{2} \partial^\mu h \partial_\mu h - \frac{1}{2} m_h^2 h^2 - \lambda v h^3 - \frac{1}{4} \lambda h^4 \\
& + [m_W^2 W_+^\mu W_\mu^- + \frac{1}{2} m_Z^2 Z_\mu^0 Z_0^\mu] (1 + h/v)^2 \\
& + i \sum_{i=1}^3 \left[\bar{\Psi}_i \not{D} \Psi_i + \bar{\ell}_i^+ \not{D} \ell_i^+ + \sum_{\text{colors}} (\bar{u}_i \not{D} u_i + \bar{d}_i \not{D} d_i) \right] \\
& - \sum_{i=1}^3 \left[m_i^\ell \bar{\ell}_i \ell_i + \sum_{\text{colors}} (m_i^u \bar{u}_i u_i + m_i^d \bar{d}_i d_i) \right] (1 + h/v) \\
& + A_\mu J^\mu + Z_\mu^0 J_0^\mu + W_\mu^- J_-^\mu + W_\mu^+ J_+^\mu .
\end{aligned} \tag{2.59}$$

⁴which follows after repeating the same steps already done to let fermions acquire mass in the former section.

The complete expression of the electroweak currents is given by

$$J^\mu = -e \sum_{i=1}^3 \left[\bar{\ell}_i \gamma^\mu \ell_i + \sum_{\text{colors}} \left(\frac{1}{3} \bar{\mathbf{d}}_i \gamma^\mu \mathbf{d}_i - \frac{2}{3} \bar{\mathbf{u}}_i \gamma^\mu \mathbf{u}_i \right) \right] \quad (2.60)$$

$$J_+^\mu = \frac{g}{\sqrt{2}} \sum_{i=1}^3 \left[\bar{\nu}_i \gamma^\mu \ell_i^- + \frac{1}{2} \sum_{\text{colors}} \bar{\mathbf{u}}_i^- \gamma^\mu (\mathbb{I} - \gamma_5) \mathbf{v}_{ij} \mathbf{d}_j \right] \equiv (J_-^\mu)^\dagger, \quad (2.61)$$

$$J_0^\mu = \frac{1}{2} \sec \theta_W \sum_{i=1}^3 \left[\bar{\nu}_i \gamma^\mu \nu_i - \bar{\ell}_i^- \gamma^\mu \ell_i^- + 2 \sin^2 \theta_W \bar{\ell}_i \gamma^\mu \ell_i \right. \\ \left. + \bar{\mathbf{u}}_i^- \gamma^\mu \mathbf{u}_i^- - \frac{1}{2} \bar{\mathbf{d}}_i \gamma^\mu (\mathbb{I} - \gamma_5) \mathbf{d}_i \right. \\ \left. + \sin^2 \theta_W \left(\frac{2}{3} \bar{\mathbf{d}}_i \gamma^\mu \mathbf{d}_i - \frac{4}{3} \bar{\mathbf{u}}_i \gamma^\mu \mathbf{u}_i \right) \right], \quad (2.62)$$

and is riassuntive of both the lepton and quark matter.

2.3 \mathcal{CP} -violation in the standard model

Being measured in several neutral K mesons decays, \mathcal{CP} -violation is still one of the most tested aspects of SM and most mysterious, at the same time. It is unlikely that the SM can describe all the \mathcal{CP} -violation in nature. It is also clear that some kind of BSM physics exists, and so it is not surprising at all that most of these extensions do incorporate some additional sources of \mathcal{CP} -violation⁵.

A glaring evidence of our limited understanding⁶ of \mathcal{CP} symmetry, is that our Universe seems to be composed mostly of ordinary matter, while antimatter is only created in high-energy events, be these of astrophysical nature, cosmic rays or our laboratories. This fact is known as the baryon asymmetry problem, and it goes under the name of baryogenesis in the primordial universe.

As we will discuss later, to correctly account for such a transition it is mandatory to have additional \mathcal{CP} -violating sources than those we know of in the SM. Another logical possibility is simply that we have not reached an energy high enough to test if the SM is capable of such violation. It could be that the energy scales involved are actually far from our experimental reach, and this directly translated in successful measurement on arguments concerning the mostly \mathcal{CP} conserving nature of the SM. Nevertheless, here we proceed by analysing the only source of \mathcal{CP} -violation present in the SM (assuming neutrino are massless, for the moment).

The SM Lagrangian provides three Yukawa interactions between the Higgs field and the fermions

$$\mathcal{L}_{\text{yuk}} = - \sum_{i=1}^3 \left\{ \sum_{j=1}^3 \sum_{\text{colors}} \left(Y_{ij}^d \bar{q}_i^- \cdot \Phi d_j^+ + Y_{ij}^u \bar{q}_i^- \cdot \tilde{\Phi} u_j^+ \right) + y_i \bar{\Psi}_i \cdot \Phi \ell_i^+ + \text{h.c.} \right\}, \quad (2.63)$$

⁵As an example, the seesaw mechanism to generate neutrino masses provides extra sources of \mathcal{CP} -violation via the Majorana phases involved in neutrinos mixing

⁶we also remind the puzzling question of strong \mathcal{CP} -violation in QCD

to be \mathcal{CP} -violating, if and only if [3]

$$\text{Im}\left\{\det\left[\mathbf{Y}^d\mathbf{Y}^{d,\dagger}, \mathbf{Y}^u\mathbf{Y}^{u,\dagger}\right]\right\} \neq 0. \quad (2.64)$$

This can intuitively be related to the structures of Yukawa terms concerned in the interactions. As an example, consider a generic fermion ψ with Yukawa coupling to the SM Higgs

$$\mathbf{Y}_{ij} \bar{\psi}_i^- \cdot \Phi \psi_j^+ + \mathbf{Y}_{ij}^* \bar{\psi}_i^+ \cdot \tilde{\Phi} \psi_j^- \quad . \quad (2.65)$$

The \mathcal{CP} acts as

$$\mathcal{CP}(\bar{\psi}_i^- \cdot \Phi \psi_j^+) \rightarrow \bar{\psi}_i^+ \cdot \tilde{\Phi} \psi_j^- \quad . \quad (2.66)$$

So, we essentially move to the Hermitian conjugated on the first term of the equation above. On the other hand, the \mathbf{Y} matrices do not get modified acting with \mathcal{CP} operator. Therefore we find the SM to be completely \mathcal{CP} -symmetric if and only if the \mathbf{Y} matrices are real, i.e. $\mathbf{Y}_{ij} = \mathbf{Y}_{ij}^*$. But how many \mathcal{CP} -violating independent phases do we have? We have three 3×3 complex Yukawa matrices, for a total of 27 complex coefficients, i.e 27 real and imaginary parts. It is possible to reduce this number via a unitary rotation which leaves invariant the three generators for each of the five representations of fermion species[3]. Doing so, we remove at most 15 real and 30 imaginary parameters. Nevertheless, a

$$\text{U}(1)_{\text{B}} \times \text{U}(1)_{\text{e}} \times \text{U}(1)_{\mu} \times \text{U}(1)_{\tau} \quad (2.67)$$

symmetry is left untouched, meaning that up to 26 imaginary parameters can be removed. As a result, we have 12 real parameters and a phase. The 12 real parameters correspond to the six quark masses, the three charged leptons masses, and three angles. The phase is the only \mathcal{CP} -violating source present in the SM, and is known as the Kobayashi-Maskawa phase.

Going back to the SM Lagrangian (2.57), after EWSB occurs the quarks masses are generated via the Higgs mechanism as shown in (2.59) by means of (2.58). This eventually takes us to writing down the vector currents in the mass eigenstate basis. It turns out that the only currents getting affected by the change of basis is

$$J_+^\mu(x) = \frac{1}{\sqrt{2}} \sum_{i=1}^3 \bar{U}_i^- \gamma^\mu \left(V_-^{\mu,\dagger} V_-^d \right)_{ij} D_j^-(x) = (J_-^\mu(x))^* \quad . \quad (2.68)$$

We now understand that the flavour changing weak interactions mix up the three quarks up and the three quark down species by the CABIBBO-KOBAYASHI-MASKAWA mixing matrix

$$V_{\text{CKM}} \equiv V_-^{u,\dagger} V_-^d \quad , \quad (2.69)$$

which is a unitary 3×3 matrix with three real angles and six phases. The form of this matrix is not unique. A standard choice consists in

- Getting rid of all the possible permutation by ordering the up and down quarks by their masses, leading to

$$V_{\text{CKM}} = \begin{pmatrix} V_{ud} & V_{us} & V_{ub} \\ V_{cd} & V_{cs} & V_{cb} \\ V_{td} & V_{ts} & V_{tb} \end{pmatrix}$$

- Defining \mathcal{P}_i to be unitary phase matrices, we can equivalently rotate to the mass eigenstates by using

$$\tilde{V}_-^i = \mathcal{P}^i V_-^i \quad \tilde{V}_+^i = \mathcal{P}^i V_+^i,$$

with the mass basis being the same under this transformation. Nevertheless the CKM matrix changes as

$$V_{CKM} \rightarrow \mathcal{P}^u V_{CKM} \mathcal{P}^{d,*}. \quad (2.70)$$

we fix this freedom [3] by requiring V_{CKM} to have the minimal number of phases compatible with the quark generations included, leading us to keep only one phase in the mixing matrix. This phase is exactly the Kobayashi-Maskawa phase, i.e., the same phase we obtained before from the three complex Yukawa matrices concerning quarks and Higgs interactions.

We end this section by writing down the standard parametrisation for the CKM matrix, suiting three Euler-like angles and the only \mathcal{CP} -violating KM phase[1]:

$$V_{CKM} = \begin{pmatrix} c_{12}c_{13} & s_{12}c_{13} & s_{13}e^{-i\delta_{KM}} \\ -s_{12}c_{23} - c_{12}s_{23}s_{13}e^{i\delta_{KM}} & c_{12}c_{13} - s_{12}s_{23}s_{13}e^{i\delta_{KM}} & s_{23}c_{13} \\ s_{12}s_{23} - c_{12}c_{23}s_{13}e^{i\delta_{KM}} & -c_{12}s_{23} - s_{12}c_{23}s_{13}e^{i\delta_{KM}} & c_{23}c_{13} \end{pmatrix}. \quad (2.71)$$

2.4 Shortcomings of the standard model

Today's measurements performed at high energy colliders, as well as in low-energy precision experiments, confirms that the SM is able to explain pretty much all the particle-physics observations with an unexpected precision. The last exciting discoveries at colliders being the Top-Quark (Fermilab, 1995 - [4]), the τ neutrino (Fermilab 2000 - [5]) and the Higgs boson (CERN, 2012 - [6]), with no convincing sign of BSM physics. On the other hand, hints of BSM physics appear to us considering theoretical considerations on the one hand and astrophysical/cosmological observations. In particular:

- we now know neutrinos to be massive, yet we do not know the mechanism through which their masses is generated. In addition, we do not know whether they are Majorana or Dirac fermions. Finally, their mixing could also be the source of additional \mathcal{CP} -violation;
- we observe a baryon-anti-baryon asymmetry in today's universe, for which mechanisms are in place in the SM but whose amount cannot be explained by SM;
- we have evidence that the Universe is mostly made by some kind of non-interacting/non-collisional kind of matter, i.e. the Dark Matter, which cannot find a full explanation in the SM.

We aim to explore whether all of these facts (and other theoretical limitations) can be explained by a BSM theory that leaves at higher energy scales.

In the last decades, different theoretical scenarios have been built trying to answer these questions. On the other hand, the phenomenological and experimental consequences of such theoretical constructions have so far eluded us. A complementary and model independent approach is to assume that the new physics energy scale Λ is beyond our reach, and only indirect effects (from the virtual exchange of new states) could be detected.

Under this hypothesis, the Effective Field Theory approach is the most promising one, as it provides a consistent QFT framework where to analyse possible deviations from the SM. In the context of the problems outlined above EFT's also offer a context where to analyse/solve problems:

- Majorana neutrino mass generation can be obtained from the only 5-dimensional, non-renormalisable, gauge independent operator which encompasses, for instance, all different types of see-saw mechanisms[7];
- by adding suitable operators to the SM, it is possible to achieve electroweak phase transition, understood to directly lead to the observed matter-antimatter asymmetry [8];
- Dark Matter candidates can be added and EFTs built to include them in rather model independent way [9];

last but not least, the EFT approach is general and can experimentally tested both in collider [10, 11] and non-collider [12, 8] experiments.

2.4.1 Electroweak baryogenesis

Electroweak baryogenesis is understood as one of the most attractive and promising ways to account for the observed baryon asymmetry of the Universe. The assumptions are simply that in the phase where hot radiation dominated universe, the electroweak symmetry $SU(2) \times U(1)_Y$ was unbroken.

As the universe temperature cooled down, the Higgs acquired a non zero VEV, breaking the EW gauge symmetry to the $U(1)_{em}$ subgroup. During this phase transition, if first order, the EWBG occurs. In short, the electroweak Phase Transition (EWPT) proceeds via bubble formation in $U(1)_{em}$ broken phase nucleating within the non-broken plasma around and then expanding. By a non-perturbative process, the so-called EW sphaleron processes [13, 14], the asymmetry between the internal and external regions of the bubbles, the presence of sufficiently large \mathcal{CP} -violation, and the fact that the bubble expand, lead to formation of a net baryon number inside the bubble which we currently call our Universe.

In 1967, Andrei Sakharov identified three minimum properties which are required for baryogenesis to occur:

- at least one baryon number violating process,
- C and \mathcal{CP} violation,

- interactions outside thermal equilibrium.

In the SM, mechanisms that lead to satisfying the three conditions above are present. On the other hand, our current understanding is that within the SM, the size of the effects are not sufficient to generate enough baryons as fast as needed to achieve EWBG [15]. This is due to the smallness of the \mathcal{CP} violation in the SM and the SM Higgs potential, which implies a second order electroweak phase transition. A strong first order phase transition could instead occur in extensions of the SM.

So the question now is :

HOW CAN WE OBTAIN BOTH A MODIFICATION OF THE HIGGS POTENTIAL AND ENOUGH \mathcal{CP} -VIOLATION BY MINIMALLY DEFORMING THE SM?

As mentioned above, it is possible to achieve baryogenesis in the framework of an EFT. This is essentially due to the fact that these conditions can be satisfied taking into account effects from **non-renormalisable/higher-dimensional operators**, generated after integrating out heavy-particles/degrees-of-freedom of a complete theory. After this short review of the SM, we are ready to consider EFTs more in detail.

In the next chapter we review the idea and some basic aspects of effective field theories, while the full discussion about which models should be considered for our goals and the corresponding theoretical/experimental/observational constraints is in the following chapters.

This chapter is dedicated to reviewing key concepts and technical developments of EFT methods. The goal is to construct a solid theoretical framework to face up the arguments discussed in the succeeding chapters.

We start with a brief introductory discussion on the motivations behind this approach in section 3.1. We review how mass and energy scales play a different role in this picture in the relative subsection 3.1.1, using [16] as the main reference.

Then, in section 3.2 we review on how the EFT approach takes place. We consider a full (referred as an ordinary field theory) spinor/meson interacting theory and show how matching to the corresponding EFT can be obtained up to the one-loop order in perturbation theory. The entire discussion is based on the work [17], with the results reproduced independently.

Finally, in section 3.3 we generalize this approach to the standard model effective field theory. We discuss on operator basis and phenomenological Lagrangians, eventually characterising an Higgs extended sector which will be introduced in chapter 4. The main review reference exploited here being [11].

3.1 Physics and philosophy behind

Most of the times, phenomena involving different scales can be analysed by considering only one relevant scale at a time. Classical Mechanics is the straightforward example in which this statement is true. If one is looking for *extreme* precision, then it is mandatory to consider classical mechanics only an approximation of reality, or according to the language to which we will refer, an effective description.

To get a whole understanding, one must take all the necessary steps into the vast area of fundamental physics, starting from special relativity and quantum mechanics, arriving to the quantum theory of fields.

The standard model is the quantum field theory of fundamental particles and interactions, and represents one of the most advanced steps in our understanding of nature. Even though, as we discussed in section 2.4, the SM is found to be an incomplete theory, which cannot be extended to arbitrary large energy-momentum scales owing to the *raw*/non-smooth structure of the quantum fields at short scales [18]. This feature inevitably degenerates into the so called ultraviolet divergences of the Feynman loop diagrams. To fix this behavior, several procedures were developed over the years.

Today, the standard method to deal with infinities is known as REGULARISATION, together with the strictly related RENORMALISATION. In a nutshell, the key concept is the possibility to separate the finite and the infinite parts of the Feynman diagrams using a proper integral-regularisation technique, and to cast away these infinities introducing counter-terms inside the Lagrangian with a proper renormalisation scheme. As several regularisation techniques and subtraction scheme can be defined, this procedure leads to arbitrariness in the finite terms, which, however, is not physical.

Nowadays, supported by an incredible matching with the experimental results, we understand these techniques to be trustful.

But what about the infinities? Why do we simply *cast away* them?

The easy way to understand this prescription is thinking at QFTs and the SM as theories constructed to describe only a finite range of energy and length scales. Integrating over loops inside Feynman diagrams does not respect this constrain, because the integration is made on the unbounded Fourier space of momenta. Regularising and then renormalising the divergences translates into an high energy-momenta cutoff, fixed to a finite and arbitrary scale.

Renormalisation can be simply thought of as a method to manage contributions from higher scales and writing an effective field theory which is not sensitive to physics happening at very high energies.

Now, after this brief discussion, in the following we will enter the details concerning the charming world of effective field theories.

3.1.1 On mass and energy scales

Before getting into the details, we briefly argue about the subtle differences between mass and interaction/effective energy scales, in order to highlight their different physical meaning and to better understand the process of matching (a distinction that helps in highlighting their different physical meaning) to an EFT.

To discuss what will follow it is necessary to partially abandon natural units, which we tacitly assumed up to know by taking $\hbar = c = 1$. To distinguish between energy E and length L^{-1} , but not between length and time T , we keep $c = 1$.

Now, a general SM Lagrangian density of dimension $[\mathcal{L}] \equiv EL^{-3}$ contains

- scalar fields $\rightarrow [\phi] \equiv (EL^{-1})^{1/2}$,
- vector field $\rightarrow [A^\mu] \equiv (EL^{-1})^{1/2}$,
- spinor fields $\rightarrow [\psi] \equiv E^{1/2}L^{-1}$,

- 4-derivatives $\rightarrow [\partial^\mu] \equiv L^{-1}$,
- Couplings $\rightarrow \begin{cases} [g] = [y] \equiv (E^{-1}L^{-1})^{1/2} , \\ [\lambda] \equiv E^{-1}L^{-1} . \end{cases}$

We maintained the same conventions of the former chapter, so that g^2, λ, y^2 are respectively, the gauge, scalar quartic and Yukawa couplings.

We remark that:

1. all the couplings appear to be dimensional, so it is worth to simplify the notations introducing the coupling and mass units as

$$\mathbf{C} \equiv 1/\sqrt{EL} , \quad \tilde{M} \equiv 1/L ; \quad (3.1)$$

2. it is possible to demonstrate that every 1-loop integral carries an \hbar , so that for each loop we have multiplicative factors of $\sim \hbar k_i / (4\pi)^2$, with $k_i = g^2, \lambda, y^2$, which do not contribute modifying the couplings dimension. This fact is also extended *mutatis-mutandis* to any loop order.

Now, considering a generic operator¹ included in \mathcal{L} as

$$\mathcal{L} \supset \frac{1}{\Lambda^{d-4}} \partial^{n_d} \Phi^{n_b} \psi^{n_f} , \quad (3.2)$$

with $\Phi = (\phi, A_\mu)$, it is possible to guess the dimensions of Λ , i.e. the effective scale.

The meaningful fields and parameter dimensions introduced above can be now expressed as functions of the units of mass and coupling.

We have

$$[\phi] = [A^\mu] \equiv \tilde{M}\mathbf{C}^{-1} , \quad [\psi] \equiv \tilde{M}^{3/2}\mathbf{C}^{-1} , \quad (3.3)$$

so that

$$[\mathcal{L}] = \frac{\tilde{M}^{n_d+n_b+\frac{3}{2}n_f}}{\mathbf{C}^{-(n_b+n_f)}\Lambda^{d-4}} . \quad (3.4)$$

Then, as $[\mathcal{L}] \equiv \tilde{M}^4/\mathbf{C}^2$, and as $n_b + \frac{3}{2}n_f + n_d = d$, we immediately obtain the dimensions of the effective scale, namely

$$[\Lambda] = \frac{\tilde{M}}{\mathbf{C}^{\frac{n-2}{d-4}}} , \quad (3.5)$$

where $n = n_b + n_f$.

Equation (3.5) gives us the minimal number of couplings required to define the scale measuring the strength of effective interactions.

we are eventually lead to understand the differences between mass and scales by the fact that the exponent of \mathbf{C} is always positive, and so scales and masses are not commensurable quantities.

¹ n_b, n_f, n_d are respectively for numbers of bosons, fermions, and derivatives.

Moreover, the physical meaning of these two quantities is intimately different, as the mass is associated with the energy at which new degrees of freedom do appear, while the energy scale is associated with the limit over which the theory becomes strongly coupled if no degrees of freedom do modify the effective description [16].

To summarize and show this fact practically, let us take a $\lambda\phi^4$ Lagrangian describing a massless complex scalar field invariant under the global group of phase transformation $U(1)$, namely

$$\mathcal{L} = \frac{1}{2}g_{\mu\nu}(\partial^\mu\phi)^*\partial^\nu\phi - \lambda\left(\phi^*\phi - \frac{v^2}{2}\right)^2. \quad (3.6)$$

Then, taking the $U(1)$ symmetry to be broken by the following field parametrisation over it's VEV

$$\phi = \frac{e^{\frac{i\chi(x)}{v}}}{\sqrt{2}}(v + \gamma(x)) \quad , \quad \langle 0|\phi|0\rangle = \frac{v}{\sqrt{2}}, \quad (3.7)$$

we are lead to

$$\mathcal{L} \supset \frac{1}{2}\left[1 + \frac{\gamma^2}{v^2} + 2\frac{\gamma}{v}\right]\partial^\mu\chi\partial_\mu\chi - \frac{1}{2}\gamma(\square + m_\gamma^2)\gamma, \quad (3.8)$$

where $m_\gamma^2 = 2\lambda v^2$, and where other terms arising were neglected, as irrelevant to this example.

Here we see two interaction vertexes concerning both χ and γ .

At energies far below the mass of γ it is possible to integrate out this field by the procedure introduced in Appendix A. Doing so, we determine the EFT that describes the interactions of the so called Nambu/Goldstone boson, namely

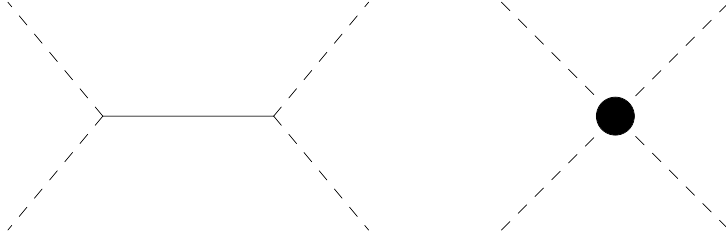


Figure 3.1: Full theory (left) vs effective theory (right) diagrams. Integrating out the radial γ field (continued line), we are left with the momentum dependent four scalar diagram in the effective theory, with the Λ scale identified in the matching procedure illustrated.

$$\mathcal{L}_{\text{eff}} = \frac{1}{2}\partial^\mu\chi\partial_\mu\chi + \frac{1}{\Lambda^4}(\partial^\mu\chi\partial_\mu\chi)^2, \quad (3.9)$$

with $\Lambda^4 = m^2v^2$.

From this formula we confirm the differences between mass and energy scales. In fact, m is the mass at which the particle responsible of the higher dimensional interaction appears, while Λ is the scale at which the theory becomes strongly coupled.

3.2 Illustrating the process

After these introductory remarks, we reserve this section to be dedicated to the introduction of EFT techniques from a quantitative perspective.

As discussed, the point of departure for EFTs is to humbly accept that any given theory is likely to have some short-distance or UV cut-off, Λ , beyond which it is invalid. Then, we proceed by *dropping* the constraining criterion of renormalisability, welcoming the introduction of $d > 4$ terms local in space-time.

That's to say that an effective Lagrangian is in principle defined by

$$\mathcal{L}_{\text{eff}} = \mathcal{L}_{d \leq 4} + \sum_{d=5}^{\infty} \frac{c_d}{\Lambda^{d-4}} \mathcal{O}_d . \quad (3.10)$$

The goal of this picture will be to describe the infrared physics of a more general full theory, taking into account how the ultraviolet physics can also influence this low energy behavior.

Following this scheme, we should consider only light degrees of freedom in the EFT, dropping the heavy ones².

Formally, these particles are INTEGRATED OUT of the action by a functional path integration over the heavy field involved.

That is, mathematically speaking³

$$\int \mathcal{D}\varphi_H \exp\left\{i \int dx \mathcal{L}(\varphi_\ell, \varphi_h)\right\} = \exp\left\{i \int dx \mathcal{L}_{\text{eff}}(\varphi_\ell)\right\} . \quad (3.11)$$

After that, it is clear that the \mathcal{L}_{eff} in (3.10) is a function of the solely light states φ_ℓ , and that the $c_d \equiv c_d(\mu)$ are the Wilson coefficients describing the dynamics of the heavy fields.

In the following section we will illustrate the procedure of MATCHING to the effective and full theory results, taking as example a Yukawa theory involving two scalar states, and more precisely an heavy and a light one.

1. In section 3.2.1 we introduce the spinor/mesons interaction model and proceed to show how the tree-level matching procedure is performed. In particular we consider the 8-dimensional EFT resulting after the integration out of the heavy scalar.
2. In section 3.2.2 we consider 1-loop corrections in the EFT. We show how these contributions affect the Wilson coefficients by renormalisation group running.
3. In section 3.2.3 we illustrate the process of matching to the 1-loop order. We start from a simplified full theory with a single heavy scalar, proceeding to match in the corresponding 6-dimensional EFT.
4. Finally, in section 3.2.4 we consider the same model of 3.2.3. We still perform 1-loop matching calculation, this time considering the fermion as the heavy degree of freedom.

²The dividing line between light and heavy states is based on whenever or not the particles can be produced on shell at the available energy.

³ ℓ is for light, h is for heavy.

3.2.1 Mathematical formulation and tree-level matching

Let \mathcal{L} be a Yukawa-like Lagrangian with two different scalar fields carrying and exchanging interactions with a matter field. In the following, without arguing about Hierarchy problems, we assume

- φ_ℓ a light scalar field of mass m ,
- φ_h a heavy scalar field of mass M ,

so that $M \gg m$.

For the sake of simplicity, we do not consider quartic interactions (and self-interactions) among scalars. So, the full theory Lagrangian reads:

$$\begin{aligned} \mathcal{L}_{\text{full}} = & i\bar{\psi}\not{\partial}\psi + \frac{1}{2}\partial^\mu\varphi_\ell\partial_\mu\varphi_\ell - \frac{m^2}{2}\varphi_\ell^2 \\ & + \frac{1}{2}\partial^\mu\varphi_h\partial_\mu\varphi_h - \frac{M^2}{2}\varphi_h^2 - \lambda\bar{\psi}\psi\varphi_h - \eta\bar{\psi}\psi\varphi_\ell. \end{aligned} \quad (3.12)$$

In ordinary (and so in effective) field theory, the S-Matrix, or scattering operator, is defined by the relation

$$S = \mathcal{T} \exp\left\{-\frac{i}{\hbar} \int_{-\infty}^{+\infty} dt V_{\text{int}}(t)\right\}, \quad (3.13)$$

where $V_{\text{int}}(t)$ is the potential in the INTERACTION PICTURE, in which the time evolution is completely determined by the free part H_0 of the complete, self-adjoint, Hamiltonian $H = H_0 + V$ of the quantum-mechanical system [1].

We would now like to match to the EFT where the heavy scalar has been integrated out. To reach this goal we consider the diagrams in 3.2, where only heavy scalars are considered as intermediate states. The only non zero S-matrix element for the corresponding scattering process is given by

$$\begin{aligned} S &= \mathbb{I} - i\lambda \int dx \left\{ \varphi_h(x)\bar{\psi}(x)\psi(x) \right\} \\ &\quad - \lambda^2 \int dx \int dy \mathcal{T} \left\{ \varphi_h(x)\bar{\psi}(x)\psi(x)\varphi_h(y)\bar{\psi}(y)\psi(y) \right\} + \dots \end{aligned} \quad (3.14)$$

Owing to the Wick Theorem, it turns out that the only non-zero S-Matrix element for the $\psi\psi \rightarrow \psi\psi$ scattering process in 3.2, is given by

$$\begin{aligned} \mathcal{A}_{\text{full}} &= (-i\lambda)^2 \langle 0 | a(p_3)a(p_4) : \bar{\psi}_3^{(+)}\psi_y^{(-)}\bar{\psi}_x^{(+)}\psi_y^{(-)} : a^\dagger(p_1)a^\dagger(p_2) | 0 \rangle \mathcal{D}_{xy} \\ &= (-i\lambda)^2 \underbrace{a(p_3)\bar{\psi}_y}_{\bar{u}(p_3)} \underbrace{\psi_y a^\dagger(p_4)}_{u(p_1)} \mathcal{D}_{xy} \underbrace{a(p_4)\bar{\psi}_x}_{\bar{u}(p_4)} \underbrace{\psi_x a^\dagger(p_2)}_{u(p_2)} \\ &= \bar{u}_3 u_1 \bar{u}_4 u_2 (-i\lambda)^2 \frac{i}{(p_3 - p_1)^2 - M^2} - 3 \leftrightarrow 4, \end{aligned} \quad (3.15)$$

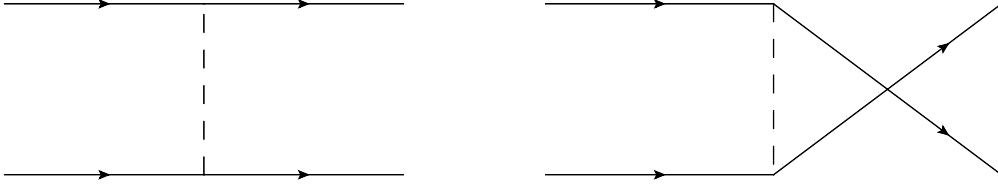


Figure 3.2: Tree-level diagrams for $\psi\psi$ scattering. The continuous lines with arrows are for the fermions, while the dashed lines for the heavy scalars. We maintain this convention till the end of this section if it is not specified differently.

where u_i indicates the spin state $u(p_i)$ and where in the last term on the r.h.s. we took into account the impulse interchange between 3 and 4.

The whole point here is that this contribution can be generated into the correspondent effective field theory.

As said, the idea behind is to include only the light degrees of freedom into a new Lagrangian. This is made by taking into account the residual interactions between light and heavy fields, which in the EFT are manifested as higher-dimensional/non-renormalisable interactions between the solely light fields.

Doing so, we understand the Yukawa interaction between the fermion and the heavy scalar to generate the (zero order momenta) Lagrangian

$$\mathcal{L}_{\text{eff}} = i\bar{\psi}\not{\partial}\psi + \frac{c}{2}\bar{\psi}\psi\bar{\psi}\psi. \quad (3.16)$$

We can reproduce the scattering amplitude we calculated in the full theory by considering the tree level diagram in 3.3.

We have

$$\mathcal{A}_{\text{eff}} = \bar{u}_3 u_1 \bar{u}_4 u_2 (ic) - 3 \leftrightarrow 4. \quad (3.17)$$

As can be easily seen, the Dirac structure of the theory is identical both on the full and the effective sides, so we can proceed by focusing on the bosonic structure.

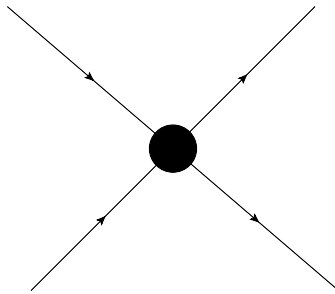


Figure 3.3: Tree-level diagram for EFT $\psi\psi\psi\psi$ scattering.

In the full theory it is possible to approximate the Klein-Gordon propagator in equa-

tion (3.15) according to

$$\begin{aligned}
A_{\text{full}} &\sim (-i\lambda)^2 \frac{i}{(p_3 - p_1)^2 - M^2} = \frac{-i\lambda^2}{M^2} \left[\frac{1}{\left(\frac{p_3 - p_1}{M}\right)^2 - 1} \right] \\
&\simeq \frac{i\lambda^2}{M^2} \left[1 + \left(\frac{p_3 - p_1}{M}\right)^2 + \mathcal{O}(p^4/M^4) \right]. \quad (3.18)
\end{aligned}$$

So, comparing this expansion to the amplitude in (3.17), the straightforward guess is $c = \frac{\lambda^2}{M^2}$.

A Dirac spinor field carries engineering dimensions in natural units of $[E]^{3/2}$. This means that a 4-spinor interacting term such as the one in (3.16) necessarily requires a squared energy-inverse coupling constant to get the action dimensionless, which is exactly what we obtained in the matching procedure.

Moving to the next order in momentum expansion we get another 4-spinor interaction defined in the Lagrangian

$$\mathcal{L}_{\text{eff}_2} = i\bar{\psi}\not{\partial}\psi + \frac{\lambda^2}{2M^2}\bar{\psi}\psi\bar{\psi}\psi + d\partial_\mu\bar{\psi}\partial^\mu\psi\bar{\psi}\psi. \quad (3.19)$$

We calculate the corresponding amplitude, proceeding then to match to the 1-st momentum dependent term of the full theory amplitude.

It is helpful to remind that, comparing full and effective theories, we can choose the external momenta to be either on or off shell. In this example is easier to put the momenta on shell, so that the amplitude follows to be dependent only by mixed momenta contributions.

In fact, if

$$p_i^2 = 0 \quad (i = 1, \dots, 4),$$

then

$$\mathcal{A}_{\text{full}} \simeq i\frac{\lambda^2}{M^2} \left(1 - 2\frac{p_1 \cdot p_3}{M^2} + \mathcal{O}((p_1 \cdot p_3/M)^4) \right) - 3 \leftrightarrow 4. \quad (3.20)$$

On the effective side, the 4-fermions d-coupled term corresponds to the amplitude

$$\mathcal{A}_{\text{eff}_2} = (id)\bar{u}_3u_1\bar{u}_4u_2(p_3 \cdot p_1 + p_2 \cdot p_4) - 3 \leftrightarrow 4. \quad (3.21)$$

As the momentum conservation implies

$$p_1 \cdot p_2 = p_3 \cdot p_4, \quad p_1 \cdot p_3 = p_2 \cdot p_4, \quad p_1 \cdot p_4 = p_2 \cdot p_3, \quad (3.22)$$

we obtain $d = -(\lambda^2/M^4)$. This time we see an $\sim 1/M^4$ behavior, as the momentum dependent term is 8-dimensional.

The d-coupled operator we introduced in $\mathcal{L}_{\text{eff}_2}$ is not the only one possible with same dimension and momenta structure. In principle, we also have the operators

$$(\partial^2\bar{\psi})\psi\bar{\psi}\psi + \text{h.c.}, \quad \partial_\mu\bar{\psi}\psi\bar{\psi}\partial^\mu\psi. \quad (3.23)$$

It is possible to show [17] that ∂^2 terms are vanishing in the EFT owing to the fermion equations of motion. For this reason, we have the following relation between the remaining derivative terms

$$\partial^\mu \bar{\psi} \psi \bar{\psi} \partial_\mu \psi + \bar{\psi} \partial^\mu \psi \bar{\psi} \partial_\mu \psi + \bar{\psi} \psi \partial^\mu \bar{\psi} \partial_\mu \psi = 0 \quad (3.24)$$

Moreover, we also mention that it would be possible to introduce the 6-dimensional operator

$$\bar{\psi} \gamma^\mu \psi \bar{\psi} \gamma_\mu \psi . \quad (3.25)$$

In effective field theory it is in principle necessary to consider all these non-equivalent operators (up to the fixed dimension considered).

Anyhow, as our principal goal here is to illustrate the main features involving EFT techniques, we will not include these operators in the description.

3.2.2 1-loop corrections and renormalisation group running

After this first example, we consider the whole effective theory picture resulting by integrating out the heavy field to the 1-loop level, focusing on how RG evolution plays a role here.

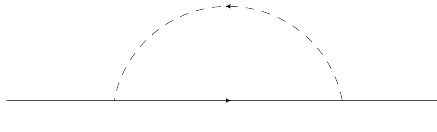
The up-to-dimension-8 effective theory Lagrangian \mathcal{L} which we will now consider is

$$\begin{aligned} \mathcal{L}_{\text{eff}_3} &= i\bar{\psi} \not{\partial} \psi + \frac{c}{2} \bar{\psi} \psi \bar{\psi} \psi + d \partial^\mu \bar{\psi} \partial_\mu \psi \bar{\psi} \psi \\ &+ \frac{1}{2} \partial^\mu \varphi_\ell \partial_\mu \varphi_\ell - \frac{m^2}{2} \varphi_\ell^2 - \eta \bar{\psi} \psi \varphi_\ell , \end{aligned} \quad (3.26)$$

with the matched parameters being

$$c = \frac{\lambda^2}{M^2} \quad , \quad d = -\frac{\lambda^2}{M^4} . \quad (3.27)$$

Our next goal will be to calculate the $\bar{\psi} \psi \rightarrow \bar{\psi} \psi$ scattering amplitude to the 1-loop order in the effective theory. We start by calculating the self-energy Σ_{eft} of the fermion. We have



$$= (-i\eta)^2 \int \frac{d^d k}{(2\pi)^d} \frac{i(\not{k} + \not{p})}{(k+p)^2} \frac{i}{k^2 - m^2} . \quad (3.28)$$

For this kind of integral is it possible to use the FEYNMAN FORMULA, which in the present case reduces to [19]

$$\frac{1}{A_1 \cdot A_2} = \int_0^1 \frac{dx}{(xA_1 + (1-x)A_2)^2} , \quad (3.29)$$

so that, with the substitution $\ell = k + xp$, the fermion self-energy follows as

$$\Sigma_{\text{eft}}(p, \eta) = \eta^2 \int_0^1 dx \int \frac{d^d \ell}{(2\pi)^d} \frac{\ell + (1-x)\not{p}}{x^2 \left(\ell^2 - \underbrace{(1-x)(p^2 - m^2)}_{\Delta^2} \right)^2}. \quad (3.30)$$

We choose to keep the singular contributions to this integral. In fact, the finite terms do not contribute to the RENORMALISATION GROUP (RG) calculations to which we are interested. For this reason, we proceed considering the second term on the right hand side.

Solving, we obtain

$$\begin{aligned} \Sigma_{\text{eft}}(\eta, p) &= \int_0^1 dx \int \frac{d^d \ell}{(2\pi)^d} \eta^2 \frac{(1-x)\not{p}}{(\ell^2 - \Delta^2)} \\ &= \int_0^1 dx \left(\frac{\eta}{4\pi} \right)^2 \left(\frac{1}{\epsilon} + \ln \frac{4\pi m^2}{\Delta^2} \right) (1-x)\not{p} + \mathcal{O}(\epsilon), \end{aligned} \quad (3.31)$$

and so

$$\Sigma_{\text{eft}}(\eta, p) = \frac{1}{\epsilon} \frac{\eta^2}{16\pi^2} \int_0^1 dx (1-x)\not{p} + \text{finite} = \frac{i\eta^2 \not{p}}{32\pi^2 \epsilon} + \text{finite}. \quad (3.32)$$

This concludes our analysis to the kinetic contribution.

Then, we may proceed with the 1-loop correction to the 4-fermions vertexes, which are shown in figure 3.4. Owing to the UV divergent nature of these diagrams, it is possible to neglect the external momenta and masses, still if we are interested to the solely divergent parts.

Realising that every top/bottom pair in figure 3.4 makes the same contribution to the scattering amplitude, we may proceed by just multiplying by 2 each topology.

The calculation follows as

$$\begin{aligned} (A_1 + A_2)_{\text{eft}} &= 2 \cdot 2\eta^2 c \int \frac{d^d k}{(2\pi)^d} \frac{k^2}{k^6} = -2\eta^2 c \gamma^\mu \gamma^\nu \int \frac{d^d k}{(2\pi)^d} \frac{k_\mu k_\nu}{k^6} \\ &= -2\eta^2 c \int \frac{d^d k}{(2\pi)^d} \frac{1}{k^4} = -\frac{2\eta^2 c}{16\pi^2 \epsilon} + \text{finite}; \end{aligned} \quad (3.33)$$

$$\begin{aligned} (B_1 + B_2)_{\text{eft}} &= 2 \cdot \eta^2 c \left(\int \frac{d^d k}{(2\pi)^d} \frac{k_\mu k_\nu}{k^6} \right) \cdot \bar{u}_3 \gamma^\mu u_1 \bar{u}_4 \gamma^\nu u_2 \\ &= \frac{2i\eta^2 c}{4(4\pi)^2 \epsilon} \cdot \bar{u}_3 \gamma^\mu u_1 \bar{u}_4 \gamma_\mu u_2 + \text{finite}; \end{aligned} \quad (3.34)$$

$$\begin{aligned}
(C_1 + C_2)_{\text{eft}} &= -2 \cdot \eta^2 c \left(\int \frac{d^d k}{(2\pi)^d} \frac{k_\mu k_\nu}{k^6} \right) \cdot \bar{u}_3 \gamma^\mu u_1 \bar{u}_4 \gamma^\nu u_2 \\
&= -\frac{2i\eta^2 c}{4(4\pi)^2} \frac{1}{\epsilon} \cdot \bar{u}_3 \gamma^\mu u_1 \bar{u}_4 \gamma_\mu u_2 + \text{finite} .
\end{aligned} \tag{3.35}$$

Eventually, these contributions add up to

$$(A_1 + A_2 + B_1 + B_2 + C_1 + C_3)_{\text{eft}} = -\frac{2\eta^2 c}{16\pi^2} \frac{i}{\epsilon} + \text{finite} , \tag{3.36}$$

which coincide with $A_1 + A_2$. In fact, the B and the C topologies are canceling each other owing to the opposite momentum directions.

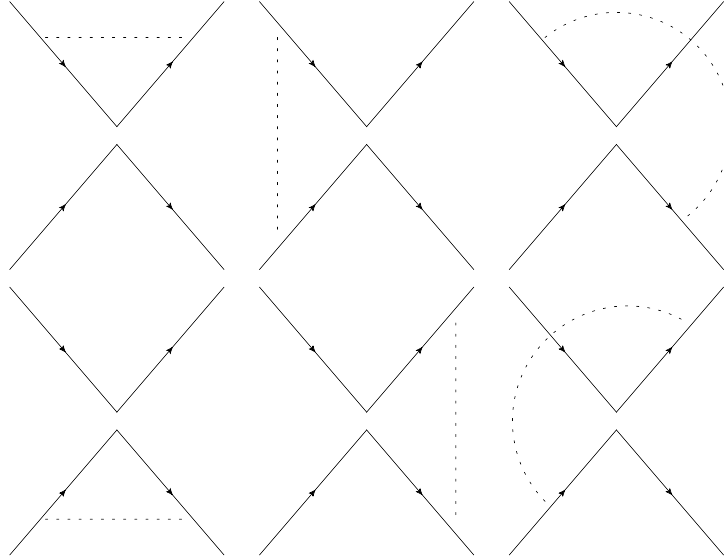


Figure 3.4: 1-loop contributions to the 4-fermions interaction vertex. The interaction is still point-like, but the fermion flow through the vertex is emphasised. We will refer to these diagrams as $(A, B, C)_{\text{eft}}$ with the suffix 1,2 indicating respectively the first and the second row.

We now introduce the bare and dressed parameters and fields in order to define the 1-loop renormalised Lagrangian. We can think of the original Lagrangian as being expressed in terms of the bare fields and bare coupling constants, and rescale

$$\psi_0 = \sqrt{Z_\psi} \psi , \quad c_0 = c \mu^{2\epsilon} Z_c , \quad \eta_0 = \eta \mu^\epsilon Z_\eta . \tag{3.37}$$

This choice on the couplings is made in order to keep fixed the dimensions in an arbitrary $d = 4 - 2\epsilon$ space-time.

The 1-loop renormalised Lagrangian reads

$$\begin{aligned} \mathcal{L}_{\text{eff,R}} &= i\bar{\psi}\not{\partial}\psi + \mu^{2\epsilon}\frac{c}{2}\bar{\psi}\psi\bar{\psi}\psi - \mu^\epsilon\eta\bar{\psi}\psi\varphi_\ell + i(Z_\psi - 1)\bar{\psi}\not{\partial}\psi \\ &+ \mu^{2\epsilon}\frac{c}{2}(Z_c Z_\psi^2 - 1)\bar{\psi}\psi\bar{\psi}\psi - \mu^\epsilon\eta(Z_\eta Z_\psi - 1)\bar{\psi}\psi\varphi_\ell , \end{aligned} \quad (3.38)$$

where the counter terms in can actually be identified as

$$Z_\psi - 1 = -\frac{\eta^2}{2(4\pi)^2}\frac{1}{\epsilon} \quad ; \quad c(Z_c Z_\psi^2 - 1) = \frac{2c\eta^2}{(4\pi)^2}\frac{1}{\epsilon} . \quad (3.39)$$

So, we easily get:

$$Z_\psi = 1 - \frac{\eta^2}{2(4\pi)^2}\frac{1}{\epsilon} , \quad (3.40)$$

$$\begin{aligned} Z_c &= \left(1 + \frac{2\eta^2}{(4\pi)^2}\frac{1}{\epsilon}\right) \cdot \left(1 - \frac{\eta^2}{2(4\pi)^2}\frac{1}{\epsilon}\right)^{-2} \\ &= \left(1 + \frac{2\eta^2}{(4\pi)^2}\frac{1}{\epsilon}\right) \cdot \left(1 + \frac{\eta^2}{(4\pi)^2}\frac{1}{\epsilon} + \mathcal{O}(1/\epsilon^2)\right) \\ &= 1 + \frac{3\eta^2}{(4\pi)^2}\frac{1}{\epsilon} + \mathcal{O}(1/\epsilon^2) . \end{aligned} \quad (3.41)$$

The standard way to calculate the RENORMALISATION GROUP EQUATIONS (RGEs) is to exploit the fact that the bare quantities do not depend on the renormalisation scale. So, considering the Lagrangian (3.38), we have

$$\mu\frac{d}{d\mu}(c\mu^{2\epsilon}Z_c) = \left(\beta_c Z_c + 2\epsilon c Z_c + c\frac{dZ_c}{d\log\mu}\right)\mu^{2\epsilon} = 0 \quad (3.42)$$

$$\frac{d\log Z_c}{d\log\mu} = -c^{-1}\beta_c - 2\epsilon \quad , \quad (3.43)$$

where the $\beta_c = \mu\frac{d}{d\mu}c$ function has been introduced.

Following the same argument, it is easy to get the β_η function from the renormalised η coupling,

$$\mu\frac{d}{d\mu}(\mu^\epsilon\eta Z_\eta) = \left(\epsilon\mu^\epsilon\eta Z_\eta + \mu^\epsilon\beta_\eta Z_\eta + \mu^\epsilon\eta\frac{dZ_\eta}{d\log\mu}\right) = 0 , \quad (3.44)$$

which implies

$$\beta_\eta = -\eta\frac{d\log Z_\eta}{d\log\mu} - \epsilon\eta . \quad (3.45)$$

Now, we know that

$$\frac{dZ_c}{d\log\mu} = \mu\frac{d}{d\mu}\left(1 + \frac{3\eta^2}{(4\pi)^2}\frac{1}{\epsilon}\right) = \frac{6\eta}{(4\pi)^2}\frac{\beta_\eta}{\epsilon} . \quad (3.46)$$

As the derivative of $\log Z_\eta$ term would give rise to an higher-order term in η , we choose to retain only $\epsilon\eta$ term in the β_η expansion in (3.45). It follows

$$\mu \frac{d}{d\mu} Z_c = -\frac{6\eta^2}{(4\pi)^2} \rightarrow \beta_c = \frac{6\eta^2}{(4\pi)^2} c, \quad (3.47)$$

$$c(m) = \frac{\lambda^2}{M^2} \left(1 - \frac{6\eta^2}{(4\pi)^2} \log \frac{M}{m} \right). \quad (3.48)$$

Then, it is possible to show that calculating the running of β_η we obtain

$$\beta_\eta = \frac{5\eta^3}{(4\pi)^2}, \quad (3.49)$$

and so

$$\mu \frac{d\eta}{d\mu} = \frac{5\eta^3}{(4\pi)^2} \quad (3.50)$$

$$\frac{d\eta}{\eta^3} = \frac{5}{(4\pi)^2} \frac{d\mu}{\mu} \quad (3.51)$$

$$-\frac{1}{2} \frac{1}{\eta^2} \Big|_{\mu_2}^{\mu_1} = \frac{5}{(4\pi)^2} \log \mu \Big|_{\mu_2}^{\mu_1} \quad (3.52)$$

$$\frac{1}{\eta^2(\mu_2)} - \frac{1}{\eta^2(\mu_1)} = \frac{10}{(4\pi)^2} \log \frac{\mu_1}{\mu_2}. \quad (3.53)$$

Substituting this behavior into the definition of β_η , we have

$$\mu \frac{dc}{d\mu} = \frac{6\eta^2}{(4\pi)^2} c, \quad \frac{dc}{c} = \frac{6\eta^2}{(4\pi)^2} d \log \mu \quad (3.54)$$

$$\frac{dc}{c} = -\frac{6}{10} \eta^2 d \left(\frac{1}{\eta^2} \right), \quad \int_m^M \frac{dc}{c} = \frac{3}{5} \int_m^M 2 \frac{d\eta}{\eta} \quad (3.55)$$

$$c(m) = c(M) \left(\frac{\eta^2(m)}{\eta^2(M)} \right)^{3/5}. \quad (3.56)$$

The important point to remark is that the Yukawa interaction $\eta \bar{\psi} \psi \varphi_\ell$ receives corrections from both the light and heavy scalar fields. Also, the lack of renormalisability never played any role in the previous calculations.

3.2.3 1-loop matching

We will now illustrate the process of matching to the 1-loop order in perturbation theory.

We take the full theory Lagrangian in (3.2), considering only the heavy scalar, and the effective theory in (3.3). We also consider a small σ mass for the fermion, in order to avoid possible infrared divergences in the loop integrals.

With these positions, the full theory Lagrangian now reads

$$\mathcal{L}_{\text{full}} = i \bar{\psi} \not{\partial} \psi - \sigma \bar{\psi} \psi + \frac{1}{2} \partial^\mu \varphi_h \partial_\mu \varphi_h - \frac{M^2}{2} \varphi_h^2 - \lambda \bar{\psi} \psi \varphi_h, \quad (3.57)$$

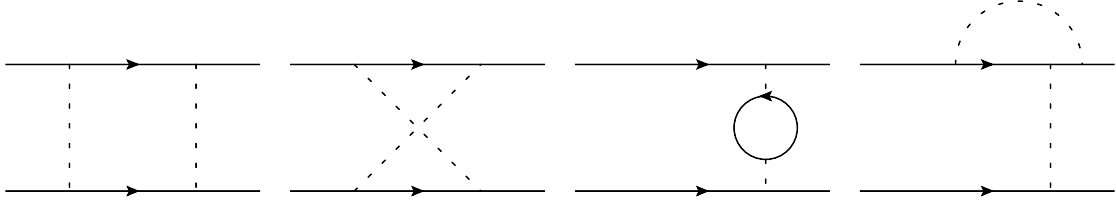


Figure 3.5: Full theory diagrams from the Lagrangian in (3.57). We will refer to them as a,b,c,d , from left to right.

with the corresponding Feynman diagrams illustrated in figure 3.5.

We then proceed with the evaluation. By using the Feynman parametric formula, and introducing

$$U_V = -\bar{u}_3 \gamma^\mu u_1 \bar{u}_4 \gamma^\nu u_2 \quad , \quad U_S = \bar{u}_3 u_1 \bar{u}_4 u_2 \quad , \quad (3.58)$$

we have

$$\begin{aligned}
(a) &= (-i\lambda)^4 \int \frac{d^d k}{(2\pi)^d} \bar{u}_3 \frac{i(\not{k} + \sigma)}{k^2 - \sigma^2} u_1 \frac{i^2}{(k^2 - M^2)^2} \bar{u}_4 \frac{i(-\not{k} + \sigma)}{k^2 - \sigma^2} u_2 \\
&= \lambda^2 \left\{ - \underbrace{\bar{u}_3 \gamma^\mu u_1 \bar{u}_4 \gamma^\nu u_2}_{U_V} \int \frac{d^d k}{(2\pi)^d} \frac{k_\mu k_\nu}{(k^2 - \sigma^2)^2 (k^2 - M^2)^2} \right. \\
&\quad \left. + \underbrace{\bar{u}_3 u_1 \bar{u}_4 u_2}_{U_S} \int \frac{d^d k}{(2\pi)^d} \frac{\sigma^2}{(k^2 - \sigma^2)^2 (k^2 - M^2)^2} \right\} \quad (3.59) \\
&= \frac{i\lambda^4}{(4\pi)^2} \left\{ \frac{U_V}{2} \int_0^1 dx \frac{x(1-x)}{xM^2 + (1-x)\sigma^2} \right. \\
&\quad \left. + \sigma^2 U_S \int_0^1 dx \frac{x(1-x)}{(xM^2 + (1-x)\sigma^2)^2} \right\} .
\end{aligned}$$

Evaluating the integrals as

$$\begin{aligned}
\int_0^1 dx \frac{x(1-x)}{xM^2 + (1-x)\sigma^2} &= \frac{(M^2 + \sigma^2) \log(M^2) - (M^2 + \sigma^2) \log(\sigma^2) - 2M^2 + 2\sigma^2}{(M^2 - \sigma^2)^3} \\
\int_0^1 dx \frac{x(1-x)}{(xM^2 + (1-x)\sigma^2)^2} &= \frac{2M^2\sigma^2 \log \sigma^2 + (M^2 + \sigma^2)(M^2 - \sigma^2) - 2M^2\sigma^2 \log M^2}{2(M^2 - \sigma^2)^3}
\end{aligned}$$

and Taylor expanding for $\sigma \rightarrow 0$, we obtain

$$(a) = \frac{i\lambda^4}{(4\pi)^2} \left(U_V \left(\frac{1}{4M^2} + \frac{\sigma^2}{4M^2} \left(3 - 2 \log \frac{M^2}{\sigma^2} \right) \right) + U_S \frac{\sigma^2}{M^2} \left(\log \frac{M^2}{\sigma^2} - 2 \right) \right) . \quad (3.60)$$

This result can be extended to the (b) diagram, inverting the sign of the momentum in one of the fermion propagators.

Doing so, we get

$$(b) = \frac{i\lambda^4}{(4\pi)^2} \left(-U_V \left(\frac{1}{4M^2} + \frac{\sigma^2}{4M^2} \left(3 - 2 \log \frac{M^2}{\sigma^2} \right) \right) + U_S \frac{\sigma^2}{M^2} \left(\log \frac{M^2}{\sigma^2} - 2 \right) \right), \quad (3.61)$$

and in the same way, we can calculate the divergent diagrams

$$(c) = -4 \frac{i\lambda^4}{(4\pi)^2} U_S \left(\frac{3}{\epsilon} + 3 \log \frac{\mu^2}{\sigma^2} + 1 \right) + \dots \quad (3.62)$$

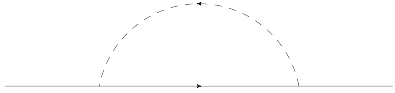
and

$$(d) = -2 \frac{i\lambda^4}{(4\pi)^2 M^2} U_S \left(\frac{1}{\epsilon} + 1 + \log \frac{\mu^2}{M^2} + \frac{\sigma^2}{M^2} \left(2 - 3 \log \frac{M^2}{\sigma^2} \right) \right) + \dots \quad (3.63)$$

Then, the sum of all of these contributions is

$$(a + \dots + d) = \frac{2i\lambda^4 U_S}{(4\pi)^2 M^2} \left(-\frac{1}{\epsilon} - 1 - \log \frac{\mu^2}{M^2} + \frac{\sigma^2}{M^2} \left(-\frac{6}{\epsilon} - 6 \log \frac{\mu^2}{\sigma^2} - 6 + 4 \log \frac{M^2}{\sigma^2} \right) \right). \quad (3.64)$$

Moreover, it is straightforward to calculate the fermion self-energy $\Sigma_{\text{full}_2}(p, M)$ contribution of the heavy scalar to the 1-loop level. We have



$$\begin{aligned} &= (-i\lambda)^2 \int \frac{d^d k}{(2\pi)^d} \frac{i(\not{k} + \not{p} + \sigma)}{(k+p)^2 - \sigma^2} \frac{i}{k^2 - M^2} \\ &= \lambda^2 \int_0^1 dx \int \frac{d^d \ell}{(2\pi)^d} \frac{\not{\ell} + (1-x)\not{p} + \sigma}{x^2(\ell^2 - \Delta^2)^2} \\ &= i\not{p} \frac{\lambda^2}{2(4\pi)^2} \left(\frac{1}{\epsilon} + \log \frac{\mu^2}{M^2} + \frac{1}{2} + \dots \right) = \Sigma_{\text{full}_2}, \end{aligned} \quad (3.65)$$

where we proceeded following the steps of the equation (3.28).

Now, we consider the effective Lagrangian

$$\mathcal{L}_{\text{eff}_4} = iz\bar{\psi}\not{\partial}\psi - \sigma\bar{\psi}\psi + \frac{c}{2}\bar{\psi}\psi\bar{\psi}\psi \quad (3.66)$$

and calculate the scattering amplitude related to the ones we calculated in the full theory.

The self-energy vanishes in this EFT, so we can proceed by evaluating the 4-fermion amplitudes.

Considering the diagrams in figure 3.6, we have

$$\begin{aligned} (a)_{\text{eft}} &= \frac{c^2}{4} \int \frac{d^d k}{(2\pi)^d} \frac{\bar{u}_3 i(\not{k} + \sigma) u_1 \bar{u}_4 i(\not{k} + \sigma) u_2}{(k^2 - \sigma^2)^2} \\ &= c^2 \int \frac{d^d k}{(2\pi)^d} \frac{U_V k^2 + U_S \sigma^2}{(k^2 - \sigma^2)^2}, \end{aligned} \quad (3.67)$$

from which we can easily isolate the divergent contribution to the σ^2 term on the r.h.s. as

$$(a)_{\text{eft}} = \frac{ic^2 U_S}{(4\pi)^2} \left(\frac{1}{\bar{\epsilon}} + \log \frac{\mu^2}{\sigma^2} \right) + \dots \quad (3.68)$$

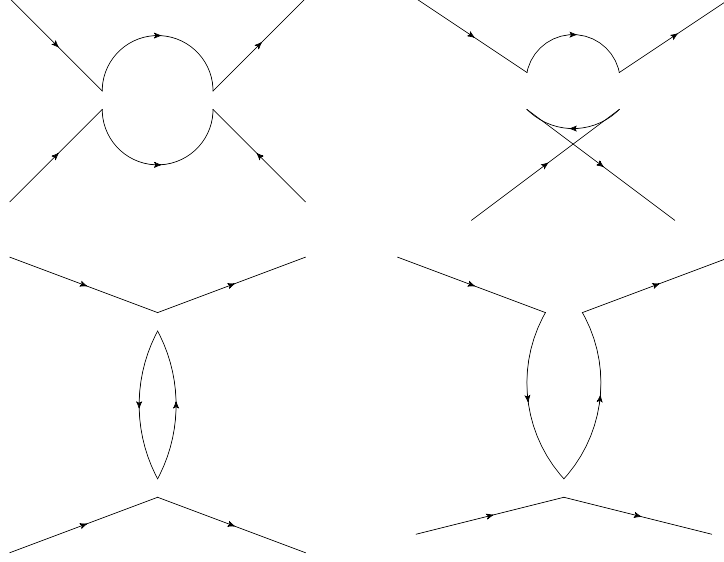


Figure 3.6: 1-loop diagrams to the c^2 order from the effective Lagrangian in (3.66). We will refer to them as $(a, b, c, d)_{\text{eft}}$, from left to right, starting from the upper row.

Then, the calculation for the (b) diagram is essentially the same. We have

$$(a + b)_{\text{eft}} = 2 \frac{ic^2 U_S}{(4\pi)^2} \left(\frac{1}{\bar{\epsilon}} + \log \frac{\mu^2}{\sigma^2} \right) + \dots, \quad (3.69)$$

where we took into account the fact that, owing to the opposite directions of the momenta flow, the U_V part of the diagrams vanish in the sum.

The same way it is possible to calculate

$$(c)_{\text{eft}} = -4 \frac{ic^2 \sigma^2}{(4\pi)^2} U_S \left(\frac{3}{\bar{\epsilon}} + 3 \log \frac{\mu^2}{\sigma^2} + 1 \right), \quad (3.70)$$

$$(d)_{\text{eft}} = 2 \frac{ic^2 \sigma^2}{(4\pi)^2} U_S \left(\frac{3}{\bar{\epsilon}} + 3 \log \frac{\mu^2}{\sigma^2} + 1 \right). \quad (3.71)$$

So that

$$\begin{aligned} (a + \dots d)_{\text{eft}} &= -\frac{2ic^2 \sigma^2}{(4\pi)^2} U_S \left(\frac{2}{\bar{\epsilon}} + 2 \log \frac{\mu^2}{\sigma^2} + 1 \right) \\ &= -\frac{2i\lambda^4 \sigma^2}{(4\pi)^2 M^4} U_S \left(\frac{2}{\bar{\epsilon}} + 2 \log \frac{\mu^2}{\sigma^2} + 1 \right). \end{aligned} \quad (3.72)$$

Notice that the degree of divergence of these EFT diagram is higher than the FT ones. For example, the (a) diagram of figure 3.6 is quadratically divergent, while the (a) diagram in figure 3.5 is finite.

The only scale which appears in last expansion is contained inside the logarithm. On the other side, taking a look to the full theory results , we easily see that multiple scales are involved. In fact, we find

$$\log \frac{\mu^2}{M^2} , \log \frac{M^2}{\sigma^2} , \log \frac{\mu^2}{\sigma^2} \quad (3.73)$$

terms.

Now, taking into account that the coefficients in the front of the $\log \sigma^2$ terms are identical both in the effective and in the full theory sides, we understand this scale to be the so called MATCHING SCALE.

In other words, we switched to an effective low-energy theory which **must** look identical to the IR behavior of the full theory, and we found back the fact that non-analytic terms involving only the light degrees of freedom are identical.

Taking the difference between the full and the effective results, evaluated on $\mu = M$, we are able to identify the 1-loop corrections to the tree-level $c = \lambda^2/M^2$ coefficient. Using the \overline{MS} subtraction scheme, we have

$$c(\mu = M) = \frac{\lambda^2}{M^2} - \frac{2\lambda^4}{M^2(4\pi)^2} - \frac{10\lambda^4\sigma^2}{M^4(4\pi)^2} . \quad (3.74)$$

Definitely, as the EFT fermion self energy vanishes, we simply identify

$$z = 1 + \frac{\lambda^2}{4(4\pi)^2} , \quad (3.75)$$

from (3.65), exploiting the \overline{MS} -scheme.

The EFT Lagrangian now reads

$$\mathcal{L}_{\text{eff}_{4,R}} = i \left(1 + \frac{\lambda^2}{4(4\pi)^2} \right) \bar{\psi} \not{\partial} \psi - \sigma \bar{\psi} \psi + \frac{1}{2} \left(\frac{\lambda^2}{M^2} - \frac{2\lambda^2}{M^2(4\pi)^2} - \frac{10\lambda^4\sigma^2}{M^4(4\pi)^2} \right) \bar{\psi} \psi \bar{\psi} \psi . \quad (3.76)$$

Finally, the physical scattering amplitude are obtained after the rescaling

$$\sqrt{z} \psi \rightarrow \psi_{\text{canonical}} . \quad (3.77)$$

This gives an additional contribution to the λ^4 term in equation (3.74), which is not obvious to consider at this level.

In fact, other 4-fermions interaction, say the d-coupled interaction vertex in (3.26), can contribute to this λ^4 order in the renormalisation group running, eventually generating the same contribution.

Anyhow, we will not argue about this eventuality for now.

3.2.4 Heavy fermion/light Scalar: Sketch of The calculations

This last subsection is reserved to the case in which the fermion is the heavy field to integrate out. We also choose to consider just a single scalar field φ .

The full theory Lagrangian reads

$$\mathcal{L}_{\text{full}_3} = i\bar{\psi}\not{\partial}\psi - M\bar{\psi}\psi - \frac{1}{2}\partial^\mu\varphi\partial_\mu\varphi - \frac{m^2}{2}\varphi^2 - \eta\bar{\psi}\psi\varphi, \quad (3.78)$$

with $M \gg m$.

No diagrams with internal fermion line are present to the tree-level, so we have to consider 1-loop diagrams. Getting started with the φ self-energy diagram in figure 3.7, we find

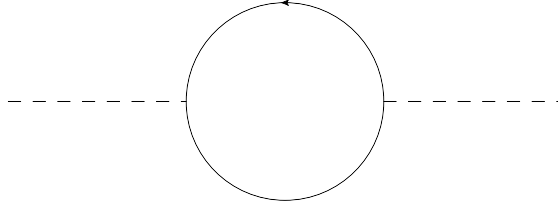


Figure 3.7: 1-loop self-energy diagram for φ .

$$\begin{aligned} \Sigma(p, M, \eta) &= (-1)(i\eta\mu^\epsilon)^2 \int \frac{d^d k}{(2\pi)^d} i^2 \frac{(\not{k} + \not{p} + M)(\not{k} + M)}{((k+p)^2 - M^2)(k^2 - M^2)} \\ &= -4\eta^2 \mu^{2\epsilon} \int \frac{d^d k}{(2\pi)^d} \frac{k^2 + kp + M^2}{(x((k+p)^2 - M^2) + (1-x)(k^2 - M^2))^2} \\ &= -4\eta^2 \mu^{2\epsilon} \int_0^1 dx \int \frac{d^d \ell}{(2\pi)^d} \frac{\ell^2 + p^2(x-1)x + M^2 + \overbrace{\ell(1-2x)p}^{\text{odd}}}{(\ell^2 - M^2)^2} \\ &= -\frac{4i\eta^2}{(4\pi)^2} \left[\left(\frac{3}{\epsilon} + 1 + 3 \log \frac{\mu^2}{M^2} \right) \left(M^2 - \frac{p^2}{6} - \frac{p^4}{20M^4} + \dots \right) \right]. \quad (3.79) \end{aligned}$$

Then, it is possible to show that the 1-loop correction in figure 3.8 can be evaluated as

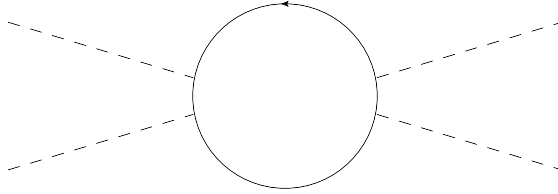


Figure 3.8: 1-loop 4-points amplitude.

$$\mathcal{Y}(M, \eta, k_i) = -1(-i\eta\mu^\epsilon)^4 \int \frac{d^d\ell}{(2\pi)^d} \frac{i(\ell + M)}{\ell^2 - M^2} \cdot \frac{i(\ell - k_1 + M)}{(\ell - k_1)^2 - M^2} \quad (3.80)$$

$$\begin{aligned} & \cdot \frac{i(\ell + k_2 + k_3 + M)}{(\ell + k_2 + k_3)^2 - M^2} \cdot \frac{i(\ell + k_2 + M)}{(\ell + k_2)^2 - M^2} + 5 \text{ permutations} \\ & = -\frac{8i\eta^4}{(4\pi)^2} \left[3 \left(\frac{1}{\epsilon} + \log \frac{\mu^2}{M^2} \right) - 8 \right] + \dots \end{aligned} \quad (3.81)$$

In the corresponding effective theory we have to integrate out the heavy spinor field. Doing so, we are left with the following tree-level free scalar field Lagrangian

$$\mathcal{L} = \frac{1}{2} \partial^\mu \varphi \partial_\mu \varphi - \frac{m^2}{2} \varphi^2. \quad (3.82)$$

Which is lacking of any interaction content.

Finally, we obtain the 1-loop effective theory Lagrangian, setting $\mu = M$ in the full theory 1-loop amplitudes, and by choosing the counter terms to cancel the $\frac{1}{\epsilon}$ poles in the previous expressions.

$$\mathcal{L}_{\text{eff}_{5,R}} = \left(1 - \frac{4\eta^2}{3(4\pi)^2} \right) \frac{(\partial^\mu \varphi)^2}{2} - \left(m^2 + \frac{4\eta^2 M^2}{(4\pi)^2} \right) \frac{\varphi^2}{2} + \frac{\eta^2}{5(4\pi)^2 M^2} \frac{(\partial^2 \varphi)^2}{2} + \frac{64\eta^2}{(4\pi)^2} \frac{\varphi^2}{4!}. \quad (3.83)$$

Once again (as done in the former case in section 3.2.3), to obtain a consistent/physical scattering amplitude we have to normalise the scalar field according to the coefficient of the kinetic operator.

3.3 The SM as an effective field theory

Notwithstanding its predictive power, nowadays the SM is not understood to be a complete theory of the microscopical world. In fact, we expect this framework to break up as we raise and raise the energy scale at which experiments are running.

This motivation, through the years, has taken researchers to invest time on the development of alternative approaches beyond the SM, to eventually be ready for some evident deviations, and to improve accuracy in the interpretation of the already gathered datas.

The standard model effective field theory turns out to be a particularly interesting framework, to describe physics beyond the standard model in a model independent way.

Moreover, projecting measurements of the interactions of the known SM states into an effective field theory framework is an important goal of the LHC physics program, so we expect to get results and answers on the correctness of this approach in the proximal future.

Utilizing the SMEFT is based on the expectation that the experimental resolution ΔE_r at LHC [11]⁴ could be (in the future) such that

$$\Delta E_r \lesssim \frac{c_i p^2}{g_{sm} \Lambda^2} . \quad (3.84)$$

It seems to be reasonable to adopt this assumption for now.

Conversely, using the standard model is equivalent to assume that

$$\Delta E_r \gg \frac{c_i p^2}{g_{sm} \Lambda^2} , \quad (3.85)$$

will always hold when interpreting the data.

The SMEFT generalizes the SM with a set of higher order $SU(3) \times SU(2) \times U(1)$ invariant operators, under the assumption that the corresponding BSM states/fields have masses greater than the measured Higgs VEV, which currently sets the mass scale of all the SM states.

The related Lagrangian is obtained with the same recipe already introduced in equation (3.10), namely

$$\mathcal{L}_{\text{SMEFT}} = \mathcal{L}_{\text{SM}} + \sum_{d=5}^{\infty} \frac{c_d}{\Lambda^{d-4}} \mathcal{O}_d . \quad (3.86)$$

The general algorithm to determine operator bases at higher orders was developed by [20].

However, in the following, we will mainly be concerned with the SMEFT Lagrangian truncated up to 6-dimensional operators. A characteristic still embedded in this construction is that the Higgs VEV gets modified by the operator $\frac{c_6}{\Lambda^2} \mathcal{O}_6$.

In fact,

$$\mathcal{L} \supset -\lambda \left(\Phi^\dagger \Phi - \frac{v^2}{2} \right)^2 + \frac{c_6}{\Lambda^2} (\Phi^\dagger \Phi)^3 , \quad (3.87)$$

leading to a new potential's minimum given by

$$\langle \Phi^\dagger \Phi \rangle = \frac{v^2}{2} \left(1 + \frac{3c_6 v^2}{4\lambda \Lambda^2} \right) . \quad (3.88)$$

3.3.1 Operator bases and reduction

In order to consider the SM extension up to dimension 6 it is required to introduce a new basis of operators. In [20] we have a set of operators respecting the gauge symmetry of the SM. Anyhow, this set of operators is over-complete. Indeed, we immediately understand a redundancy⁵ issue after including every term compatible with the truncated (3.86) Lagrangian.

As discussed by [21], it is possible to fix this behavior by using the following substitutions⁶ on the SM fields:

⁴Here c_i is a Wilson coefficient in the effective theory corresponding to the expansion p^2/Λ^2 .

⁵Which we already encountered in the examples developed in 3.2.

⁶We remark that removing these redundant operators have always to be done in a gauge independent manner, as the procedure is justified by the invariance of observables under gauge independent field redefinitions [11].

Bosons

$$\begin{aligned}
\Phi'_j &\rightarrow \Phi_j + \frac{a_1}{\Lambda^2} D^2 \Phi_j + \frac{a_2}{\Lambda^2} \bar{\ell}^+ \Psi_j \mathbf{y} + \frac{a_3}{\Lambda^2} \bar{d} q_j \mathbf{Y}_d + \frac{a_4}{\Lambda^2} (\bar{u} \epsilon q_j)^* \mathbf{Y}_u^* + \frac{a_5}{\Lambda^2} (\Phi^\dagger \Phi) \Phi_j, \\
B'_\mu &\rightarrow B_\mu + \frac{b_1}{\Lambda^2} \bar{\psi} \gamma_\mu \psi + \frac{b_2}{\Lambda^2} \Phi^\dagger i \overleftrightarrow{D}_\mu \Phi + \frac{b_3}{\Lambda^2} D^\nu B_{\nu\mu} + \frac{b_4}{\Lambda^2} (\Phi^\dagger \Phi) B_\mu, \\
W_\mu^{a'} &\rightarrow W_\mu^a + \frac{c_1}{\Lambda^2} \bar{q} \sigma^a \gamma_\mu q + \frac{c_2}{\Lambda^2} \bar{\ell} \sigma^a \gamma_\mu \ell + \frac{c_3}{\Lambda^2} \Phi^\dagger \overleftrightarrow{D}_\mu^a \Phi + \frac{c_4}{\Lambda^2} [D^\nu, W_{\nu\mu}]^a + \frac{c_5}{\Lambda^2} (\Phi^\dagger \Phi) W_\mu^a, \\
G_\mu^{A'} &\rightarrow G_\mu^A + \frac{d_1}{\Lambda^2} \bar{q} \mathbf{T}^A \gamma_\mu q + \frac{d_2}{\Lambda^2} \bar{d} \mathbf{T}^A \gamma_\mu d + \frac{d_3}{\Lambda^2} \bar{u} \mathbf{T}^A \gamma_\mu u + \frac{d_4}{\Lambda^2} [D^\nu, G_{\nu\mu}]^A + \frac{d_5}{\Lambda^2} (\Phi^\dagger \Phi) G_\mu^A.
\end{aligned} \tag{3.89}$$

Left-handed fermions

$$\begin{aligned}
q'_j &\rightarrow q_j + \frac{f_1}{\Lambda^2} u i \not{D} \tilde{\Phi}_j \mathbf{Y}_u^\dagger + \frac{f_2}{\Lambda^2} u i \overleftarrow{\not{D}} \tilde{\Phi}_j \mathbf{Y}_u^\dagger + \frac{f_3}{\Lambda^2} d i \not{D} \tilde{\Phi}_j \mathbf{Y}_d^\dagger + \frac{f_4}{\Lambda^2} d i \overleftarrow{\not{D}} \tilde{\Phi}_j \mathbf{Y}_d^\dagger \\
&\quad + \frac{f_5}{\Lambda^2} (\Phi^\dagger \Phi) q_j + \frac{f_6}{\Lambda^2} D^2 q_j, \\
\Psi'_j &\rightarrow \Psi_j + \frac{g_1}{\Lambda^2} \ell^+ i \not{D} \Phi_j \mathbf{y}^\dagger + \frac{g_2}{\Lambda^2} \ell^+ i \overleftarrow{\not{D}} \Phi_j \mathbf{y}^\dagger + \frac{g_3}{\Lambda^2} (\Phi^\dagger \Phi) \Psi_j + \frac{g_4}{\Lambda^2} D^2 \Psi_j.
\end{aligned} \tag{3.90}$$

Right-handed fermions

$$\begin{aligned}
\ell^{+'} &\rightarrow \ell^+ + \frac{h_1}{\Lambda^2} \bar{\Psi} i \not{D} \Phi \mathbf{y}^\dagger + \frac{h_2}{\Lambda^2} \bar{\Psi} i \overleftarrow{\not{D}} \Phi \mathbf{y}^\dagger + \frac{h_3}{\Lambda^2} (\Phi^\dagger \Phi) \ell^+ + \frac{h_4}{\Lambda^2} D^2 \ell^+, \\
d' &\rightarrow d + \frac{j_1}{\Lambda^2} \bar{q} i \not{D} \Phi \mathbf{Y}_d^\dagger + \frac{j_2}{\Lambda^2} \bar{q} i \overleftarrow{\not{D}} \Phi \mathbf{Y}_d^\dagger + \frac{j_3}{\Lambda^2} (\Phi^\dagger \Phi) d + \frac{j_4}{\Lambda^2} D^2 d, \\
u' &\rightarrow u + \frac{k_1}{\Lambda^2} \bar{q} i \not{D} \Phi \mathbf{Y}_u^\dagger + \frac{k_2}{\Lambda^2} \bar{q} i \overleftarrow{\not{D}} \Phi \mathbf{Y}_u^\dagger + \frac{k_3}{\Lambda^2} (\Phi^\dagger \Phi) u + \frac{k_4}{\Lambda^2} D^2 u.
\end{aligned} \tag{3.91}$$

With these substitutions we are eventually lead to the WARSAV BASIS, which is the first complete set of SM field operators respecting the SM gauge group up to dimension 6.

We refer the reader to references [11, 20, 21] for further informations on this topic.

3.3.2 Phenomenological lagrangians

The concept of phenomenological Lagrangian is introduced to characterize a subset of events occurring at LHC.

Instead of specifying all of the SMEFT Lagrangian, we focus on a specific sector, giving rise, for example, to the SILH (Strong Interacting Light Higgs) [22] Lagrangian⁷.

It is worth to specify that a phenomenological Lagrangian is by no means a basis for the SMEFT operators. Technical aspects about this topic are discussed in [23, 24, 25].

For what concerns this work, we will be mainly interested in the Higgs extended sector. The natural phenomenological Lagrangian describing this sector is exactly the

⁷This Lagrangian is inspired by a scenario in which the Higgs is part of a strongly interacting sector [22].

SILH Lagrangian. Following [26, 22], we decompose the standard model effective field theory Lagrangian as

$$\mathcal{L}_{\text{SMEFT}} = \mathcal{L}_{\text{SM}} + \mathcal{L}_{\text{SILH}} + \mathcal{L}_{\text{G}} + \mathcal{L}_{\text{CP}} + \mathcal{L}_{\text{F1}} + \mathcal{L}_{\text{F2}} + \mathcal{L}_{\text{F3}} . \quad (3.92)$$

In particular, we have the SILH Lagrangian to contain the 6-dimensional self-interacting Higgs operators

$$\mathcal{L}_{\text{SILH}} \supset \frac{c_h}{2\Lambda^2} \partial^\mu (\Phi^\dagger \Phi) \partial_\mu (\Phi^\dagger \Phi) - \frac{c_6}{\Lambda^2} (\Phi^\dagger \Phi)^3 , \quad (3.93)$$

which will be essential for the discussions in the following chapters.

Minimally extending the standard model

In the former chapter we introduced and discussed the framework of effective field theories. Our aim now is to make use of these techniques to analyse some possible beyond standard model scenarios featuring a real scalar singlet.

We have already pointed out that the standard model still lacks an explanation for (say) the origin of the baryon asymmetry of the universe, dark matter and neutrino masses and how these evidences motivates the study of physics beyond the standard model. Among the BSM proposals one can identify three minimal scenarios where the new physics is connected to the SM through so-called portal interactions and the field content of the SM is minimally extended.

These three scenarios respectively include the following new states:

1. scalar singlet (both real and complex),
2. right-handed/sterile neutrino,
3. dark photon.

In this thesis we will focus on the scenario 1. The main reason behind this choice is the next experimental program of the LHC and the future ILC [11, 27]. Indeed, this will aim at measuring the trilinear Higgs coupling, which is shifted after taking into account effective operators generated by integrating out these new singlet states.

For simplicity and without affecting the main conclusions of our investigation we will restrict to the simplified case in which there is only one new real scalar.

The main goal of this chapter is to systematically analyze this model focusing on the resulting deviations in the Higgs couplings. In particular we will concentrate on the corresponding EFT operators that are generated in this class of models when the new state is heavy and is integrated out.

We will explore the different possible realisations of this model (with or without a conserved \mathbb{Z}_2 symmetry acting on the singlet). In this investigation, we reproduce independently the results already presented in the literature, but we also extend some of the computations to higher order in the EFT expansion.

This section is organised as follow:

We start by introducing the real scalar singlet portal, previously studied in e.g. [26, 28, 29, 30, 31, 32]. In section 4.1.1 we review the EFT structure [27] which results after integrating out the singlet.

Then we introduce two different scenarios, taking into account (sections 4.2 , 4.4) or not (section 4.3) the possibility of an explicit \mathbb{Z}_2 symmetry.

We describe the structures of the full theories, eventually proceeding by mapping to the EFT with two different approaches, in order to evaluate and double check the Wilson coefficients necessary to the analysis which will follow in sections 5 and 6.

4.1 The real scalar singlet portal

We now introduce and discuss the real singlet scalar portal, which is one of the simplest possible renormalisable extension of the SM involving the Higgs sector.

The most important event at LHC is without any doubt the discovery of the Higgs Boson. This confirms the Higgs Mechanism of the SM. After electroweak symmetry breaking (EWSB) occurs, every particle interacting with the Higgs acquires mass. Moreover, linear, cubic and quartic self-interaction terms do appear for the physical Higgs boson.

It is known that the quartic self-interaction term is very hard to probe at LHC nowadays. Conversely the cubic self-interaction can be investigated by searching for double-Higgs final states and loop induced single Higgs productions [27]. In particular, a detailed analysis of this sector and a precise measure of the coupling would definitely test the electroweak sector of the SM by the reconstruction of the scalar Higgs potential.

As mentioned, we still do not know the structure of the potential and the physics behind the electroweak symmetry breaking. In particular, beyond standard model scenarios could modify significantly the SM physics.

As we will find out in the sequel, including a real scalar singlet as a BSM particle will modify the temperature dependent Higgs effective potential. This is crucial to get the strong first order electroweak phase transition [29, 13] which is necessary for electroweak baryogenesis (see section 2.4), in an attempt to explain the baryon asymmetry of Universe. Singlet scalars are indeed among the *most-hidden* particles that can increase the strength of this EW transition. Moreover, the existence of this particle can have implications for the Higgs searches at LHC.

Motivated by the lack of significant deviations from the SM global data set [11], we will extensively study this scenario by using the framework of EFTs introduced and discussed in the former section. Essentially, we will proceed by matching tree-level and 1-loop level results into the EFT which results after integrating out the singlet particle.

To get started, let us introduce the most general/ \mathbb{Z}_2 -breaking SM Higgs potential extended with the $SU(3) \times SU(2) \times U(1)$ real singlet scalar:

$$V(\Phi, s) = -\mu_h^2 |\Phi|^2 + \lambda |\Phi|^4 - \frac{\mu_s^2}{2} s^2 + \underbrace{\frac{\lambda_m}{2} |\Phi|^2 s^2 + \frac{\mu_3}{3} s^3 + \frac{\lambda_s}{4} s^4}_{\text{portal}} + \mu_4 |\Phi|^2 s. \quad (4.1)$$

Here, Φ is the Higgs field, which is a doublet laying into one of the fundamental representation of the $SU(2) \times U(1)$ gauge group, and s is the real singlet. Then, starting from this potential, many different scenarios could arise as the singlet takes a vacuum expectation value or not. Furthermore, this general potential could also be reduced to a \mathbb{Z}_2 preserving one, which is of particular interest if we are looking for a reliable dark matter candidate¹.

The \mathbb{Z}_2 -preserving potential can be quickly obtained taking μ_4, μ_3 to zero in (4.1).

Summarising, in the following we discuss the singlet extension of the SM analyzing both the possibilities of a \mathbb{Z}_2 preserving or breaking potential, and the cases in which the singlet do get a vacuum expectation value or not.

We will perform a map into the effective Higgs potential introduced below, where local operators respecting the symmetries of the gauge group are inserted inside the SM Lagrangian as

$$\mathcal{L}_{\text{eff}} = \mathcal{L}_{\text{SM}} + \frac{c_h}{2\Lambda^2} \partial^\mu \left(\Phi^\dagger \Phi - \frac{v^2}{2} \right) \partial_\mu \left(\Phi^\dagger \Phi - \frac{v^2}{2} \right)^2 + \sum_{n=3}^{\infty} \frac{c_{2n}}{\Lambda^{2n-4}} \left(\Phi^\dagger \Phi - \frac{v^2}{2} \right)^n, \quad (4.2)$$

where Λ is the effective scale, and where $c_{2n} \equiv c_{2n}(\mu)$ are the Wilson coefficients of the higher dimensional Higgs operators. For now, we will only consider scalar operators up to dimension 8. Moreover, we will extend our investigations up to the 1-loop level in perturbation theory.

It turns out that

1. c_h corrects the Higgs field wave function renormalisation, and globally shifts all the other Higgs couplings,
2. c_6 corrects the 3,4,5,6 - Higgs self-interactions,
3. c_8 corrects both the 4,5,6,7,8 - Higgs self-interactions.

We will adopt the following conventions² in the whole chapter:

¹Indeed, the absence of odd interaction vertexes do stabilise the singlet, and it is clear that a dark matter particle have to respect this feature, otherwise it wouldn't be possible to obtain the relic abundance measure up-to-date.

²If it is not otherwise specified.

- the gauge bosons acquire mass after the Higgs field gets a VEV according to the gauge choice:

$$\Phi(x) = \frac{U_\chi(x)}{\sqrt{2}} \begin{pmatrix} 0 \\ h(x) + v \end{pmatrix}, \quad U_\chi(x) = e^{\frac{i\tau_a \chi^a(x)}{v}}, \quad v^2 = \frac{\mu_h^2}{2\lambda}, \quad (4.3)$$

where $h(x)$ is the Higgs field, $U_\chi(x)$ is a unitary matrix containing the three Goldstone bosons $\chi_a(x)$ and v is the Higgs vacuum expectation value.

- Every internal line in the Feynman diagrams of this section is referred to the singlet, which is represented by a continuous line.
- Every external line represents the Higgs, referring in the same way to the broken phase or the symmetric one.
- Dimensional regularization will be used in all the 1-loop calculations unless it is explicitly stated.
- We mainly use the $\overline{\text{MS}}$ renormalisation scheme, defining the Euler Γ function simple poles as

$$\frac{1}{\bar{\epsilon}} = \frac{1}{\epsilon} - \gamma,$$

with γ being the Euler-Mascheroni constant.

4.1.1 The effective theory

Here we introduce the self-interacting sector of the Higgs effective potential relevant to our investigations. The results obtained in the full theories will be matched in this effective theory, following the recipe already discussed in 3.2.

We start from the phenomenological SILH Lagrangian [11] introduced in (3.93) extended with the 8-dimensional $(\Phi^\dagger \Phi)^4$ operator.

In the symmetric phase we have³

$$\mathcal{L}_{\text{eff}} \supset -\frac{c_h}{2\Lambda^2} \left(\Phi^\dagger \Phi - \frac{v^2}{2} \right) \square \left(\Phi^\dagger \Phi - \frac{v^2}{2} \right) - \frac{c_6}{\Lambda^2} \left(\Phi^\dagger \Phi - \frac{v^2}{2} \right)^3 - \frac{c_8}{\Lambda^4} \left(\Phi^\dagger \Phi - \frac{v^2}{2} \right)^4. \quad (4.4)$$

Then, after the Higgs gets a VEV according to (4.3), every term up to the power of 8 appears.

We have

$$\begin{aligned} \mathcal{L}_{\text{eff}} \supset & \frac{c_h}{2\Lambda^2} (h+v)^2 \partial^\mu h \partial_\mu h - \frac{c_6}{\Lambda^2} \left(\frac{h^6}{8} + v^3 h^3 + \frac{3h^5 v}{4} + \frac{3h^4 v^2}{2} \right) \\ & - \frac{c_8}{\Lambda^4} \left(\frac{h^8}{16} + \frac{h^7 v}{2} + 2h^5 v^2 + \frac{3h^6 v^2}{2} + h^4 v^4 \right). \end{aligned} \quad (4.5)$$

³The 6-dimensional derivative operator is identical to the one in equation (4.2) up to a total derivative.

In particular, it follows that:

- c_h contributes to the renormalisation of the Higgs wave function as

$$\frac{1}{2} \left(1 + \underbrace{\frac{c_h v^2}{\Lambda^2}}_{\bar{c}_h} \right) \partial^\mu h \partial_\mu h; \quad (4.6)$$

- c_6 do modify the \mathbf{hhh} self-interaction vertex as

$$\lambda v h^3 \rightarrow v \lambda \left(1 + \underbrace{\frac{c_6 v^2}{\lambda \Lambda^2}}_{\bar{c}_6} \right) h^3; \quad (4.7)$$

- c_6 and c_8 do modify the \mathbf{hhhh} self-interaction vertex as

$$\frac{1}{4} \lambda h^4 \rightarrow \frac{1}{4} \lambda \left(1 + \underbrace{\frac{6c_6 v^2}{\lambda \Lambda^2}}_{6\bar{c}_6} + \underbrace{\frac{4c_8 v^4}{\lambda \Lambda^4}}_{\bar{c}_8} \right) h^4. \quad (4.8)$$

For convenience, we also define the ratios

$$k_3 = \frac{\lambda_3}{\lambda_{3,\text{SM}}} = 1 + \bar{c}_6 \quad , \quad k_4 = \frac{\lambda_4}{\lambda_{4,\text{SM}}} = 1 + 6 \bar{c}_6 + \bar{c}_8. \quad (4.9)$$

To take into account the BSM contributions to the interaction vertexes we will be using two different techniques.

Specifically:

1. We will integrate out the singlet by using its equations of motion, as exemplified in appendix [A](#).
2. We will compare the full theory and effective theory complementary scattering amplitudes, following the example discussed in [3.2](#).

Being mainly interested in the renormalisable self-interacting Higgs couplings, we will focus our attention to the value of c_h , c_6 and c_8 in the singlet extended models introduced. Then, we will show how different form for the singlet scalar potential will lead to modifications of interaction vertexes both at tree and 1-loop level.

4.2 \mathbb{Z}_2 preserving potential: spontaneous symmetry breaking

For the sake of simplicity, we proceed by increasing difficulty, starting from the easiest extension consisting of just a single coupling between the Higgs and the singlet. As the title suggests, this corresponds to a \mathbb{Z}_2 preserving potential.

The case is interesting when the scalar field mass mixing occurs from $\propto hs$ terms appearing after both the fields acquire a VEV. Moreover, as introduced, a \mathbb{Z}_2 preserving model could eventually ensure stability to the singlet. This feature would make it a possible Dark Matter candidate.

Anyhow, here the \mathbb{Z}_2 symmetry will be spontaneously broken after the singlet acquires a VEV, forbidding this kind of identification which we will discuss in section 4.4.

The \mathbb{Z}_2 preserving potential reads

$$V(\Phi, s) = -\mu_h^2 |\Phi|^2 + \lambda |\Phi|^4 - \frac{\mu_s^2}{2} s^2 + \frac{\lambda_s}{4} s^4 + \frac{\lambda_m}{2} |\Phi|^2 s^2. \quad (4.10)$$

Substituting the EWSB condition from (4.3) and letting s acquire a non zero VEV by $s \rightarrow s + v_s$, we have:

$$\begin{aligned} V(h, s) &= -\frac{\mu_h^2}{2}(h^2 + 2vh + v^2) + \frac{\lambda}{4}(h^4 + v^4 + 6h^2v^2 + 4v^3h + 4vh^3) \\ &\quad - \frac{\mu_s^2}{2}(s^2 + 2vs + v^2) + \frac{\lambda_s}{4}(s^4 + v_s^4 + 6v_s^2s^2 + 4v_s^3s + 4v_s s^3) \\ &\quad + \frac{\lambda_m}{4}(h^2 + v^2 + 2vh)(s^2 + v_s^2 + 2v_s s) \\ &= \left(-\mu_h^2 v + \lambda v^3 + \frac{\lambda_m}{2} v v_s^2\right) h + \left(-\frac{\mu_h^2}{2} + \frac{3}{2} \lambda v^2 + \frac{\lambda_m}{4} v_s^2\right) h^2 \\ &\quad + \left(-\mu_s^2 v_s + \lambda_s v_s^3 + \frac{\lambda_m}{2} v_s v^2\right) s + \left(-\frac{\mu_s^2}{2} + \frac{3}{2} \lambda_s v_s^2 + \frac{\lambda_m}{4} v^2\right) s^2 \\ &\quad + \frac{\lambda}{4} h^4 + v \lambda h^3 + \frac{\lambda}{4} v^4 + \frac{\lambda_s}{4} s^4 + \lambda_s v_s s^3 + \frac{\lambda_s}{4} v_s^4 \\ &\quad + \frac{\lambda_m}{4} h^2 s^2 + \frac{\lambda_m v}{2} h s^2 + \lambda_m v v_s h s + \frac{\lambda_m v_s}{2} h^2 s. \end{aligned} \quad (4.11)$$

After the introduction of masses m_h, m_s and tadpoles $\mathfrak{T}_h, \mathfrak{T}_s$ (which can be identified respectively from the squared and linear terms in the last equation), we have

$$\begin{aligned} V(h, s) &= \frac{m_h^2}{2} h^2 + \mathfrak{T}_h h + \frac{m_s^2}{2} s^2 + \mathfrak{T}_s s + \frac{\lambda}{4} h^4 + v \lambda h^3 + \frac{\lambda}{4} v^4 + \frac{\lambda_s}{4} s^4 + \lambda_s v_s s^3 \\ &\quad + \frac{\lambda_s}{4} v_s^4 + \frac{\lambda_m}{4} h^2 s^2 + \frac{\lambda_m v}{2} h s^2 + m_h^2 h s + \frac{\lambda_m v_s}{2} h^2 s. \end{aligned} \quad (4.12)$$

We immediately note a mass mixing term arising. In order to get a clear understanding of the respective singlet and Higgs masses, it is necessary to diagonalize the mass matrix of the system. Essentially, we move from (h, s) to the mass eigenstates (h_1, h_2) .

For this task, we start by employing the tadpole conditions, namely

$$\mathfrak{T}_s = \mathfrak{T}_h = 0 .$$

We have

$$-\mu_h^2 v + \lambda v^3 + \frac{\lambda_m}{2} v_s^2 v = 0 \quad \rightarrow \quad \boxed{\mu_h^2 = \lambda v^2 + \frac{\lambda_m}{2} v_s^2} ; \quad (4.13)$$

$$-\mu_s^2 v_s + \lambda_s v_s^3 + \frac{\lambda_m}{2} v_s v^2 = 0 \quad \rightarrow \quad \boxed{\mu_s^2 = \lambda_s v_s^2 + \frac{\lambda_m}{2} v^2} . \quad (4.14)$$

By substituting these conditions into the definition of the mass parameters of the system, we obtain

$$\boxed{m_h^2 = 2\lambda v^2 \quad | \quad m_s^2 = 2\lambda_s v_s^2} . \quad (4.15)$$

Thus, we now understand (from the potential (4.12)) the mass of the system to be embedded in the matrix product

$$\begin{pmatrix} h & s \end{pmatrix} \begin{pmatrix} 2\lambda v^2 & \lambda_m v v_s \\ \lambda_m v v_s & 2\lambda_s v_s^2 \end{pmatrix} \begin{pmatrix} h \\ s \end{pmatrix} . \quad (4.16)$$

Rotating to the mass eigenstates by means of

$$\begin{pmatrix} h_1 \\ h_2 \end{pmatrix} = \begin{pmatrix} \cos \theta & -\sin \theta \\ \sin \theta & \cos \theta \end{pmatrix} \begin{pmatrix} h \\ s \end{pmatrix} , \quad \theta = \frac{1}{2} \arctan \left(\frac{2m_{hs}^2}{m_s^2 - m_h^2} \right) , \quad (4.17)$$

gives us with the two correspondent mass eigenvalues, namely

$$\begin{aligned} m_{1,2}^2 &= \frac{1}{2} \left(m_h^2 + m_s^2 \mp (4m_{hs}^4 + (m_h^2 - m_s^2)^2)^{1/2} \right) \\ &= \frac{1}{2} \left(m_h^2 + m_s^2 \pm \frac{m_h^2 - m_s^2}{\cos 2\theta} \right) . \end{aligned} \quad (4.18)$$

Taking the limit in which the singlet VEV v_s is much larger than the Higgs VEV v is equivalent to assume a very small mixing angle. In fact, owing to equation (4.17), it follows:

$$\theta \simeq \frac{1}{2} \arctan \left(\frac{2m_{hs}^2}{\left(1 - \frac{m_h^2}{m_s^2}\right) m_s^2} \right) = \frac{1}{2} \arctan 2y \simeq y , \quad (4.19)$$

where we defined y as the ratio $\lambda_m v / 2\lambda_s v_s$.

Moreover, we also have the following mass ratios to be small in the same limit:

$$x = \frac{m_h}{m_s} \ll 1 \quad ; \quad y = \frac{m_{hs}^2}{m_s^2} \simeq \frac{\lambda_m v}{2\lambda_s v_s} \ll 1 . \quad (4.20)$$

After this process, the Higgs modified couplings to fermions and weak gauge bosons do follow straightforwardly. In fact, it is just necessary to introduce the rotated/mixed

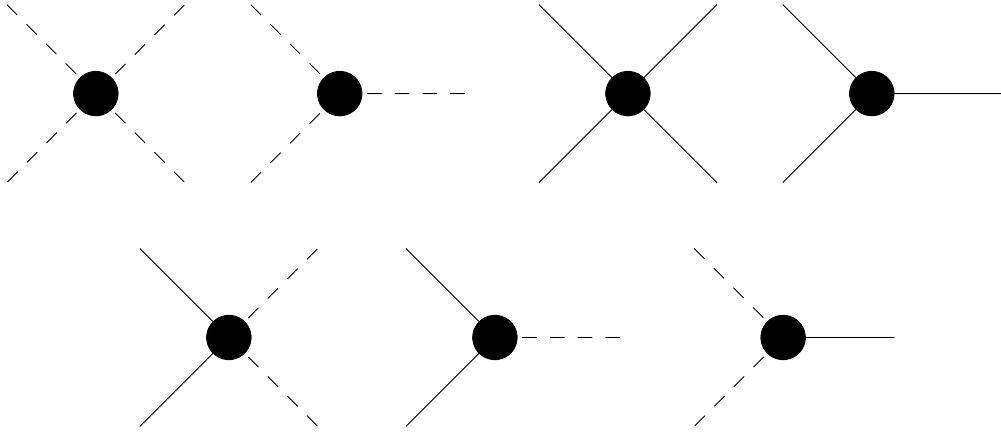


Figure 4.1: Interaction vertexes between the standard model Higgs and the singlet scalar field, after EWSB and $v \rightarrow s + v_s$. The dashed lines corresponding to the SM Higgs boson h , and the filled lines to the real scalar singlet s . The last interaction vertex is suppressed in the leading v/v_s approximation.

definition of h from (4.52) (with the appropriate limit on v and v_s) inside the usual definition of the Higgs couplings with the SM.

For example, we have the gauge bosons couplings modified after the field rotation

$$h \rightarrow h_1 \cos \theta - h_2 \sin \theta \quad \simeq h_1 \left(1 - \frac{\theta^2}{2}\right) - h_2 \theta \quad (4.21)$$

$$\simeq h \left(1 - \frac{y^2}{2}\right) - ys, \quad (4.22)$$

as [26]

$$W_\mu^+ W_\mu^- \left[gm_W \left(1 - \frac{y^2}{2}\right) h + \frac{g^2}{4}(1 - y^2)h^2 - (gm_W y)s \right], \quad (4.23)$$

$$Z_\mu Z^\mu \left[\frac{gm_W}{2 \cos \theta_W} \left(1 - \frac{y^2}{2}\right) h^2 + \frac{g^2}{4(\cos \theta_W)^2}(1 - y^2)h^2 - \left(\frac{gm_W}{2 \cos \theta_W} y\right)s \right]. \quad (4.24)$$

Finally, restricting our attention to the leading order in the mixing angle, the mass eigenvalues are just

$$m_1^2 = m_s^2(x^2 - y^2) \simeq m_h^2 \quad ; \quad m_2^2 = m_s^2(1 + y^2) \simeq m_s^2, \quad (4.25)$$

i.e. , the masses do not mix anymore.

Eventually, we are lead to the broken phase potential

$$\begin{aligned} V(h_1, h_2) \simeq V(h, s) &= \frac{1}{2}m_s^2 s^2 + \frac{1}{2}m_h^2 h^2 + \frac{\lambda}{4}h^4 + \lambda v h^3 + \frac{\lambda_m}{4}h^2 s^2 \\ &+ \frac{\lambda_m v_s}{2}h^2 s + \frac{\lambda_s}{4}s^4 + \lambda_s v_s s^3, \end{aligned} \quad (4.26)$$

in which only the leading terms in $v_s \gg v$ are considered.

4.2.1 Integrating out the singlet via E.O.M.

We now proceed with the matching to the effective theory introduced in section 4.1.1. It is possible to quantify the IR physics of this real scalar singlet BSM model by integrating it out via its EOM.

We start writing down the full theory Lagrangian

$$\begin{aligned} \mathcal{L} = & \frac{1}{2} \partial^\mu s \partial_\mu s + \frac{1}{2} \partial^\mu h \partial_\mu h - \frac{1}{2} m_s^2 s^2 - \frac{1}{2} m_h^2 h^2 - \frac{\lambda}{4} h^4 \\ & + \lambda v h^3 - \frac{\lambda_m}{4} h^2 s^2 - \frac{\lambda_m v_s}{2} h^2 s - \frac{\lambda_s}{4} s^4 - \lambda_s v_s s^3 . \end{aligned} \quad (4.27)$$

Then, following the procedure illustrated in A by:

1. solving the equations of motion for s by considering up to s^3 terms in \mathcal{L} ,
2. proceeding by expanding the *correct*⁴ solution in powers of $1/m_s$,
3. plugging the result for s inside (4.27),

we are lead to the effective Lagrangian:

$$\begin{aligned} \mathcal{L}_{\text{eff}} \supset & \frac{\lambda_m^2 v_s^2}{8m_s^4} \partial_\mu (h^2) \partial^\mu (h^2) - \frac{m_h^2}{2} h^2 - \lambda v h^3 - \left(\frac{\lambda}{4} - \frac{\lambda_m^2 v_s^2}{8m_s^2} \right) h^4 \\ & - \frac{\lambda_m^3 v_s^2}{16m_s^6} (m_s^2 - 2\lambda_s v_s^2) h^6 + \frac{\lambda_m^4}{64m_s^{10}} (2m_s^4 v_s^2 + 18\lambda_s^2 v_s^6 - 13m_s^2 \lambda_s v_s^4) h^8 . \end{aligned} \quad (4.28)$$

Then, by the tadpole condition $m_s^2 = 2\lambda_s v_s^2$, it follows that $\boxed{c_6 = c_8 = 0}$.

Moreover, in this case we also that every c_{2n} coefficient defined in (4.2) is null. This can be easily showed considering the full equations of motion for s without expanding for large m_s . In fact, plugging the full expression for s inside (4.27), we eventually have

$$\mathcal{L}_{\text{eff}} \supset \frac{\lambda_m^2}{4\lambda_s m_s^2} h^2 \partial_\mu h \partial^\mu h - \frac{m_h^2}{2} h^2 - \lambda v h^3 - \left(\frac{\lambda}{4} - \frac{\lambda_m^2 v_s^2}{8m_s^2} \right) h^4 . \quad (4.29)$$

Thus, we only have a non zero value for

$$\frac{c_h}{\Lambda^2} = \frac{\lambda_m^2}{2\lambda_s m_s^2} \quad \rightarrow \quad \frac{c_h v^2}{\Lambda^2} = y^2 \quad (4.30)$$

is found⁵.

As c_h renormalises the broken phase Higgs field wave function, it also modifies all the Higgs couplings to the SM once we canonically normalise the corresponding kinetic term.

⁴The solution which vanishes as the Higgs field h goes to zero.

⁵We have recognised the same combination corresponding to the parameter y^2 defined in (4.22).

In fact, from equation (4.6) it follows that the correct wave function normalisation is found after the shift

$$h \rightarrow \left(1 - \frac{c_h v^2}{2\Lambda^2}\right) h . \quad (4.31)$$

With this substitution, we eventually recover equations (4.23),(4.24), where the Higgs coupling to gauge bosons is modified by the Higgs/singlet mixing. This also provides us a consistency check of the integrating out procedure.

At last, an interesting phenomenological observation related to the Wilson coefficient c_h is that, as discussed by [26, 32], it modifies the electroweak precision observables.

In particular the S and T parameters are modified as follows

$$S = \frac{1}{6\pi} (c_h) \log \frac{m_s}{m_W} , \quad (4.32)$$

$$T = -\frac{3}{8\pi \cos^2 \theta_W} (c_h) \log \frac{m_s}{m_W} , \quad (4.33)$$

where m_W is the W_{\pm}^{μ} bosons mass, and where θ_W is the Weinberg angle.

4.2.2 Matching to the EFT with amplitudes

Here we proceed by employing the other matching method introduced, which essentially consists of a comparison between scattering amplitudes in the full and effective theories.

Specifically, in order to estimate the 6-Higgs effective coupling it is necessary to evaluate the full theory diagrams in 4.2. Starting from the diagram on left we have:

$$\mathcal{A}_1 = -\left(\frac{\lambda_m v_s}{2}\right)^3 \frac{\lambda_s v_s}{\left(\frac{\ell^2}{m_s^2} - 1\right)^3 m_s^6} \simeq \frac{\lambda_m^3 v_s^4 \lambda_s}{8m_s^6} . \quad (4.34)$$

Then, the second diagram gives:

$$\mathcal{A}_2 = \frac{\lambda_m}{4} \left(\frac{\lambda_m v_s}{2}\right)^2 \frac{1}{\left(\frac{\ell^2}{m_s^2} - 1\right)^2 m_s^4} \simeq -\frac{1}{16} \frac{\lambda_m^3 v_s^2}{m_s^4} . \quad (4.35)$$

Taking into account the combinatorial factors, we arrive to a null value for the c_6 coefficient at the tree level.

In fact, as can be easily checked

$$c_6 = \frac{3}{8} \left(\frac{2\lambda_s v_s^2}{m_s^2} - 1\right) \frac{\lambda_m^3 v_s^2}{m_s^4} = 0 , \quad (4.36)$$

in agreement with the result in (4.29).

Moving on, we calculate the 8-Higgs effective coupling. The diagrams involved are in figure 4.3.

Starting from the first on left, we have

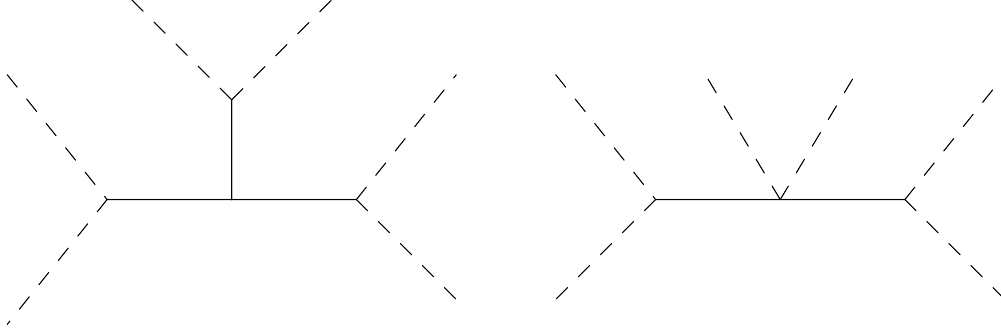


Figure 4.2: Tree-level diagrams to match in the EFT to calculate the value of the \bar{c}_6 Wilson coefficient.

$$\begin{aligned}
\mathcal{A}_3 &= -i \left(-i \frac{\lambda_m v_s}{2} \right)^4 \left(-i \frac{\lambda_s}{4} \right) \frac{i^4}{\frac{1}{m_s^8} \left(\frac{\ell^2}{m_s^2} - 1 \right)^4} \\
&\simeq - \underbrace{\frac{\lambda_m^4 v_s^4 \lambda_s}{32 m_s^8}}_{\frac{\lambda_m^4}{\lambda_s} \frac{1}{16 \cdot 2 m_s^4}} \left[1 + 4 \frac{\ell^2}{m_s^2} + \mathcal{O} \left(\frac{\ell^4}{m_s^4} \right) \right].
\end{aligned} \tag{4.37}$$

Then, moving to the second in the same row, we have:

$$\begin{aligned}
\mathcal{A}_4 &= -i \left(-i \frac{\lambda_m v_s}{2} \right)^2 \left(-i \frac{\lambda_m}{4} \right)^2 \frac{i^3}{\frac{1}{m_s^6} \left(\frac{\ell^2}{m_s^2} - 1 \right)^3} \\
&\simeq \underbrace{\frac{\lambda_m^4 v_s^2}{64 m_s^6}}_{\frac{\lambda_m^4}{\lambda_s} \frac{1}{16 \cdot 8 m_s^4}} \left[1 + 3 \frac{\ell^2}{m_s^2} \mathcal{O} \left(\frac{\ell^4}{m_s^4} \right) \right].
\end{aligned} \tag{4.38}$$

Finally, the last two diagrams contributes as (starting from left)

$$\begin{aligned}
\mathcal{A}_5 &= -i \left(-i \frac{\lambda_m v_s}{2} \right)^4 \left(-i \lambda_s v_s \right)^2 \frac{i^5}{\frac{1}{m_s^{10}} \left(\frac{\ell^2}{m_s^2} - 1 \right)} \\
&\simeq \underbrace{\frac{\lambda_m^4 \lambda_s^2 v_s^6}{16 m_s^{10}}}_{\frac{\lambda_m^4}{\lambda_s} \frac{1}{16 \cdot 8 m_s^4}} \left[1 + 5 \frac{\ell^2}{m_s^2} + \mathcal{O} \left(\frac{\ell^4}{m_s^4} \right) \right],
\end{aligned} \tag{4.39}$$

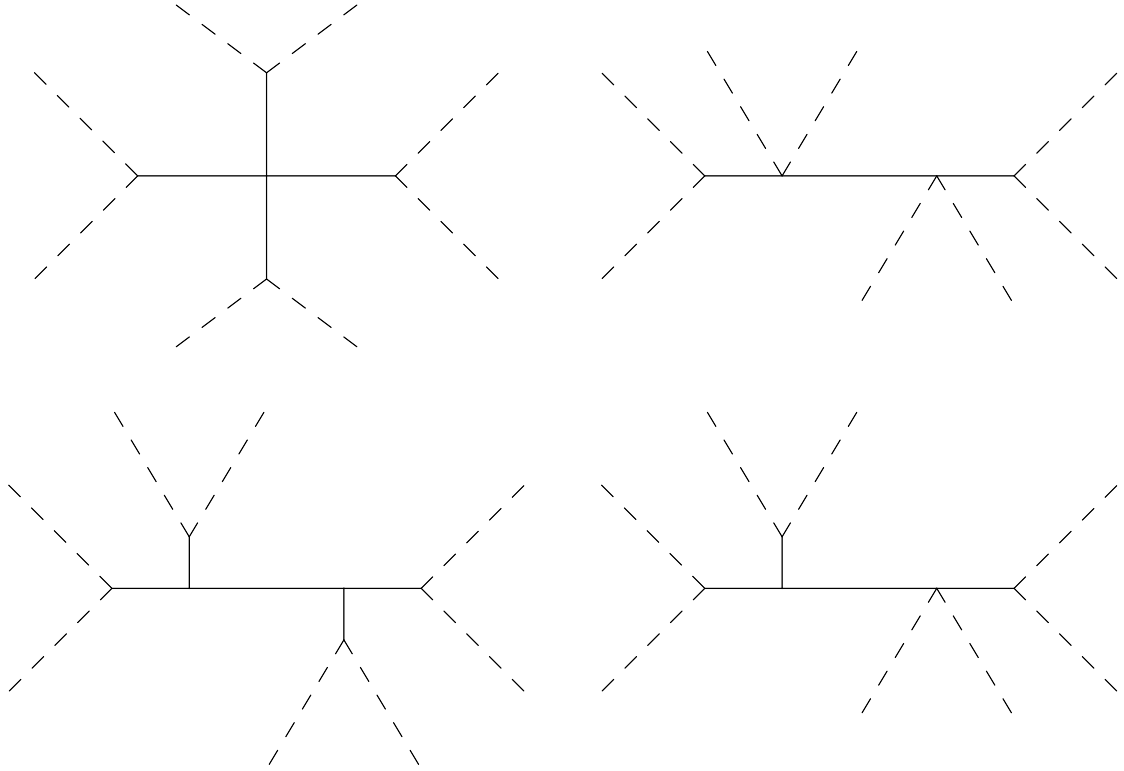


Figure 4.3: Diagrams contributing to the \bar{c}_8 coefficient at the tree level.

$$\begin{aligned}
\mathcal{A}_6 &= -i \left(-i \frac{\lambda_m v_s}{2} \right)^3 (-i \lambda_s v_s) \left(-i \frac{\lambda_s}{4} \right) \frac{i^4}{\frac{1}{m_s^8} \left(\frac{\ell^2}{m_s^2} - 1 \right)^4} \quad (4.40) \\
&\simeq - \underbrace{\frac{\lambda_m^4 \lambda_s v_s^4}{16 \cdot 2 m_s^8}}_{\frac{\lambda_m^4}{\lambda_s} \frac{1}{16 \cdot 8 m_s^4}} \left[1 + 4 \frac{\ell^2}{m_s^2} + \mathcal{O} \left(\frac{\ell^4}{m_s^4} \right) \right].
\end{aligned}$$

Summing up all the contributions above with the relative combinatorial factors, we have

$$c_8 = \frac{\lambda_m^4}{16 \cdot 8 \cdot \lambda_s m_s^4} \left(\frac{9}{2} + 2 - \frac{13}{2} \right) = 0. \quad (4.41)$$

In this section we showed that the model with a \mathbb{Z}_2 preserving potential with spontaneous symmetry breaking induces a modification of the Higgs wave function, captured in the EFT framework by a non vanishing Wilson coefficient c_h . On the contrary, we showed that the contribution to the EFT operators c_{6,c_8} and c_{2n} do eventually vanish.

4.3 \mathbb{Z}_2 explicit breaking potential

Here we discuss the most general potential for the singlet/Higgs sector, including \mathbb{Z}_2 -breaking terms, and in which both fields acquire a non zero VEV. The starting point being equation (4.1) in which all the possible interaction terms between the two fields are included.

The potential reads

$$V(\Phi, s) = \mu_h^2 |\Phi|^2 + \lambda |\Phi|^4 + \frac{\mu_s^2}{2} s^2 + \frac{\lambda_m}{2} |\Phi|^2 s^2 + \frac{\mu_3}{3} s^3 + \frac{\lambda_s}{4} s^4 + \mu_4 |\Phi|^2 s. \quad (4.42)$$

This case turns out to share some common features with the one we discussed in section 4.2, as mass mixing do also occur. As we had already analysed the common terms in 4.2, we are just left with expanding

$$\frac{\mu_3}{3} (s + v_s)^3 = \frac{\mu_3}{3} (s^3 + v_s^3 + 3v_s^2 s + 3v_s s^2); \quad (4.43)$$

and

$$\mu_4 |\Phi|^2 s = \frac{\mu_4}{2} (h^2 s + h^2 v_s + 2hsv + 2hvv_s + v^2 s), \quad (4.44)$$

so that we eventually arrive to the modified interaction potential

$$\begin{aligned} V(h, s) = & h \left(\mu_h^2 v + \frac{1}{2} v \lambda_m v_s^2 + \lambda v^3 + v v_s \mu_4 \right) + h^2 \left(\frac{\mu_h^2}{2} + \frac{1}{4} \lambda_m v_s^2 + \frac{3\lambda v^2}{2} + \frac{v_s \mu_4}{2} \right) \\ & + s \left(\frac{1}{2} v^2 \lambda_m v_s + \lambda_s v_s^3 + \mu_s^2 v_s + \mu_3 v_s^2 + \frac{\mu_4 v^2}{2} \right) + \frac{\lambda_m}{4} s^2 h^2 + (\lambda_m v_s + \mu_4) \frac{sh^2}{2} \\ & + s^2 \left(\frac{1}{4} v^2 \lambda_m + \frac{1}{2} \mu_s^2 + \frac{3}{2} \lambda_s v_s^2 + \mu_3 v_s \right) + \frac{\lambda}{4} h^4 + \lambda v h^3 \\ & + \frac{\lambda_m v}{2} h s^2 + \left(\lambda_m v_s + \frac{\mu_4}{2} \right) h s + \frac{\lambda_s}{4} s^4 + s^3 \left(\frac{\mu_3}{3} + \lambda_s v_s \right). \end{aligned} \quad (4.45)$$

In particular, from the tadpole conditions, we find out

$$-\frac{1}{2} v^2 \lambda_m v_s - \lambda_s v_s^3 - \mu_s^2 v_s - \mu_3 v_s^2 - \frac{\mu_4 v^2}{2} = 0, \quad (4.46)$$

$$-\mu_h^2 v - \frac{1}{2} v \lambda_m v_s^2 - \lambda v^3 - v_s v \mu_4 = 0, \quad (4.47)$$

and so the Higgs and the singlets masses follows as

$$\frac{m_s^2}{2} = \lambda_s v_s^2 + \frac{\mu_3 v_s}{2} - \frac{\mu_4 v^2}{4 v_s} \rightarrow \boxed{m_s^2 = 2\lambda_s v_s^2 + \mu_3 v_s - \frac{\mu_4 v^2}{4 v_s}}, \quad (4.48)$$

$$\frac{m_h^2}{2} = \lambda v^2 \rightarrow \boxed{m_h^2 = 2\lambda v^2}. \quad (4.49)$$

We now have the broken phase potential:

$$V(h, s) = \frac{1}{2}m_s^2 s^2 + \frac{1}{2}m_h^2 h^2 + \frac{h^4 \lambda}{4} + h^3 \lambda v + \frac{\lambda_m}{4} s^2 h^2 + (\lambda_m v_s + \mu_4) \frac{sh^2}{2} \quad (4.50)$$

$$+ \frac{\lambda_m v}{2} h s^2 + m_{hs}^2 h s + \frac{1}{4} s^4 \lambda_s + s^3 \left(\frac{\mu_3}{3} + \lambda_s v_s \right) ,$$

which features the mass matrix

$$M = \begin{pmatrix} m_h^2 & m_{hs}^2 \\ m_{hs}^2 & m_s^2 \end{pmatrix} = \begin{pmatrix} 2\lambda v^2 & \lambda_m v v_s + \frac{\mu_4 v}{2} \\ \lambda_m v v_s + \frac{\mu_4 v}{2} & 2\lambda_s v_s^2 + \mu_3 v_s - \frac{\mu_4 v^2}{4v_s} \end{pmatrix} . \quad (4.51)$$

Rotating to the mass eigenstates (h_1, h_2) by means of

$$\begin{pmatrix} h_1 \\ h_2 \end{pmatrix} = \begin{pmatrix} \cos \theta & -\sin \theta \\ \sin \theta & \cos \theta \end{pmatrix} \begin{pmatrix} h \\ s \end{pmatrix} , \quad \theta = \frac{1}{2} \arctan \left(\frac{2m_{hs}}{m_s - m_h} \right) , \quad (4.52)$$

we arrive to the mass eigenvalues

$$m_{1,2}^2 = \frac{1}{2} \left(m_h^2 + m_s^2 \mp (4m_{hs}^2 + (m_h^2 - m_s^2)^2)^{1/2} \right) . \quad (4.53)$$

Then, inverting the rotation matrix, we find

$$\begin{cases} h = h_1 \cos \theta + h_2 \sin \theta , \\ s = -h_1 \sin \theta + h_2 \cos \theta , \end{cases} \quad (4.54)$$

and thus, e.g. , the trilinear Higgs coupling in the mass eigenstates basis reads

$$v \lambda h^3 = v \lambda \left(h_1 \cos^3 \theta + h_2 \sin^3 \theta + 3h_1^2 h_2 \cos^2 \theta \sin \theta + 3h_2^2 h_1 \sin^2 \theta \cos \theta \right) . \quad (4.55)$$

The same way all the other terms get shifted. Thus, collecting all the couplings in front of h_1^3 (which we identify as the SM Higgs) and taking into account the symmetry factors, we are ready to write down the modified/shifted trilinear Higgs coupling, namely:

$$6 \tilde{\lambda}_3 = 6\lambda v \cos^3 \theta - (3\mu_4 + 3\lambda_m v_s) \cos^2 \theta \sin \theta \quad (4.56)$$

$$+ 3\lambda_m v \cos \theta \sin^2 \theta - \sin^3 \theta (2\mu_3 + 6v_s \lambda_s) . \quad (4.57)$$

Proceeding the same way for the four Higgs coupling, we obtain

$$4! \cdot \tilde{\lambda}_4 = 4! \cdot \left(\lambda \cos^4 \theta + \frac{\lambda_m}{2} \cos^2 \theta \sin^2 \theta + \frac{\lambda_s}{4} \sin^4 \theta \right) . \quad (4.58)$$

In particular, as a cross-check, it is possible to link this framework to the one discussed in section 4.2 by taking the limits $\mu_3, \mu_4 \rightarrow 0$, and by the assumption⁶ $y \rightarrow 0$.

⁶We remind the reader that y is identifiable with the mixing angle.

Taking the limit in which $\mu_3, \mu_4 \rightarrow 0$, we have:

$$6 \tilde{\lambda}_3 = 6\lambda v \cos^3 \theta - 3\lambda_m v_s \cos^2 \theta \sin \theta + 3\lambda_m v \cos \theta \sin^2 \theta - 6v_s \lambda_s \sin^3 \theta \simeq 6\lambda v , \quad (4.59)$$

$$4! \tilde{\lambda}_4 = 4! \cdot \left(\lambda \cos^4 \theta + \frac{\lambda_m}{2} \cos^2 \theta \sin^2 \theta + \frac{\lambda_s}{4} \sin^4 \theta \right) \simeq 4! \lambda , \quad (4.60)$$

that is, if $\theta \rightarrow 0$, then

$$\tilde{\lambda}_3 \rightarrow \lambda v \text{ then } k_3 = \frac{\lambda_3}{\lambda_{3,SM}} = 1 , \quad (4.61)$$

$$\tilde{\lambda}_4 \rightarrow \lambda \text{ then } k_4 = \frac{\lambda_4}{\lambda_{4,SM}} = 1 . \quad (4.62)$$

Eventually, we have that in this limit both c_6 and c_8 are zero at the tree level, matching the result from 4.2.

4.3.1 Integrating out the singlet via E.O.M.

Here we discuss what happens integrating out the singlet via equations of motion. As shown in section 4.2 this approach turns out to be fully equivalent to the scattering amplitude matching, therefore we will use only this for reasons of convenience.

We will thus provide an explicit expression of the c_h, c_6, c_8 at the tree-level, which turn out to be non zero, owing to the presence of explicit \mathbb{Z}_2 -breaking terms that do modify the singlet mass/VEV relation found before via tadpole conditions.

Calling back the potential and the definitions developed in 4.3, we have, after EWSB and $s \rightarrow s + v_s$

$$\begin{aligned} \mathcal{L} \supset & \frac{1}{2} \partial_\mu h \partial^\mu h + \frac{1}{2} \partial_\mu s \partial^\mu s - \frac{1}{2} m_s^2 s^2 - \frac{1}{2} m_h^2 h^2 - \frac{\lambda}{4} h^4 - \lambda v h^3 - \frac{\lambda_m}{4} s^2 h^2 \\ & - \frac{\lambda_m v_s + \mu_4}{2} s h^2 - \frac{\lambda_m v}{2} h s^2 - m_{hs}^2 h s + \frac{\lambda_s}{4} s^4 - \left(\frac{\mu_3}{3} - \lambda_s v_s \right) s^3 . \end{aligned} \quad (4.63)$$

Then, moving to the mass eigenstates already introduced, and considering the leading approximation in v/v_s (which essentially means to take the mixing angle $\theta \simeq 0$) we have

$$\begin{aligned} \mathcal{L} \supset & -\frac{1}{2} m_s^2 s^2 - \frac{1}{2} m_h^2 h^2 - \frac{\lambda}{4} h^4 + \lambda v h^3 - \frac{\lambda_m}{4} s^2 h^2 \\ & - \frac{\lambda_m v_s + \mu_4}{2} s h^2 - \frac{\lambda_s}{4} s^4 - \left(\frac{\mu_3}{3} - \lambda_s v_s \right) s^3 , \end{aligned} \quad (4.64)$$

in which only the relevant interaction terms are present.

Then, solving the equations of motion for the heavy field, and substituting the value of s_{\min} inside the Lagrangian (4.64), we obtain the effective Lagrangian containing the resulting interactions involving just the light field h .

Considering just the c_h , c_6 and c_8 relevant terms, we do have:

$$\begin{aligned}
\mathcal{L}_{\text{eff}} \supset & \frac{(\mu_4 + \lambda_m v_s)^2}{2m_s^4} h^2 \partial^\mu h \partial_\mu h & (4.65) \\
& - \left\{ \frac{\lambda_m (\mu_4 + \lambda_m v_s)^2}{16m_s^4} - \frac{\lambda_s v_s (\mu_4 + \lambda_m v_s)^3}{8m_s^6} \right\} h^6 \\
& - \frac{(\mu_4 + \lambda_m v_s)^2}{64m_s^{10}} \left\{ 2\lambda_m^2 m_s^4 - m_s^2 \lambda_s (\mu_4^2 + 14\mu_4 \lambda_m v_s + 13\lambda_m^2 v_s^2) \right. \\
& \left. + 2(9\lambda_s^2 v_s^2 - \mu_3^2) (\mu_4 + \lambda_m v_s)^2 \right\} h^8 .
\end{aligned}$$

We conclude

$$c_h/\Lambda^2 = \frac{(\mu_4 + \lambda_m v_s)^2}{m_s^4} , \quad (4.66)$$

$$c_6/\Lambda^2 = \frac{(\mu_4 + \lambda_m v_s)^2}{2m_s^4} \left(\lambda_m - 2\frac{\lambda_s v_s}{m_s^2} (\mu_4 + \lambda_m v_s) \right) , \quad (4.67)$$

$$\begin{aligned}
c_8/\Lambda^4 = & \frac{(\mu_4 + \lambda_m v_s)^2}{4m_s^{10}} \left[2\lambda_m^2 m_s^4 - m_s^2 \lambda_s (\mu_4^2 + 14\mu_4 \lambda_m v_s + 13\lambda_m^2 v_s^2) \right. & (4.68) \\
& \left. + 2(9\lambda_s^2 v_s^2 - \mu_3^2) (\mu_4 + \lambda_m v_s)^2 \right] .
\end{aligned}$$

If $\mu_3, \mu_4 \rightarrow 0$ both c_6 and c_8 are zero owing once again to the tadpole condition, which in this case simplifies as $m_s^2 = 2\lambda_s v_s^2$. Moreover, $\bar{c}_h = y^2$, so we get back to the results already obtained in section 4.2.

In this section we showed that the model with a \mathbb{Z}_2 breaking potential with spontaneous symmetry breaking induces a modification of the Higgs wave function, captured in the EFT framework by the non vanishing Wilson coefficient c_h, c_6 and c_8 . Moreover, we also showed how in the limit in which the \mathbb{Z}_2 breaking coefficients are null we recover the \mathbb{Z}_2 preserving case in which $c_6 = c_8 = 0$.

4.4 \mathbb{Z}_2 preserving potential : 1-loop matching

Finally, let us now consider the case in which only the standard model Higgs gets a VEV, moving to the 1-loop level to see how the couplings do get affected.

In this case, as opposed to 4.2, the singlet can also be a reliable DM candidate owing to the absence of (as we shall see) the $s \rightarrow hh$ interaction vertex generated after the singlet gets a VEV.

Employing the parameterization in equation (4.3) inside the potential in (4.1), it follows:

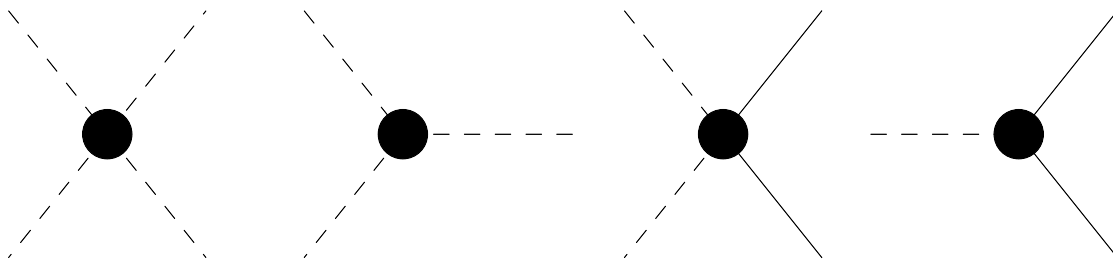


Figure 4.4: Feynman Diagrams resulting from the expansion in (4.70). The dashed lines corresponding to the standard model Higgs field, and the continuous lines with the scalar singlet field.

$$\begin{aligned}
 V(h, s) &= \left[-\frac{\mu_h^2}{2} + \frac{\lambda}{4}(v^2 + h^2 + 2hv) \right] (v^2 + h^2 + 2hv) - & (4.69) \\
 &+ \frac{\mu_s^2}{2}s^2 + \frac{\lambda_s}{4}s^4 + \frac{\lambda_m}{4}(v^2 + h^2 + 2hv)s^2 \\
 &= \left(-\frac{\mu_h^2}{2} + \frac{3}{2}\lambda v^2 \right) h^2 + (-\mu_h^2 v + \lambda v^3)h + \frac{\lambda}{4}h^4 + \lambda v h^3 \\
 &+ \left(-\frac{\mu_s^2}{2} + \frac{\lambda_m}{4}v^2 \right) s^2 + \frac{\lambda_s}{4}s^4 + \frac{\lambda_m}{4}h^2 s^2 + \frac{\lambda_m}{2}v h s^2 .
 \end{aligned}$$

After the obvious definition of the coefficients in the last row, and after imposing the tadpole condition $\mu_h^2 = 2\lambda v^2$, it follows:

$$V(h, s) \doteq \frac{m_h^2}{2}h^2 + \lambda v h^3 + \frac{\lambda}{4}h^4 + \frac{m_s^2}{2}s^2 + \frac{\lambda_s}{4}s^4 + \frac{\lambda_m}{4}h^2 s^2 + \frac{\lambda_m}{2}v h s^2 . \quad (4.70)$$

The corresponding interaction vertices are summarised by the Feynman diagrams in 4.4. It turns out that no mass mixing arises in this particular case, i.e. the mass matrix is diagonal.

4.4.1 Matching by scattering amplitudes

To correctly calculate contributions to c_6 , c_8 and c_h , we have to consider all the Feynman diagrams that generate the corresponding effective interaction vertexes after integrating out the singlet.

We can immediately see that these contributions are not found at tree level here, since six and four external SM Higgs legs connected by only internal singlets are topological impossible with this kind of interactions. This is just equivalent to take the case discussed in 4.2 in the limit in which $v_s \rightarrow 0$, where by this prescription we also see c_h to become null.

Conversely, at the 1-loop level, a non zero value for all the Wilson coefficients do arise. Starting from c_h by considering the diagrams in figure 4.5, we have, for the left one:

$$\begin{aligned} \mathcal{A}_7 \equiv B_0(p^2, m_s^2, m_s^2) &= 2 \cdot \left(-i \frac{\lambda_m v}{2} \right)^2 \int \frac{d^d \ell}{(2\pi)^d} \frac{i}{\ell^2 - m_s^2} \frac{i}{(\ell - q)^2 - m_s^2} \\ &= 2 \cdot \left(\frac{\lambda_m v}{2} \right)^2 \int \frac{d^d \ell}{(2\pi)^d} \int_0^1 dx [\ell(\ell - 2qx) + q^2 x - m_s^2]^{-2}, \end{aligned} \quad (4.71)$$

which simplifies after the substitution $\ell' = \ell - qx$ as

$$\begin{aligned} \mathcal{A}_7 &= 2 \cdot \left(\frac{\lambda_m v}{2} \right)^2 \int_0^1 dx \int \frac{d^d \ell'}{(2\pi)^d} \left[\ell'^2 - \underbrace{q^2 x^2 + q^2 x - m_s^2}_{M_s^2(x, m_s)} \right]^{-2} \\ &= 2 \cdot \left(\frac{\lambda_m v}{2} \right)^2 \frac{1}{16\pi^2} \left[\frac{1}{\epsilon} + \ln \frac{4\pi\mu^2}{m_s^2} - \int_0^1 dx \ln \left(1 + \frac{x(x-1)q^2}{m_s^2} \right) \right]. \end{aligned} \quad (4.72)$$



Figure 4.5: 1-loop contributions to the c_h coefficient.

So, the lowest order contribution from this diagram, after renormalising, is

$$\delta Z = - \frac{d\mathcal{A}_7}{dq^2} \Big|_{q^2=0} = \frac{1}{96} \frac{\lambda_m^2 v^2}{2\pi^2 m_s^2}. \quad (4.73)$$

Then, we move on calculating the second diagram. This particular one can easily be calculated adopting the cut-off regularization technique [19, 1].

Introducing Λ_c as the cut-off scale in the momenta space, we thus get:

$$\begin{aligned}
\mathcal{A}_8 \equiv B_0(p^2, m_s^2) &= 2 \cdot \frac{\lambda_m}{2} \int \frac{d^4\ell}{(2\pi)^4} \Theta(\Lambda_c^2 - \ell^2) \frac{i}{\ell_0^2 - \vec{\ell}^2 - m_s^2} \\
&= \frac{\lambda_m}{2} \int \frac{d\vec{\ell}}{(2\pi)^3} \Theta(\Lambda_c^2 - \ell^2) \frac{1}{\sqrt{\ell^2 + m_s^2}} \\
&= \frac{\lambda_m}{2\pi^2} \int_0^{\Lambda_c} d\ell \frac{\ell^2}{\sqrt{\ell^2 + m_s^2}} \\
&= \frac{\lambda_m}{4\pi^2} \left\{ \Lambda_c^2 - m_s^2 \left(\ln \frac{\Lambda_c^2}{m_s^2} - \frac{1}{2} + \ln 2 \right) \right\},
\end{aligned} \tag{4.74}$$

where $\langle \rho \rangle$ is the vacuum energy expectation value.

This particular diagram is finite and momentum independent, so it does not contribute to the c_h coefficient while matching on-shell.

Thus, we match the previous computations to the corresponding contribution in the effective theory which arises by a tree level diagram involving the Wilson coefficient c_h (which modifies the Higgs wave function).

We conclude that the operator

$$\frac{c_h v^2}{2\Lambda^2} \partial^\mu h \partial_\mu h, \tag{4.75}$$

is generated at one loop with $c_h/\Lambda^2 = \lambda_m^2/96\pi^2 m_s^2$, as derived in [30].

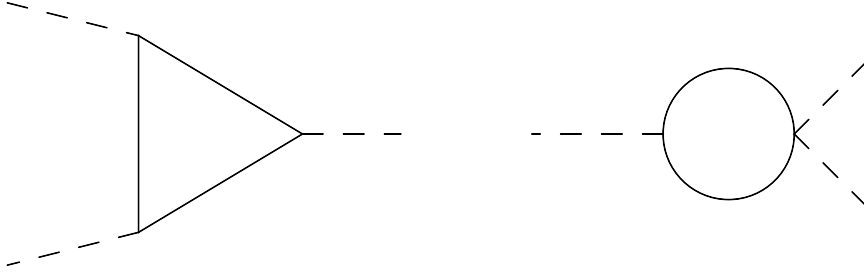


Figure 4.6: 1-loop contributions to the c_6 coefficient.

We then proceed to the calculation involving c_6 . The diagrams are shown in 4.6. Starting from the triangle, we have

$$i\mathcal{A}_9 = \left(-\frac{i\lambda_m v}{2} \right)^3 \int \frac{d^d\ell}{(2\pi)^d} \frac{i^3}{(\ell^2 - m_s^2)((\ell + p)^2 - m_s^2)((\ell - q)^2 - m_s^2)}. \tag{4.76}$$

Then, using the Feynman Parametric Formula, we get:

$$\begin{aligned}
i\mathcal{A}_9 &= 2 \left(\frac{\lambda_m v}{2} \right)^3 \int_0^1 dx \int_0^{1-x} dy \int \frac{d^d \ell}{(2\pi)^d} \left[(1-x-y)(\ell^2 - m_s^2) \right. \\
&\quad \left. + x((\ell - q)^2 - m_s^2) - y((\ell + p)^2 - m_s^2) \right]^{-3} \\
&= 2 \left(\frac{\lambda_m v}{2} \right)^3 \int_0^1 dx \int_0^{1-x} dy \int \frac{d^d \ell}{(2\pi)^d} \left[\ell^2 - m_s^2 + 2\ell(qx - py) + q^2 x + p^2 y \right]^{-3}.
\end{aligned} \tag{4.77}$$

Shifting the integration variable as $\ell' = \ell - qx + py$ reduces the amplitude to

$$\begin{aligned}
\mathcal{A}_9 &= -i 2 \left(\frac{\lambda_m v}{2} \right)^3 \int_0^1 dx \int_0^{1-x} dy \int \frac{d^d \ell}{(2\pi)^d} \left[\ell^2 - \underbrace{m_s^2 - (qx - py)^2 + q^2 x + p^2 y}_{-M_s^2(x, y, p, q)} \right]^{-3} \\
&= -\frac{1}{32\pi^2} \frac{\lambda_m^3 v^3}{4} \int_0^1 dx \int_0^{1-x} dy \left[(4\pi)^\epsilon \frac{\Gamma(1 + \epsilon)}{M_s(x, y, p, q)^{2(1+\epsilon)}} \right],
\end{aligned} \tag{4.78}$$

In particular, letting $\epsilon \rightarrow 0$, and considering the combinatorial factor of 8, we obtain:

$$\mathcal{A}_9 = -\frac{\lambda_m^3 v^3}{16\pi^2} \int_0^1 dx \int_0^{1-x} dy \frac{1}{M_s^2}. \tag{4.79}$$

Thus, we are only left with the other diagram in figure 4.6:

$$\begin{aligned}
i\mathcal{A}_{10} &= \frac{-i\lambda_m - i\lambda_m v}{4} \int \frac{d^d \ell}{(2\pi)^d} \frac{i^2}{((\ell - q)^2 - m_s^2)(\ell^2 - m_s^2)} \\
&= \frac{\lambda_m^2 v}{8} \int_0^1 dx \int \frac{d^d \ell}{(2\pi)^d} \left[(1-x)(\ell^2 - m_s^2) + x((\ell - q)^2 - m_s^2) \right]^{-2} \\
&= \frac{\lambda_m^2 v}{8} \int_0^1 dx \int \frac{d^d \ell}{(2\pi)^d} \left[\ell^2 - m_s^2 - 2kqx + q^2 x \right]^{-2} \\
&= \frac{\lambda_m^2 v}{8} \int_0^1 dx \int \frac{d^d \ell}{(2\pi)^d} \left[\ell^2 - \underbrace{q^2 x^2 - m_s^2 + q^2 x}_{-M_s^2(x, q)} \right]^{-2}.
\end{aligned} \tag{4.80}$$

Thus, with the combinatorial factor of 2, we are lead to

$$i\mathcal{A}_{10} = i \frac{\lambda_m^2 v}{64\pi^2} \left[\frac{1}{\bar{\epsilon}} + \ln \frac{4\pi\mu^2}{m_s^2} - \int_0^1 dx \ln \left(1 - \frac{x(1-x)q^2}{m_s^2} \right) \right]. \tag{4.81}$$

Summing up the the two diagrams, we obtain

$$\begin{aligned}
\mathcal{A}_9 + \mathcal{A}_{10} &= \frac{\lambda_m^2 v}{64\pi^2} \left[\frac{1}{\bar{\epsilon}} + \ln \frac{4\pi\mu^2}{m_s^2} - \int_0^1 dx \ln \left(1 - \frac{x(1-x)q^2}{m_s^2} \right) \right] \\
&\quad - \frac{\lambda_m^3 v^3}{16\pi^2} \int_0^1 dx \int_0^{1-x} dy \frac{1}{M_s^2}.
\end{aligned} \tag{4.82}$$

Then, owing to the expansion made in equation (4.7), we are legitimate to match (this time) c_6 with the sum of the two diagrams calculated above.

Considering the tree-level three point function in the EFT, already defined in 4.1.1, we have

$$-i 3! \frac{c_6 v^3}{\Lambda^2} = i\mathcal{A}_9 + i\mathcal{A}_{10} . \quad (4.83)$$

Eventually, at $q^2 = p^2 = 0$, a non zero value for c_6 appears at 1-loop:

$$c_6/\Lambda^2 = \frac{\lambda_m^3}{192\pi^2 m_s^2} . \quad (4.84)$$

Lastly, we consider the diagrams in figure 4.7, to match in the effective theory to obtain the c_8 coefficient and to finally have a full picture of the λ_4 behavior in this 8-dimensional effective theory.

Considering the first diagram on the left, it follows

$$\begin{aligned} i\mathcal{A}_{11} &= \left(\frac{\lambda_m v}{2}\right)^4 \int \frac{d^d \ell}{(2\pi)^d} \frac{1}{(\ell^2 - m_s^2)((\ell + p)^2 - m_s^2)((\ell - q)^2 - m_s^2)((\ell + k)^2 - m_s^2)} \quad (4.85) \\ &= \int_{\ell} \int_{x,y,z} \left[\ell^2 - m_s^2 - x(2\ell p + p^2) + y(2\ell(p + q) + p^2 - q^2) \right. \\ &\quad \left. - z(2\ell(q + k) - q^2 + k^2) \right]^{-4} \\ &= \int_{\ell} \int_{x,y,z} \left[\ell(\ell - 2(p(x + y) + q(y - z) - kz) - p^2(x - y) - q^2(y - z) - k^2 z) \right]^{-4} \\ &= \int_{\ell} \int_{x,y,z} \left\{ \left[\ell - (p(x - y) + q(y - z) - kz) \right] \left[\ell + (p(x - y) + q(y - z) - kz) \right] \right. \\ &\quad \left. - p^2(x - y) - q^2(y - z) - k^2 z \right\}^{-4} \\ &= \int_{\ell} \int_{x,y,z} \left\{ \underbrace{\ell^2 - m_s^2 - (p(x - y) + q(y - z) - kz)^2 - p^2(x - y) - q^2(y - z) - k^2 z}_{-M_s^2(x,y,z,p,q,k,m_s^2)} \right\}^{-4} \\ &= 6 \left(\frac{\lambda_m v}{2}\right)^4 \int \frac{d^d \ell}{(2\pi)^d} \int_0^1 dx \int_0^{1-x} dy \int_0^{1-y} dz \left[\ell^2 - M_s^2 \right]^{-4} \\ &= \frac{6}{16\pi^2} \left(\frac{\lambda_m v}{2}\right)^4 \int_0^1 dx \int_0^{1-x} dy \int_0^{1-y} dz M_s^{-4} . \end{aligned}$$

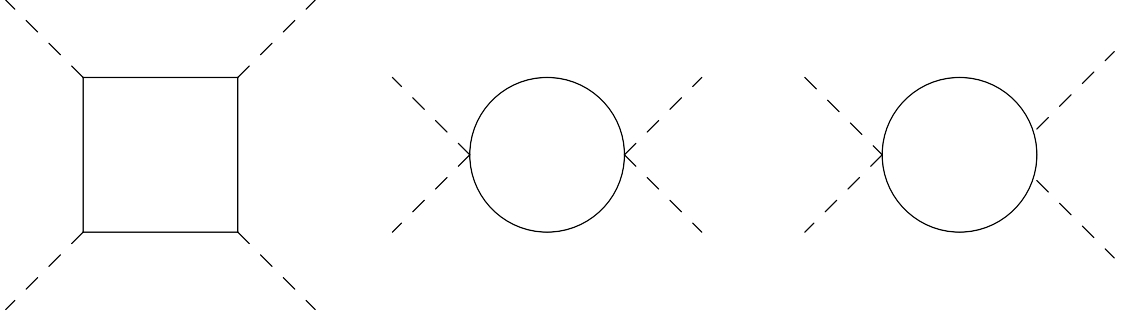


Figure 4.7: 1-loop contributions to the c_8 coefficient.

While the second diagram gives

$$\begin{aligned}
i\mathcal{A}_{12} &= \frac{\lambda_m^2}{16} \int \frac{d^d \ell}{(2\pi)^d} \frac{1}{(\ell^2 - m_s^2)((\ell - p)^2 - m_s^2)} \\
&= \frac{\lambda_m^2}{16} \int \frac{d^d \ell}{(2\pi)^d} \int_0^1 dx \left(\ell(\ell - 2px) - m_s^2 + p^2 x \right)^{-2} \\
&= \frac{\lambda_m^2}{16} \int \frac{d^d \ell}{(2\pi)^d} \int_0^1 dx \left(\ell^2 - p^2 x^2 - m_s^2 + p^2 x \right)^{-2} \\
&= \frac{\lambda_m^2}{16} \frac{i}{16\pi^2} \left\{ \frac{1}{\bar{\epsilon}} + \ln 4\pi\mu^2 - \int_0^1 dx \ln(q^2 x^2 + m_s^2 - q^2 x) \right\}.
\end{aligned} \tag{4.86}$$

Finally, the last diagram gives

$$\begin{aligned}
i\mathcal{A}_{13} &= \left(-i \frac{\lambda_m}{4} \right) \left(-\frac{i\lambda_m v}{2} \right)^2 \int \frac{d^d \ell}{(2\pi)^d} \frac{i^3}{(\ell^2 - m_s^2)((\ell + p)^2 - m_s^2)((\ell - q)^2 - m_s^2)} \\
&= 2 \left(\frac{\lambda_m^3 v^2}{16} \right) \int_0^1 dx \int_0^{1-x} dy \int \frac{d^d \ell}{(2\pi)^d} \left\{ \ell^2 - m_s^2 + 2\ell(qx - py) + q^2 x + p^2 y \right\}^{-3} \\
&= 2 \left(\frac{\lambda_m^3 v^2}{16} \right) \int_0^1 dx \int_0^{1-x} dy \int \frac{d^d \ell}{(2\pi)^d} \left\{ \ell^2 - \underbrace{m_s^2 - (qx - py)^2 + q^2 x + p^2 y}_{M_s^2(x,y,p,q)} \right\}^{-3} \\
&= \frac{1}{16\pi^2} \left(\frac{\lambda_m^3 v^2}{8} \right) \int_0^1 dx \int_0^{1-x} dy \left[(4\pi)^\epsilon \frac{\Gamma(1+\epsilon)}{M_s(x,y,p,q)^{2(1+\epsilon)}} \right],
\end{aligned} \tag{4.87}$$

so that, letting $\epsilon \rightarrow 0$, we obtain:

$$\mathcal{A}_{13} = \frac{1}{16\pi^2} \frac{\lambda_m^3 v^2}{8} \int_0^1 dx \int_0^{1-x} dy \frac{1}{M_s^2}. \tag{4.88}$$

Summing up the results for $p, q, k = 0$, with the related combinatorial factor, we find

$$\mathcal{A}_{11} + \mathcal{A}_{12} + \mathcal{A}_{13} = -\frac{\lambda_m^2}{16\pi^2} \left[\frac{1}{\bar{\epsilon}} + \ln \frac{4\pi\mu^2}{m_s^2} \right] + \frac{1}{8\pi^2} \frac{(\lambda_m v)^4}{m_s^4} + \frac{\lambda_m^3 v^2}{16\pi^2 m_s^2}. \tag{4.89}$$

Then, we repeat the procedure already employed for c_6 . Considering the EFT tree level contributions arising from the 8-dimensional operator, we have

$$\mathcal{A}_6 + \mathcal{A}_7 + \mathcal{A}_8 = 4! \frac{c_8 v^4}{\Lambda^4} . \quad (4.90)$$

Then, using the minimal subtraction scheme, and matching on $\mu = m_s$, we are left with

$$c_8/\Lambda^4 = \frac{1}{v^2 m_s^2} \frac{\lambda_m^3}{16 \cdot 4! \cdot \pi^2} \left(1 + \frac{2\lambda_m v^2}{m_s^2} \right) . \quad (4.91)$$

4.5 Singlet models showdown

To better rearrange the whole discussion and to make evident the EFT structure concerning the singlet models analysed, here we summarize all of the results for c_h and c_6 obtained in the chapter⁷.

We discussed the \mathbb{Z}_2 -breaking potential

$$V(\Phi, s) = \mu_h^2 |\Phi|^2 + \lambda |\Phi|^4 + \frac{\mu_s^2}{2} s^2 + \frac{\lambda_m}{2} |\Phi|^2 s^2 + \frac{\mu_3}{3} s^3 + \frac{\lambda_s}{4} s^4 + \mu_4 |\Phi|^2 s . \quad (4.92)$$

in the case in which the singlet and the Higgs fields do acquire a VEV.

We also discussed the \mathbb{Z}_2 -preserving potential⁸

$$V(\Phi, s) = -\mu_h^2 |\Phi|^2 + \lambda |\Phi|^4 - \frac{\mu_s^2}{2} s^2 + \frac{\lambda_s}{4} s^4 + \frac{\lambda_m}{2} |\Phi|^2 s^2 , \quad (4.93)$$

with the Higgs always acquiring a VEV, and the singlet acquiring a VEV or less.

It is easy to see that c_6 and c_8 cannot be generated at tree-level if the potential is \mathbb{Z}_2 symmetric (see sections 4.2 , 4.4). Moreover, it turns out that every c_{2n} coefficient of the effective theory would be null in this case. Nevertheless, moving to next orders in perturbation theory, we find these coefficients to be non zero. We also have that c_h is generated at tree-level only if mixing occurs between the Higgs and the singlet⁹(see section 4.2). If this is not the case, we have c_h generated at 1-loop (see section 4.4).

Conversely, the explicit \mathbb{Z}_2 breaking scenarios do always supply non zero values for the Wilson coefficients, also if we take the limit of vanishing singlet VEV (see section 4.3).

All the formulas in the following table are featuring a non zero VEV v_s for the singlet are valid under the hypothesis of $v_s \gg v$, with v the Higgs field VEV. We also include the \mathbb{Z}_2 -breaking potential in the $v_s \rightarrow 0$ case, in which we can still find non vanishing values for the Wilson coefficients of the effective theory.

⁷ c_8 is missing mainly as its not relevant for the two next chapters. The long expression (see (4.66) would also be difficult to display clearly here.

⁸Which can be obtained taking the limit $\mu_3, \mu_4 \rightarrow 0$ and inverting the Higgs and singlet mass signs.

⁹That is the case in which both the fields acquire a VEV.

tree-level	c_h/Λ^2	c_6/Λ^2
$V_{\mathbb{Z}_2}, v_s = 0$	0	0
$V_{\mathbb{Z}_2}, v_s \neq 0$	$\lambda_m^2 v_s^2/m_s^4$	0
$V_{\mathbb{Z}_2}, v_s = 0$	μ_4^2/m_s^4	$\lambda_m \mu_4^2/2m_s^4$
$V_{\mathbb{Z}_2}, v_s \neq 0$	$(\lambda_m v_s + \mu_4)^2/m_s^4$	$\kappa \left(\lambda_m - 2 \frac{\lambda_s v_s}{m_s^2} (\mu_4 + \lambda_m v_s) \right)$
1-loop	c_h/Λ^2	c_6/Λ^2
$V_{\mathbb{Z}_2}, v_s = 0$	$\lambda_m^2/96\pi^2 m_s^2$	$\lambda_m^3/192\pi^2 m_s^2$

where

$$\kappa = \frac{(\mu_4 + \lambda_m v_s)^2}{2m_s^4}.$$

5.1 Introduction

The matter/antimatter asymmetry of today's universe remains still an open issue: the ratio between matter and radiation, which characterizes this asymmetry, is¹ $\eta = (n_B - n_{\bar{B}})/n_\gamma \sim 6,14 \cdot 10^{-10}$.

We expect inflation to produce an equal number of particles and antiparticles, as any existing asymmetry found before will be diluted by the large amount of entropy generated in the reheating phase.

We could also expect to have a large scale universe populated with regions in which baryons and antibaryons are separately dominating. Anyhow, this would directly translate in a rate of annihilation between baryons and antibaryons dominated region, owing to the large hydrogen gas clouds observed[33] between galaxy clusters. Eventually, this should produce a large amount of observed gamma rays which are not observed.

The first explanation of the observed Baryon Asymmetry of the Universe (BAU) was given by Sakharov and his famous mechanism of baryogenesis. As we already introduced in 2.4, the necessary conditions, the Sakharov conditions, to any baryogenesis to occur are

- Baryon number violation.
- \mathcal{CP} and \mathcal{C} - violation.
- Absence of thermal equilibrium.

It turns out that the SM is in principle capable of accommodating these three conditions, and that the baryogenesis occurs during the electroweak phase transition. However,

¹ n is for density of B-baryons, \bar{B} -antibaryons, and γ -photons

the actual parameters of the SM (masses and couplings) are such that, while met, such conditions do not generate enough BAO. First, an additional source of \mathcal{CP} -violation is required. Second, the mass of the Higgs is too light (and so the self-coupling is too small) to achieve a strong first order electroweak phase transition necessary to accommodate a departure from thermal equilibrium. This necessarily forces us to the introduction of new BSM physics at the electroweak scale.

First of all, we give a basic description of how the three Sakharov conditions are found in the SM [33, 34] in Section 5.2. An important role in the determination of the phase transition is given by the study of the effective potential for the Higgs field, including thermal effects.

Hence, we first discuss in Section 5.3 the Coleman-Weinberg potential for a scalar QED model, and we re-derive in details the symmetry breaking mechanism via radiative corrections.

Then we review the finite temperature corrections to the 1-loop effective potential in Section 5.4 following [35, 34].

Finally, in Section 5.5 we proceed by discussing the singlet real scalar extension of the SM with \mathbb{Z}_2 symmetric potential (described in the section 4.4) as a possible BSM scenario to realize a strong first order EWPT.

We investigate the conditions to achieve the SFOPT in such BSM theory and we reproduce independently results already existing in the literature (see e.g. [29]).

5.2 Sakharov conditions in the standard model

5.2.1 Baryon number violation

In the SM we understand baryon number violation to occur via the SPHALERON PROCESS. The starting point is the ADLER-BELL-JACKIW ANOMALY concerning the axial currents in gauge theories. The process in figure 5.1 (that is the sphaleron process) with 3 left-handed leptons (one for each generation) and 9 left-handed quark ($\text{SU}(2)$ doublets, three for each generation), is indeed possible according to the baryon/lepton current²[33, 36, 2]

$$\partial_\mu J_{\text{B}_L+\text{L}_L}^\mu = \frac{3g^2}{32\pi^2} \epsilon_{\alpha\beta\gamma\delta} W_a^{\alpha\beta} W_a^{\gamma\delta}. \quad (5.1)$$

Here g is the $\text{SU}(2)$ coupling and $W^{\mu\nu a}$ is the $\text{SU}(2)$ non-abelian strength tensor. From this process results a baryon number violation of three³.

This baryon number violation occurs in every perturbative process, and is associated with the vacuum structure of the SM. More precisely, the violation is due to the vacuum structure of spontaneously broken $\text{SU}(N)$ gauge theories [39, 36, 40].

²Conversely, the difference between the total number of baryons and leptons $\text{B} - \text{L}$ and the related $J_{\text{B}_L-\text{L}_L}^\mu$ current vanish in the sphaleron process, and so we also have $\Delta\text{B} = \Delta\text{L}$.

³A similar scenario is also found in GUT and supersymmetric theories [37, 38].

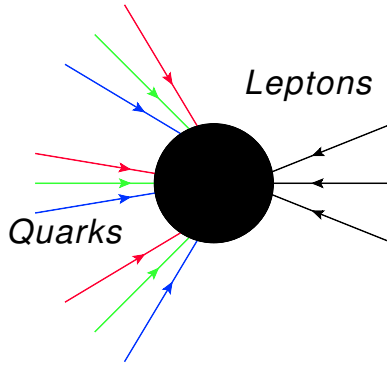


Figure 5.1: The sphaleron process. We see a total of 9 quarks in the initial and 3 leptons in the final states, leading to the baryon asymmetry.

To explain this fact we introduce the Chern-Simons number N_{CS} [41], which is obtained from the current

$$K^\mu = \frac{g^2}{32\pi^2} \epsilon^{\mu\nu\alpha\beta} \left(W_{\nu\alpha}^a A_\beta^a - \frac{g}{3} \epsilon_{abc} A_\nu^a A_\alpha^b A_\beta^c \right) , \quad (5.2)$$

as

$$N_{\text{CS}} = \int d\vec{x} K^0(t, \vec{x}) . \quad (5.3)$$

The Chern-Simons current K^μ features the property

$$\partial_\mu K^\mu = \frac{g^2}{32\pi^2} W_{\mu\nu}^a \tilde{W}_a^{\mu\nu} , \quad (5.4)$$

where

$$\tilde{W}_a^{\mu\nu} = \frac{1}{2} \epsilon^{\mu\nu\delta\gamma} W_{\delta\gamma a} . \quad (5.5)$$

The *topological* nature of the Chern-Simons number becomes clear considering pure gauge configurations at some fixed times.

Labeling these fixed times as t_2 and t_1 and evaluating the difference

$$N_{\text{CS}}(t_2) - N_{\text{CS}}(t_1) = \int_{t_1}^{t_2} dt \int d^3x \partial_\mu K^\mu = \nu , \quad (5.6)$$

we have that ν is found to be always an integer, which is a winding number. It is also possible to demonstrate that in correspondence of these integer values we find the degenerate vacuum states⁴ of the system [41, 33].

We can think at the gauge field $A^\mu(x)$ as a map between the physical space and the manifold of the gauge group⁵ $\text{SU}(2)$. Given a family of static gauge configurations with

⁴These states are characterised by vanishing energy and field strength tensor.

⁵From now on we will restrict our considerations to the $\text{SU}(2)$ gauge group, as we are interested to connections between the C-S current/number and the ABJ current.

N_{CS} continuously varying, we see the strength tensor $W^{\mu\nu a}$ and the energy to be zero in the degenerate vacua, but in every configuration between $(\nu, \nu + i)$, they are not.

It turns out that every of these vacua is a valid perturbative state of the theory [40].

Now, if we take (5.4), we see that

$$\begin{aligned} \partial^\mu K_\mu &= \frac{g^2}{32\pi^2} \epsilon_{\mu\nu\alpha\beta} \left\{ \partial^\mu W_{\nu\alpha}^a A_\beta^a + W_{\nu\alpha}^a \partial_\mu A_\beta^a \right. \\ &\quad \left. - \frac{g}{3} \epsilon_{abc} \left(\partial_\mu A_\nu^a A_\alpha^b A_\beta^c + A_\nu^a \partial_\mu A_\alpha^b A_\beta^c + A_\nu^a A_\alpha^b \partial_\mu A_\beta^c \right) \right\} \\ &= \frac{g^2}{32\pi^2} \epsilon^{\mu\nu\alpha\beta} W_{\alpha\beta}^a W_{\mu\nu}^a = \frac{g^2}{32\pi^2} W^{\alpha\beta a} \tilde{W}_{\alpha\beta}^a, \end{aligned} \quad (5.7)$$

and so

$$\partial_\mu J_{\text{B}+\text{L}}^\mu = N_f \partial_\mu K^\mu. \quad (5.8)$$

Here N_f is the number of families, which in the present case is 3 as the generations of quarks and leptons.

Now, integrating the equation above in space time on both sides, we have⁶

$$\int dt \int d\vec{x} \left[\partial_t J_{\text{B}+\text{L}}^0 - \vec{\nabla} \cdot \vec{J}_{\text{B}+\text{L}} \right] = N_f \int dt \int d\vec{x} \left[\partial_t K^0 - \vec{\nabla} \cdot \vec{K} \right] \quad (5.9)$$

$$\frac{d}{dt} \int dt \int d\vec{x} J_{\text{B}+\text{L}}^0 = N_f \frac{d}{dt} N_{\text{CS}}, \quad (5.10)$$

$$\text{and so it follows : } 3 \frac{d}{dT} N_{\text{CS}} = \frac{d}{dT} N_{\text{B}} = \frac{d}{dT} N_{\text{L}}. \quad (5.11)$$

We conveniently defined the number of baryons and leptons in the last equation.

From this equation we understand a violation of three units in the baryon and lepton number. It was demonstrated that this violations occur as a consequence of tunnel effects between two neighbors degenerate vacua.

The field configurations involved in the tunneling process are called instantons, and are defined as the field configurations fulfilling the classical EOM in Euclidean space-time.

The amplitude of tunneling was calculated in [42] and turns out to be proportional to the energy gap between the degenerate vacua considered. Considering e.g. two next neighbors it was found [33] that the tunneling amplitude is $E \sim 10^{-173}$, which is extremely small. This amplitude would not be sufficient to generate any kind of baryon number violation in the early universe.

The scenario changes if we keep in mind finite temperature effects. At higher temperature quantum fluctuations support the possibility to *jump* over the energy barriers instead of tunneling through. This behavior gives rise to the sphaleron process, which is illustrated in Figure 5.1. This process requires at least a temperature of $\sim 100\text{GeV}$ to occur[14], and the thermal hopping must pass at least one time next to the sphaleron energy, which is defined as the max value between the two vacua⁷.

⁶The spatial divergences integrate to zero.

⁷This just acquires as long as $T \geq E_{\text{sph}}$. If $T \gg E_{\text{sph}}$ this conditions has not to be fulfilled anymore.

The rate of *hopping* can be written down starting from the energy gap proportional amplitude as [33]

$$\frac{\Gamma}{V} = k \left(\frac{E_{\text{sph}}}{T} \right)^3 \left(\frac{M_W(T)}{T} \right)^4 T^4 e^{-E_{\text{sph}}/T}, \quad (5.12)$$

which is valid as long as $T < E_{\text{sph}}$. In fact, as this condition is not fulfilled, EWSB does not occur, and so the M_W mass is not defined. To determine this ratio above the EWPT it is necessary to appeal lattice simulations, as an analytic expression is still not found. The result has been fixed by [43] as $\Gamma/V = (1.06 \pm 0.08) \times 10^{-6} T^4$. Then, looking to when the sphalerons were in thermal equilibrium, we assume a thermal volume of $1/T^3$ for each particle inside the thermal bath, so that $\Gamma \sim 10^{-6} T$. Finally, comparing this expression to the Hubble expansion rate, we see the equilibrium temperature to be⁸

$$\Gamma = H \sim \frac{\sqrt{g^*} T^2}{M_P} \rightarrow T \simeq 10^{-6} \sqrt{g^*} M_P \sim 10^{13} \text{ GeV}, \quad (5.13)$$

and so baryogenesis to be affected from the sphaleron process if it is occurring in the GUT era.

5.2.2 \mathcal{CP} -violation from the Quark sector

As we introduced in 2.3, the only \mathcal{CP} -violation source of the SM is the CKM mixing matrix defined in (2.71), in particular, the only free KM-phase embedded in the definition. To really understand how much \mathcal{CP} -violation we do have in the SM it is necessary to define an invariant phase, i.e. a phase that can not be removed by transformations acting on the fields or on the Lagrangian.

Invariant phase: As an example, let's consider a scalar theory described by

$$\mathcal{L} = -\mu^2 \Phi^2 + g \Phi^4 + \text{h.c.} . \quad (5.14)$$

Then, the \mathcal{CP} transformation acts as

$$\mathcal{L} \rightarrow \mathcal{L}_{cpv} = -\mu^2 (\Phi^2)^* + g (\Phi^4)^* + \text{h.c.} , \quad (5.15)$$

and thus, if μ^2 and g are not both real, these terms are not \mathcal{CP} -invariant.

Then, explicitly writing

$$\mu^2 = -|\mu|^2 e^{i\alpha} \quad | \quad g = |g| e^{i\beta} ,$$

we do have

$$\mathcal{L} = -|\mu|^2 e^{i\alpha} \Phi^2 + |g| e^{i\beta} \Phi^4 + \text{h.c.} . \quad (5.16)$$

So, we see that is possible to eliminate the phase on the squared field term by the redefinition $\Phi \rightarrow e^{-i\alpha/2} \Phi$. Nevertheless, this leads us to

$$\mathcal{L} \rightarrow \mathcal{L}_{cpv} = -|\mu|^2 \Phi^2 + |g| e^{i(\beta-2\alpha)} \Phi^4 + \text{h.c.} , \quad (5.17)$$

⁸ M_p is the Plank mass, g^* is the number of degrees of freedom at T .

where now $\gamma = \beta - 2\alpha$ should be defined as the invariant phase according to the definition given above.

Turning back to the CKM matrix, the corresponding invariant phase turns out to be not uniquely defined, as it is process dependent. In [44] a next-to-general procedure to extrapolate this phase was developed by calculating the determinant between the up and down quarks squared mass matrices, i.e.

$$J = \det\{[m_{up}^2, m_{dw}^2]\} . \quad (5.18)$$

Starting from this equation it is possible to show that SM is not provided with enough \mathcal{CP} -violation to let EWBG occur. In fact, trying to define a dimensionless measure, we can consider the ratio J/T^2 . In particular, taking T to match the lower bound necessary for EWPT, we obtain $J/T^2 \sim 10^{-20}$. As the observed BAU is estimate by $\eta \sim 10^{-10}$, there is no chance for the SM to account to the full \mathcal{CP} -violation required [33].

Additional discussions on how precise (and *good*) is this definition of J can be found in [44, 45, 46].

5.2.3 Departure from Thermal Equilibrium: Strong First Order Phase Transition

This last requisite is the least easy to obtain. Going out of thermal equilibrium, in fact, requires the EWPT to be strongly of first order (SFOPT), otherwise the magnitude of the SM couplings is not sufficiently small to let the transition occur[34].

The type of transition can be seen by the behavior of the Higgs Effective Potential at finite temperature, which will be extensively discussed in the next section. In particular:

IN THE FOPT, THE POTENTIAL DEVELOPS A BUMP IN CORRESPONDENCE OF THE CRITICAL TEMPERATURE. THIS BUMP SEPARATES THE BROKEN AND SYMMETRIC PHASES. WE THEN CAN DISTINGUISH THREE DEGENERATE VACUA CONFIGURATIONS IN THE BROKEN PHASE, AND ONLY ONE VACUUM IN THE SYMMETRIC ONE, WITH THE TRANSITION PROCEEDING BY THE EXPANSION OF BROKEN PHASE BUBBLES VIA NUCLEATION.

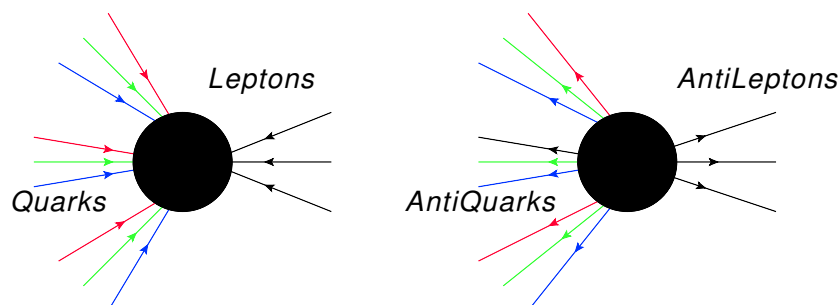


Figure 5.2: The Sphaleron Process

The Higgs VEV and all the SM particles masses are non vanishing inside the bubble, while in the external side the VEV and SM masses are still vanishing, so that sphalerons are in equilibrium.

Then, the process follows in these steps:

1. in the inside \mathcal{CP} -violating interactions do bias different quantum reflections of right/left-handed quarks, generating a chiral asymmetry with more $q_L + \bar{q}_R$ than $q_R + \bar{q}_L$.
2. The contrary just happens on the outside.
3. The sphaleron process relax this \mathcal{CP} asymmetry, as sphalerons do just interact with left handed particles.
4. The processes described by the two diagrams in figure 5.2 occur with different rates. The first causes a baryon number violation of -3 , while the second of $\Delta B = 3$. As the one on left is slower [13], we see the \mathcal{CP} -asymmetry to be converted into a Baryon asymmetry in front of the wall, while keeping the internal side untouched owing to the Higgs VEV magnitude.

We are thus left to the calculation of the Effective potential and the critical temperature identification.

5.3 The Effective Potential

Here we write down the Finite Temperature Effective Potential in all of its components, starting from the definition of the 1-loop Coleman-Weinberg potential, proceeding with finite temperature effects, and ending with Daisy correction, necessary to avoid infrared divergences occurring in the Higgs and Goldstone Bosons propagators.

5.3.1 Symmetry breaking via radiative corrections: the Coleman-Weinberg potential

The Coleman-Weinberg potential [47] can be easily derived in a scalar QED picture where just a small scalar mass is took into account, leaving aside possible Proca mass terms. Then, playing with this mass sign, one asks if it is possible to get the Lagrangian symmetry spontaneously broken.

The starting point is

$$\mathcal{L} = -\frac{1}{4}F^{\mu\nu}F_{\mu\nu} + (D^\mu\Phi)^\dagger(D_\mu\Phi) - m^2\Phi^\dagger\Phi - \frac{\lambda}{6}(\Phi^\dagger\Phi)^2. \quad (5.19)$$

The coupling between scalar and vector bosons is embedded in the covariant derivative, which is defined as

$$D^\mu\Phi(x) = (\partial^\mu + ieA^\mu(x))\Phi(x). \quad (5.20)$$

Here e stands for the electric charge of the complex scalar field. We can immediately find the minimal configuration for the field Φ . If we take $m^2 = -\mu^2 < 0$, it follows

$$\Phi_0^\dagger \Phi_0 = \frac{3}{\lambda} \mu^2 . \quad (5.21)$$

Then, we can actually say that $\mu^2 = \frac{\lambda}{3} \Phi_0^2$, and proceed to expand the Lagrangian around this constant field configuration. For this task, we introduce two real scalar fields σ, π , and we let

$$\Phi \rightarrow \Phi_0 + \frac{1}{\sqrt{2}}(\sigma(x) + i\pi(x)) . \quad (5.22)$$

Then, we have to work out all the single parts of the Lagrangian. Starting with the kinetical term, we find

$$\begin{aligned} (D^\mu \Phi)^\dagger D_\mu \Phi &= \partial^\mu \Phi^\dagger \partial_\mu \Phi + e^2 A^\mu A_\mu \Phi^\dagger \Phi + ieA\Phi^\dagger \overleftrightarrow{\partial} \Phi \\ &= \partial^\mu \left(\Phi_0 + \frac{1}{\sqrt{2}}(\sigma(x) - i\pi(x)) \right) \partial_\mu \left(\Phi_0 + \frac{1}{\sqrt{2}}(\sigma(x) + i\pi(x)) \right) \\ &\quad + e^2 A^\mu A_\mu \left(\Phi_0 + \frac{1}{\sqrt{2}}(\sigma(x) - i\pi(x)) \right) \left(\Phi_0 + \frac{1}{\sqrt{2}}(\sigma(x) + i\pi(x)) \right) \\ &\quad + ieA \left(\Phi_0 + \frac{1}{\sqrt{2}}(\sigma(x) - i\pi(x)) \right) \overleftrightarrow{\partial} \left(\Phi_0 + \frac{1}{\sqrt{2}}(\sigma(x) + i\pi(x)) \right) \\ &= \frac{1}{2} \partial^\mu \sigma \partial_\mu \sigma + \frac{1}{2} \partial^\mu \pi \partial_\mu \pi + \frac{e}{\sqrt{2}} A_\mu (\sigma \partial^\mu \pi - \pi \partial^\mu \sigma) + e^2 \Phi_0^2 A^2 \\ &\quad + \sqrt{2} e^2 \Phi_0 A^2 \sigma + \frac{e^2}{2} A^2 (\sigma^2 + \pi^2) . \end{aligned} \quad (5.23)$$

Then, using the fact that

$$\Phi^\dagger \Phi = \Phi_0^2 + \frac{\sigma^2}{2} + \sqrt{2} \Phi_0 \sigma + \frac{\pi^2}{2} ,$$

and substituting the minimum condition, we can easily come to the full expanded Lagrangian as

$$\begin{aligned} \mathcal{L} &\doteq -\frac{1}{4} F^{\mu\nu} F_{\mu\nu} + \frac{1}{2} \partial^\mu \sigma \partial_\mu \sigma + \frac{1}{2} \partial^\mu \pi \partial_\mu \pi + \frac{e}{\sqrt{2}} A_\mu (\sigma \partial^\mu \pi - \pi \partial^\mu \sigma) \\ &\quad + e^2 \Phi_0^2 A^2 + \sqrt{2} e^2 \Phi_0 A^2 \sigma + \frac{e^2}{2} A^2 (\sigma^2 + \pi^2) \\ &\quad - \frac{\lambda}{3\sqrt{2}} \Phi_0 \sigma (\sigma^2 + \pi^2) - \frac{\lambda}{24} (\sigma^2 + \pi^2)^2 - \frac{\lambda}{3} \Phi_0^2 \sigma^2 . \end{aligned} \quad (5.24)$$

Where, embracing the Landau gauge, we neglected terms which contain $\partial_\mu A^\mu$ up to a total derivative. Now, we move to calculating the correspondent part in the Effective Potential. For this task we need to start from the definition of the Generating Functional, i.e.

$$\mathcal{Z}[J] = \int \mathcal{D}\phi \exp \left\{ i \int d^4x \mathcal{L}[\Phi] + J(x)\Phi(x) \right\} , \quad (5.25)$$

where ϕ is intended as a field in the general sense of a function from the Minkowski space to a target space. The logarithm of the generating functional Z can be identified with the total energy of the system $E[J]$. One then defines the *classical* field $\Phi_{cl}(x)$ as the expectation value of Φ on the vacuum state of the system, that can be computed as

$$\frac{\delta}{\delta J} E[J] = \frac{\int \mathcal{D}\Phi \exp\{i \int dx (\mathcal{L} + J\Phi)\} \Phi}{\int \mathcal{D}\Phi \exp\{i \int dx (\mathcal{L} + J\Phi)\}} = -\langle \Omega | \Phi(x) | \Omega \rangle_J \equiv -\Phi_{c1}(x) . \quad (5.26)$$

The EFFECTIVE ACTION is then the Legendre transform of the total energy functional $E[J]$ of the system

$$\Gamma[\Phi_{c1}(x)] = E[J] - \int dx J(x) \Phi_{c1}(x) . \quad (5.27)$$

We thus see the functional derivative of the Effective Action w.r.t the classical field being related to the source . In particular, it follows

$$\frac{\delta \Gamma}{\delta \Phi_{c1}(x)} = -J(x) \quad , \quad \boxed{J = 0 \rightarrow \frac{\delta \Gamma}{\delta \Phi_{c1}(x)} = 0} . \quad (5.28)$$

In other words, the stable states of the system are characterised by a null value of the Effective Action derivative. This can be easily seen from the definition. In fact, if $J = 0$, the effective action is precisely the total energy functional, thus if the r.h.s. of (5.28) is true, then we are in a stable state for definition. This condition can also be expressed in terms of an ordinary derivative by introducing the EFFECTIVE POTENTIAL. Factorizing out the Minkowski space volume from the integrals as $-VT$, where V stays for the spatial volume and where T it's for the time propagation interval, we come to the expression

$$\Gamma[\Phi_{c1}] = -VT \cdot \mathcal{V}_{\text{eff}}(\Phi_{c1}) , \quad (5.29)$$

and thus

$$\frac{\partial}{\partial \Phi_{cl}} \mathcal{V}_{\text{eff}}(\Phi_{cl}) = 0$$

indeed characterize the stable states of the system. The lowest energy state can be easily recognised at this point. Following the idea behind [2] the calculation of the Effective Potential follows by

$$\Gamma[\Phi_{c1}] = \frac{i}{2} \log \det \left\{ -\frac{\delta^2 \mathcal{L}}{\delta \Phi_{c1} \delta \Phi_{c1}} \right\} . \quad (5.30)$$

In most of the cases, we are dealing with determinants of Klein-Gordon like operator, so it's worth to make some remark on the calculation of this easiest case. Assuming

$$\frac{\delta^2 \mathcal{L}}{\delta \Phi_{c1} \delta \Phi_{c1}} = -k^2 + m^2 = k_E^2 + m^2 ,$$

we have

$$\begin{aligned}
i \log \det\{k_E^2 + m^2\} &= i \text{Tr} \log(k_E^2 + m^2) \\
&= iT \int \frac{d^4 k_E}{(2\pi)^4} \log(k_E^2 + m^2) \\
&= VT \frac{\Gamma(-d/2)}{(4\pi)^{d/2}} \frac{1}{m^{-d}} .
\end{aligned} \tag{5.31}$$

Thus,

$$\frac{1}{VT} \log \det\{k_E^2 + m^2\} = -i \frac{\Gamma(-d/2)}{(4\pi)^{d/2}} \frac{1}{m^{-d}} . \tag{5.32}$$

Then we have to identify the correct mass terms in the presence of the background field Φ_{c1} . We already computed the mass term for the vector boson in the case of a VEV for Φ , and the same results apply here with the identification $\Phi_0 = \Phi_{c1}$. Instead, for the scalars we have to redo the computation and expand around Φ_{c1} . We will not rewrite all the steps since the procedure is analogous.

Substituting

$$\Phi(x) \rightarrow \Phi_{c1} + \frac{1}{\sqrt{2}}(\sigma(x) + i\pi(x)) , \tag{5.33}$$

and taking the second derivatives of the new potential⁹ evaluated for Φ_{c1} , we can legitimately identify the masses

$$m_{A^\mu}^2 \rightarrow 2e^2 \Phi_{c1}^2 ; \tag{5.34}$$

$$m_\sigma^2 \rightarrow m^2 + \lambda \Phi_{c1}^2 ; \tag{5.35}$$

$$m_\pi^2 \rightarrow m^2 + \frac{\lambda}{3} \Phi_{c1}^2 . \tag{5.36}$$

From the last equation we also see the (now massive) $\pi(x)$ field to be massless if we let $\Phi_{c1} = \Phi_0$, recovering the former case.

We then move on to the evaluation of the determinants. Starting from the massive vector field, we have to write the kinetic operator in a more transparent way as

$$\begin{aligned}
-\frac{1}{4} F^{\mu\nu} F_{\mu\nu} + 2e^2 \Phi_{c1}^2 A^2 &= \frac{1}{2} A_\mu ((\square + 2e^2 \Phi_{c1}^2) g^{\mu\nu} + \partial^\mu \partial^\nu) A_\nu \\
&= \frac{1}{2} A_\mu (\square + 2e^2 \Phi_{c1}^2) A^\mu ,
\end{aligned} \tag{5.37}$$

where we used the Landau gauge condition. Three degrees of freedom are left for the massive vector field. Then, the evaluation of the path integrals follows easy by calculating the determinants of the previously introduced operators with the appropriate powers¹⁰.

⁹With respect to the A^μ, σ, π fields.

¹⁰Which follow considering the independent degrees of freedom of the fields.

We have

$$\det\{\square + 2e^2\Phi_{c1}^2\}^{-3/2} \quad ; \quad (5.38)$$

$$\det\{\square + m^2 + \lambda\Phi_{c1}^2\}^{-1/2} \quad ; \quad (5.39)$$

$$\det\left\{\square + m^2 + \frac{\lambda}{3}\Phi_{c1}^2\right\}^{-1/2} . \quad (5.40)$$

Eventually, considering $d = 4 - 2\epsilon$ space-time dimensions, we obtain

$$\mathcal{V}_{\text{eff}}(\Phi_{c1}) = -\frac{\Gamma(-d/2)}{(4\pi)^{d/2}} \left[\frac{3}{2}(2e^2\Phi_{c1}^2)^{d/2} + \frac{1}{2}(m^2 + \lambda\Phi_{c1}^2)^{d/2} + \frac{1}{2}(m^2 + \frac{\lambda}{3}\Phi_{c1}^2)^{d/2} \right] , \quad (5.41)$$

with the expansion of the Γ function being

$$\Gamma(-d/2) = \frac{1}{2} \left(\frac{1}{\epsilon} + \log 4\pi + \frac{3}{2} \right) .$$

Then, introducing the arbitrary mass scale μ , expanding the powers in the limit $\epsilon \rightarrow 0$, and employing the $\overline{\text{MS}}$ subtraction scheme, we are left with the 1-Loop renormalised Effective Potential

$$\begin{aligned} \mathcal{V}_{\text{R,eff}} = & m^2\Phi_{c1}^2 + \frac{\lambda}{6}\Phi_{c1}^4 + \frac{1}{64\pi^2} \left\{ 3(2e^2\Phi_{c1}^2)^2 \left(\ln \frac{2e^2\Phi_{c1}^2}{\mu^2} - \frac{3}{2} \right) \right. \\ & \left. + (m^2 + \lambda\Phi_{c1}^2)^2 \left(\ln \frac{m^2 + \lambda\Phi_{c1}^2}{\mu^2} - \frac{3}{2} \right) + (m^2 + \frac{\lambda}{3}\Phi_{c1}^2)^2 \left(\ln \frac{m^2 + \frac{\lambda}{3}\Phi_{c1}^2}{\mu^2} - \frac{3}{2} \right) \right\} . \end{aligned} \quad (5.42)$$

Eventually, we can see the symmetry breaking to occur via 1-loop radiative corrections letting $m \rightarrow 0$ and assuming $\lambda \propto e^4 \ll 1$, namely

$$\mathcal{V}_{\text{eff}} = \frac{\lambda}{6}\Phi_{c1}^4 + \frac{3e^4}{16\pi^2}\Phi_{c1}^4 \ln \frac{2e^2\Phi_{c1}^2}{\mu^2} . \quad (5.43)$$

Then, we find the new vacuum of the potential as

$$\frac{\partial\mathcal{V}_{\text{eff}}}{\partial\Phi_{c1}^2} = 0 \quad \rightarrow \quad \frac{\lambda}{3} + \frac{3e^4}{16\pi^2} \left(1 + 2 \ln \frac{2e^2\Phi_{c1}^2}{\mu^2} \right) = 0 , \quad (5.44)$$

and so

$$\Phi_{c1}^2 \equiv \Phi_{c1,\text{min}}^2 = \frac{\mu^2}{2e^2} \exp\left\{ -\frac{16\pi^2\lambda}{9e^4} - \frac{1}{2} \right\} , \quad (5.45)$$

confirming the symmetry breaking to occur owing to the 1-loop corrections even in the massless case. To visualize what is happening, we plot this function for $\lambda = \lambda_{SM} = 0.13$ and $e = 1$ in Figure 5.3. We end this section by including the general 1-Loop Coleman-

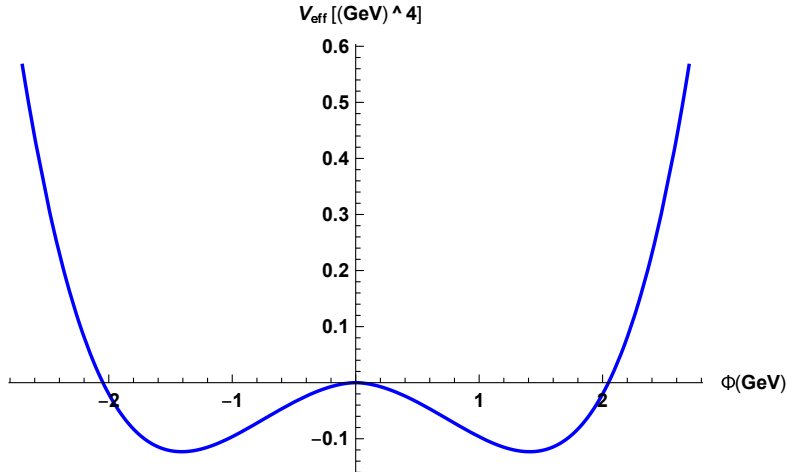


Figure 5.3: Plot of the effective potential for $m = 0$ and $\mu = 1$ TeV, highlighting the new vacua to be not in zero as in the corresponding tree-level potential.

Weinberg potential formula, which can be derived straightforwardly by extending the result showed in this section. It follows [47]:

$$V_0^1(h) = \sum_i \frac{g_i (-1)^{\mathcal{F}_i}}{64\pi^2} \left[m_i^4(h) \left(\log \frac{m_i^2(h)}{\mu^2} - \frac{3}{2} \right) \right] ; \quad (5.46)$$

which is often presented as

$$V_0^1(h) = \sum_i \frac{g_i (-1)^{\mathcal{F}_i}}{64\pi^2} \left[m_i^4(h) \left(\log \frac{m_i^2(h)}{m_i^2(v)} - \frac{3}{2} \right) + 2m_i^2(h)m_i^2(v) \right] , \quad (5.47)$$

where cut-off regularization is used and the on-shell renormalisation conditions

$$\boxed{V_0'(h)|_{h=v} = 0 \quad V_0''(h)|_{h=v} = 0} . \quad (5.48)$$

are endorsed.

This prescription turns out to be very useful, since the tree level definitions of the Higgs mass and VEV are left unmodified.

5.4 Finite Temperature Effective potential

Finite temperature QFT was firstly motivated by the study of cosmological problems [35, 34], with todays applications which are also concerning high energy physics, referring in particular on the dynamics of phase transitions.

We are specifically interested about the dynamics of phase transitions in the primordial universe. In fact, it turns out that it is indispensable to calculate the thermal

corrections to the 1-loop effective potential in order to fully understand the dynamics behind the EWPT and the related EWBG. The goal of this section will thus be to write down a full effective 1-Loop potential including temperature effects.

Following the apparatus constructed in the previous section, we can decompose the effective potential into the sum of

$$\mathcal{V}_{\text{eff}}(\Phi_{\text{c1}}) = \mathbf{V}_0^0(\Phi_{\text{c1}}) + \mathbf{V}_0^1(\Phi_{\text{c1}}) + \mathbf{V}_\beta^1(\Phi_{\text{c1}}, 1/\beta) + \mathbf{V}_r(\Phi_{\text{c1}}, 1/\beta) , \quad (5.49)$$

where the first two terms have been discussed in the previous sections. The last term is the finite temperature effective potential at 1-loop. As in previous notations, we remind that Φ_{c1} is a constant field configuration over which we expanded the original Lagrangian, that is used to identify the shifted mass terms and to perform path integration.

Now, after the introduction of the explicit $\beta = 1/T$ dependent 1-loop thermal potential correction, which is defined by

$$\mathbf{V}_\beta^1(\Phi_{\text{c1}}) = \frac{i}{VT} \ln \int \mathcal{D}\Phi_{\text{c1}} \exp \left\{ i \int d^4x \mathcal{L}_0(\Phi_{\text{c1}}, \Phi) \right\} , \quad (5.50)$$

and by endorsing the imaginary time formalism Feynman rules [34] :

- **Boson propagator:** $i/(p^2 - m^2)$ with $p^\mu = [2ni\pi\beta^{-1}, \vec{p}]$;
- **Fermion propagator:** $i/(\not{p} - m)$ with $p^\mu = [(2n + 1)i\pi\beta^{-1}, \vec{p}]$;
- **Loop integral :**

$$\frac{i}{\beta} \sum_{n=-\infty}^{\infty} \int \frac{d^3\vec{p}}{(2\pi)^3} ;$$

- **Vertex:**

$$-i\beta(2\pi)^3 \delta_{\sum_i \omega_i} \delta^{(3)} \left(\sum_i \vec{p}_i \right) ,$$

it is possible to write down the 1-loop corrected potential at non zero temperature for a $\lambda\phi^4$ theory.

Following the arguments of [47, 34, 35], we have

$$\mathbf{V}_\beta^1(\Phi_{\text{c1}}^2) = \frac{1}{2\pi^2\beta^4} \int_0^\infty dx x^2 \left(1 - e^{-\sqrt{x^2 + \beta^2 M^2(\Phi_{\text{c1}}^2)}} \right) . \quad (5.51)$$

Eventually, it is possible to extended the whole discussion to the SM by summing up all possible contributions coming from scalars, fermions, and gauge fields; namely [47, 34, 35],

$$\mathbf{V}_\beta^1(\Phi_{\text{c1}}^2) = \sum_{i=0,\pm 1,\dots} \frac{g_i (-1)^{\mathcal{F}_i}}{2\pi^2\beta^4} \int_0^\infty dx x^2 \left(1 - (-1)^{\mathcal{F}_i} e^{-\sqrt{x^2 + \beta^2 M_i^2(\Phi_{\text{c1}}^2)}} \right) . \quad (5.52)$$

Here g_i is a factor depending on the nature of fields, \mathcal{F}_i is the fermion number, and $M_i^2(\Phi_{\text{c1}}^2) = M_{0,i}^2 + a_i \Phi_{\text{c1}}^2$.

Finally, we can now resume all of the relevant coupling for the SM after parametrising $\Phi = (G^+, (h + iG^0)/\sqrt{2})$, and using h^2 as the background field. We have¹¹ [29]

$$i = t, W, Z, h, G \quad ; \quad (5.53)$$

$$M_{0,i}^2 = (0, 0, 0, -\mu_h^2, -\mu_h^2) \quad ; \quad (5.54)$$

$$a_i = \left(\frac{\lambda_t^2}{2}, \frac{g^2}{4}, \frac{g^2 + g'^2}{4}, 3\lambda, \lambda \right) ; \quad (5.55)$$

$$g_i = (12, 6, 3, 1, 1) \quad . \quad (5.56)$$

5.4.1 Daisy Resummation

It is well known that the high temperature behavior of gauge theories is unreliable from the perturbative point of view [34]. The problem is found to be related to the presence of diagrams giving $(T/M)^n$ contributions, and thus leading to a series of infrared divergences in the theory. These divergences can be *cured* by summing all the daisy/tadpole diagrams of the theory due to the interactions with the surrounding hot-phase/*plasma*. This would essentially lead us to shift the masses of the theory with a resummed masses with the structure $M(m, T) = m^2 + \Delta(T)$, with Δ to be identified according to the nature of the theory.

Taking, once again, a $\lambda\Phi^4$ as example, we have the renormalised Lagrangian

$$\mathcal{L} = \frac{1}{2}g^{\mu\nu}\partial_\mu\Phi\partial_\nu\Phi - \frac{m^2}{2}\Phi^2 - \frac{\lambda}{4!}\Phi^4 + \frac{\delta_z}{2}g^{\mu\nu}\partial_\mu\Phi\partial_\nu\Phi - \frac{\delta m^2}{2}\Phi^2 - \frac{\delta\lambda}{4!}\Phi^4. \quad (5.57)$$

Then, adding and subtracting the same temperature dependent term, we obtain

$$\mathcal{L} \supset \frac{m^2 + \Delta(T)}{2}\Phi^2 - \frac{\Delta(T)}{2}\Phi^2 + \frac{\delta m^2}{2}\Phi^2, \quad (5.58)$$

where we now consider the added term as part of the Lagrangian, while the subtracted as a 1-loop thermal counterterm. This is the essence of resummation.

The *best* value for $\Delta(T)$ can be found by imposing the 1-Loop self energy to be zero, namely

$$\Pi(p=0, \Delta(T)) - \Delta(T) = 0, \quad (5.59)$$

and by solving this "gap" equation for $\Delta(T)$.

This argument can be extended to the standard model, eventually leading to [15, 29, 34, 13, 49] as

$$\mathbf{v}_r = \sum_i \frac{T}{12\pi} \text{Tr} \left(M_i^3(h) - (M_i^2(h) - \Pi_i(0))^{3/2} \right). \quad (5.60)$$

¹¹We use the same definitions of [48].

Here i takes into account the solely Bosonic degrees of freedom, while the zero momenta self-energies are

$$\Pi_h(0) = T^2 \left(\frac{3g^2}{16} + \frac{g'^2}{16} + \frac{y_t^2}{4} + \frac{\lambda}{2} \right); \quad (5.61)$$

$$\Pi_{G.B.}(0) = \frac{11}{6} T^2 \text{diag}(g^2, g^2, g^2, g'^2), \quad (5.62)$$

with the gauge bosons mass in the unitary gauge being

$$M_{G.B.}^2(h) = \frac{h^2}{4} \begin{pmatrix} g^2 & 0 & 0 & 0 \\ 0 & g^2 & 0 & 0 \\ 0 & 0 & g^2 & -gg' \\ 0 & 0 & -gg' & g'^2 \end{pmatrix}.$$

5.5 A \mathbb{Z}_2 singlet portal for electroweak baryogenesis

As we said in 2.4, and as can be seen in [50, 15, 13], it is quite hard to introduce the strong first order phase transition in EWBG by solely using the SM. For this reason, different extended scenarios have been studied through the years to enhance this phase transition and eventually improve the \mathcal{CP} -violating sector of the SM, in order to completely satisfy the Sakharov conditions.

In the attempt to provide this enhancement, and motivated by DM searches, here we'll argue about how achieving the transition could be characterised by a BSM sector of physics containing a single $\text{SU}(3) \times \text{SU}(2) \times \text{U}(1)$ scalar singlet, referring in particular to the already introduced scenario of 4.4.

We'll demonstrate that the transition could be obtained by thermal and loop induced effects in a strongly selected region of the full theory parameter space. Every consideration regarding strength of the transition will be made by employing the condition $\boxed{v_c/T_c \geq 1}$, introduced by [29, 51], where v_c corresponds to the symmetric vacuum configuration w.r.t. to zero, at the critical temperature T_c .

We write our own code in MATHEMATICA to verify and reproduce the results of [29].

5.5.1 Phase Transition in the Full Theory

Here, a brief discussion of the underlying mechanism in the full theory framework is given: As we've discussed in the former section, it is possible to get a modification of the Higgs potential by Loop radiative corrections and finite temperature effects by introducing the effective potential at the 1-Loop order. Here, essentially, it is given by the sum of 4 terms, namely

$$\mathcal{V}_{\text{eff}}(h, 1/\beta) = \mathbf{v}_0^0(h) + \mathbf{v}_0^1(h) + \mathbf{v}_\beta^1(h, 1/\beta) + \mathbf{v}_r(h, 1/\beta), \quad (5.63)$$

where the superscript and the subscript indicates the loop order and the temperature, respectively.

Everything inside the expression is untouched w.r.t. the SM case, except the i index in the sums which now runs also over the singlet. Following the arguments of [29], we see the zero temperature contribution reducing the energy difference between the EWSB vacuum and the origin, so that, at higher temperatures the global minima of the system will be in zero.

Then, lowering the temperature and considering the loop effects from the CW potential, we eventually reach the 1-st order transition critical temperature to correspond in a three degenerate vacua configuration.

Finally, lowering further the temperature, the effective potential behavior is essentially the tree-level Higgs one, as we came up to end in the EWSB vacuum. The process is illustrated in figure 5.4.

Now, as all the thermal mass for the SM particles were already defined in 5.4, we just supply the singlet thermal mass. Considering the relevant terms in the potential

$$V(\Phi, s) \supset \frac{\mu_s^2}{2}s^2 + \frac{\lambda_m}{2}|\Phi|^2s^2 + \frac{\lambda_s}{4}s^4, \quad (5.64)$$

and by parametrizing $\Phi = (\mathbf{G}^+, (h + i\mathbf{G}^0)/\sqrt{2})$, we obtain $m_s^2 = \mu_s^2 + \frac{\lambda_m}{2}h^2$.

Also, the zero momentum self energy comes as

$$\Pi_s(0) = T^2 \left(\frac{\lambda_m}{3} + \frac{\lambda_s}{4} \right). \quad (5.65)$$

Now, it is finally time to define the viable region of parameter space to define a trustful investigation. It is found that:

- A small value of the λ_m portal coupling would not enhance the phase transition making it strongly of first order. Still, for $\lambda_m/2 \geq 2$, we are able to see this behavior. Anyhow, as pointed in [29], calculations with $\lambda_m/2 \geq 5$ may not be trustful because of perturbativity arguments.
- λ_s does almost not contribute to the phase transition in the case we're discussing, as it is not related to the singlet thermal mass. Its only appearance is inside the zero momenta self-energy tensor of the singlet, and it is found that a non zero-value of the coupling would just slightly weaken the transition. So, we proceed by considering $\lambda_s = 0$ as assumption.
- in this regime of values of λ_m and λ_s , with $\mu_s^2 > 0$ the SFOPT is occurring with a singlet thermal mass m_s range between approximately 400 and 800 GeV. Also, the transition could be possible taking into account a negative singlet squared mass $\mu_s^2 < 0$, *i.e.* the case in which both the scalars get a VEV presented in 4.2, but we will not consider this case for now, eventually excluding the related region in a final plot.
- An EFT approach would be trustful just in a more selected region of the parameter space, as the perturbativity upper bound on λ_m forces us to consider small masses compared to the regime in which an EFT is expected to be valid.

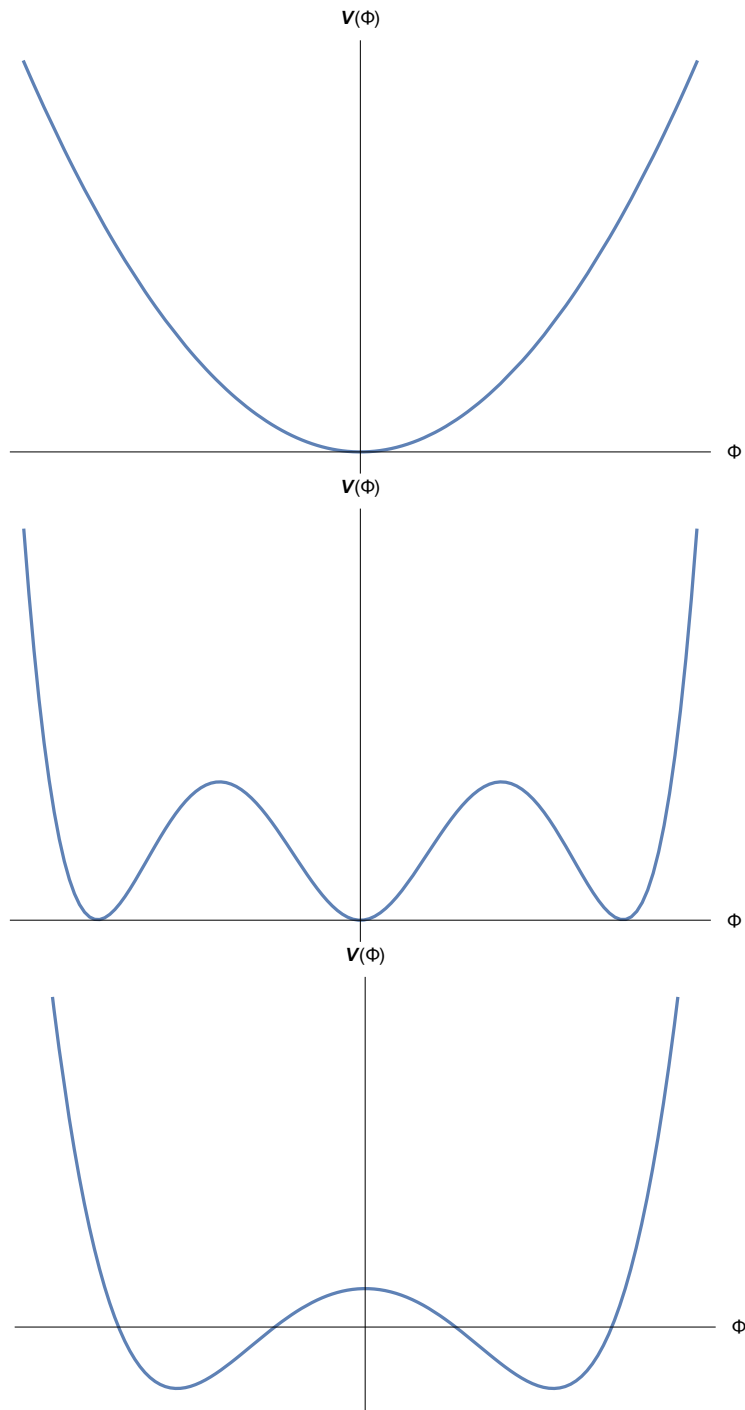


Figure 5.4: Illustrative behavior of the first order transition. The potential changes shape as a function of the temperature. In the 1st figure we see the high temperature symmetric phase. In the 2nd figure we have the three degenerate vacua corresponding to the critical temperature. In the third figure we end in the EW broken phase (the Coleman-Weinberg potential is still present).

Results This last paragraph concerns the identification of the region of the $(\lambda_m/2, m_s)$ plane in which the 1-st order 1-step phase transition takes place.

The **violet shaded region** corresponding to the strong transition, and thus are reliable for EWBG to occur. Conversely, in the white region below, the transition is still weak. Finally, the gray shaded region corresponds to $\mu_s^2 < 0$ values, which are not taken into account in the analysis.

We can see that there is a sizeable portion of parameter space where the phase transition is first order and strong. For very large λ_m one should in principle investigate whether there exist perturbativity constraints, that we do not study here (we refer to [52, 53] for such analysis).

The viable region extends from singlet mass around 400 GeV to higher masses. For large mass a larger value of λ_m is required to obtain SFOPT.

In the small singlet mass regime we expect the EFT description to not be reliable, while for large singlet mass the full theory and the EFT should reproduce the same results¹².

We will further investigate the correspondence between full theory and EFT in the next section where we will discuss the signature of this model at the LHC. In the plot in Figure 5.5 we also display the **red contours** of \bar{c}_6 which is

$$\bar{c}_6 = \frac{\lambda_m^3 v^2}{192\pi^2 \lambda m_s^2}. \quad (5.66)$$

As one can observe, the region of SFOPT span values of \bar{c}_6 leading possibly also to large deviations in the Higgs trilinear self coupling with respect to the SM value.

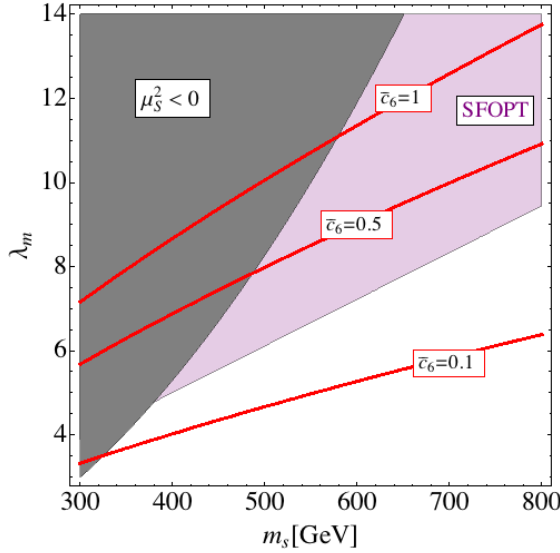


Figure 5.5: Parameter space region where the FOPT is expected to be viable.

¹²For a study of the strong first order EW phase transition in the effective theory see [54, 52].

Singlet Phenomenology at Colliders

In the previous section we identified the parameter space of the full singlet extended \mathbb{Z}_2 model where EWBG is viable. To test if this particle effectively exists, we proceed to consider collider experiment concerning some selected differential distributions of possible singlet dependent scatterings. In particular, the \mathbb{Z}_2 singlet model modifies the Higgs trilinear coupling, and hence we need to look at processes containing the corresponding interaction vertex.

The double Higgs production via gluon fusion is the most important channels of production of the Higgs particle at the LHC. It is essentially mediated by a top-quark loop which can produce the two final states Higgs, or a single s-channel virtual state decaying into two real Higgs bosons. In this process the Higgs trilinear coupling is involved. Consequently, a detailed analysis of this process can be an interesting probe of our scenario.

In this chapter we will analyze the differential distributions of Higgs pair production at the LHC in the full \mathbb{Z}_2 -preserving singlet model and in the corresponding EFT, and we compare them with the SM. For this purpose we will implement the new physics models in the framework of MADGRAPH [55].

We proceed by introducing in Section 6.1 the full singlet extended theory with the \mathbb{Z}_2 -preserving potential, arguing on how this affects the Higgs pair production at LHC, and showing how these contributions are taken into account for our simulations.

Then, the corresponding effective theory is introduced in Section 6.2 and it is discussed how the Wilson coefficients do modify the SM Higgs couplings and interactions after integrating out the singlet.

Finally, in Section 6.3, we consider several (λ_m, m_s) benchmarks identifying those where it is possible to achieve the SFOPT. We highlight the conditions under which the effective theory is capable to behave as the full theory in 6.3.1 (eventually showing how in the SFOPT region the EFT seems to be a trustful approximation), and the conditions

in which the singlet extended theory behaves differently from the SM in 6.3.2.

The results obtained in this chapter represent an original contribution of this thesis.

6.1 Full Theory Analysis

The Standard double Higgs production at LHC occurs owing to the 1-loop diagrams in figure 6.1. All quarks contribute in the loop, however, as the top is the heaviest, and so strongly coupled to the Higgs, we expect the leading contribution to belong solely from two diagrams, with the corresponding permutations.

The scattering amplitudes for the process are well known. Anyhow, as we are looking forward to implement everything in MADGRAPH, here below we will be mainly concerned in how the modifications with respect to the SM are taken into account in the analysis.

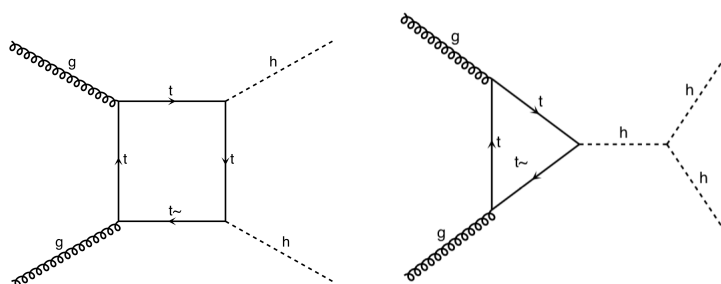


Figure 6.1:

In the \mathbb{Z}_2 -preserving singlet extended SM we see the right diagram in figure 6.1 to be modified by the singlet itself, which is running inside the loop corresponding to the trilinear Higgs vertex. Taking into account the interaction vertexes in the electroweak broken phase, we have

$$\mathcal{L} \supset \frac{\lambda_m v}{2} h s^2 + \frac{\lambda_m}{4} h^2 s^2 .$$

These interaction vertexes lead to the relevant topologies in figure 6.2, that we will include into the form factor in figure 6.3.

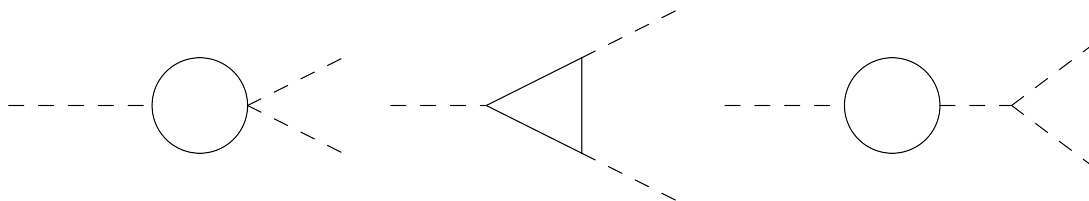


Figure 6.2: Relevant topologies to consider in the form factor

The corresponding functions in LoopTools are written¹, from left to right, as

¹the convention for Feynman diagrams as LoopTools functions is available in the user manual <http://www.feynarts.de/looptools/LT25Guide.pdf>.

1. `B0i(bb0,p1sq,ms*ms,ms*ms)`, the bubble-like function. We have three functions of this kind, one for each momenta, as other permutations of this diagrams are possible to get the same initial and final states.
2. `C0i(cc0, p1sq, p3sq, p2sq, ms*ms, ms*ms, ms*ms)`, the symmetric triangle function.
3. `1/(psqmax-MH*MH) * B0i(bb0,psqmax,ms*ms,ms*ms)`, the bubble correction to the Higgs propagator ending in the two Higgs final states via the tri-linear coupling.

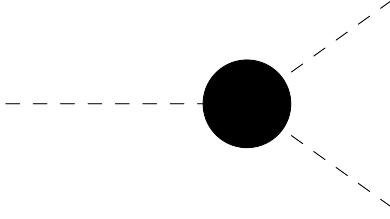


Figure 6.3: the trilinear form factor

The renormalisation scale will be fixed on $\mu = m_s$ and the \overline{MS} subtraction scheme will be employed. It is worthwhile to spend some words on the last diagram. Here `psqmax` is imposed to be the largest momenta after the loop in the last diagram. Essentially, this is done in order to consider just the off-shell contribution of this diagram, as the on-shell part corresponding to the external legs consists in a renormalisation of the Higgs field, which turns out to be a small overall shift w.r.t. the SM.

In order to implement the singlet loop corrections we define the Lorentz structures corresponding to the previous loop diagrams in figure 6.2. We multiply these structures by the couplings obtained in section 4.4. We redefine the Higgs trilinear vertex as the form factor in figure 6.3.

6.2 Effective Theory Analysis

In the effective theory we expect to see the residual effects of the 1-loop diagrams above.

As we had already calculated c_6 and c_h , the calculation follows straightforwardly by implementing the corresponding shifts in the relevant coupling defined in MADGRAPH. Calling back the framework and the definitions made in 4.1.1, we see c_h to rescale the Higgs field, and c_6 to modify the Higgs trilinear as in (4.7). Consequently, every Higgs coupling with the SM is rescaled by $(1 - n\frac{c_h}{2})$, where n is the power of the Higgs field involved in the interaction.

In these diagrams we see the only particle interacting with the Higgs being the top-quark, except the Higgs itself. So, we find the top-Higgs coupling to be rescaled as

$$\frac{y_t}{\sqrt{2}} \left(1 - \frac{\bar{c}_h}{2}\right) h \bar{t}_L t_R = \frac{y_t}{\sqrt{2}} \left(1 - \frac{c_h v^2}{2\Lambda^2}\right) h \bar{t}_L t_R, \quad (6.1)$$

and the Higgs trilinear to be rescaled both by c_6 and c_h as

$$\lambda v \left(1 - \frac{3}{2}\bar{c}_h\right) (1 + \bar{c}_6) h^3 = \lambda v \left(1 - \frac{3c_h v^2}{2\Lambda^2}\right) \left(1 + \frac{c_6 v^2}{\Lambda^2}\right) h^3. \quad (6.2)$$

The implementation in the SM@NLO extension of MADGRAPH5 follows essentially by modifying these two couplings and by introducing c_h , c_6 and Λ as new parameters. We will control the mapping between the UV model parameter and the EFT parametrisation using the coefficients in the last line of the table in 4.5.

singlet-Higgs coupling λ_m , as it is embedded in their definition, and we still identify the effective scale Λ to be the singlet mass m_s .

As it will be discussed in the benchmarks, we see the EFT analysis to better fit the full theory in *high* values of m_s and *small* values of λ_m . From the results we show, it also seems that the EFT is a good approximation of the full theory at the points where it is possible to achieve the SFOPT.

6.3 Benchmarks

Here we consider several benchmarks for the two Higgs invariant mass² in the final states in order to get an understanding of how this observable gets modified both in the full and effective theories.

We study simulations in correspondence of the SFOPT compatible region of parameter space and we also consider the case of a light singlet out of SFOPT region.

All of the simulations were made running two 7 TeV beams and by taking into account 20000 events in MadGraph.

6.3.1 Full-theory and EFT comparison

We start performing three simulations taking into account three different assignments of λ_m and m_s . We want to show here how the EFT is capable of reproducing the full theory's predictions as we change the coupling and mass.

Here it is a summary table including values of the effective theory's Wilson coefficients and the cross sections (both in the full and effective theory) in the different benchmarks performed. The values of the cross sections are expressed in pb, with the corresponding percent error. Every value should be compared to the SM cross section for the related event, which is 0.017 pb.

We also introduce the quantities³

$$\text{diff} = \sum_i |\text{FT}_i - \text{EFT}_i|, \quad \Delta\sigma/\sigma_{\text{tot}} = \frac{|\sigma_{\text{FT}} - \sigma_{\text{EFT}}|}{\sigma_{\text{FT}} + \sigma_{\text{EFT}}}, \quad (6.3)$$

in order to have a quantitative understanding of the shape and cross section differences.

(λ_m, m_s)	\bar{c}_h	\bar{c}_6	σ_{EFT}	σ_{FT}	SFOPT	diff	$\Delta\sigma/\sigma_{\text{tot}}$
(14,800)	0.019	1.05	0.0079	0.0079	Yes	0.0701	0
(12,600)	0.025	1.18	0.0075	0.0073	Yes	0.0835	0.013
(6,200)	0.057	1.32	0.0072	0.0068	No	0.6660	0.028

²The most relevant variable in the process as the $\cos\theta$ dependence is weak.

³ FT_i and EFT_i correspond respectively to the full theory and EFT normalised bins.

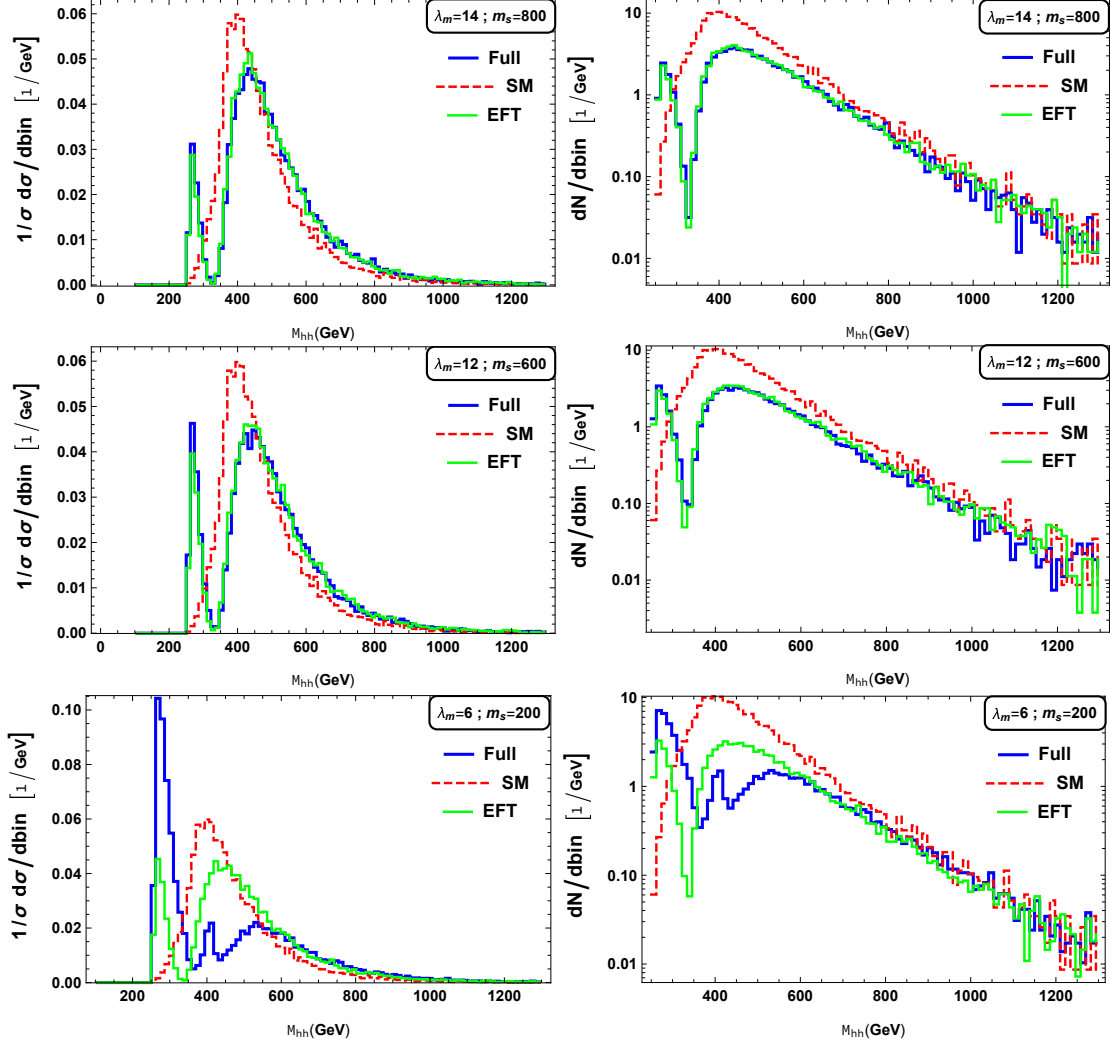


Figure 6.4: Selected benchmarks for the two final state Higgs invariant mass. We see the [full theory](#), [effective theory](#) and the [standard model](#) at comparison. The left column features histograms which are normalised to one (using a bin size of 12 GeV). The right column features logarithmic scale of the same histograms normalised to the integrated luminosity of 10^{-1} fb.

From the benchmarks in figure 6.4 we can see if the EFT is capable of reproducing the full theory result. From the first four graphs we find the EFT to be a valid approximation of the full theory on the first two benchmarks.

Conversely, in the last graph, we see how the EFT is not a valid approximation in the third benchmark. In particular, the low energy behaviors appear to be quite different. Moreover, we notice a shape difference in correspondence of $2m_s$, where the singlet loops do eventually break down as the particle production threshold is reached⁴.

⁴This feature appears to lack in the other two graphs as $2m_s$ is too high.

6.3.2 BSM theory and SM comparison

In this section we choose six different benchmarks in the strong first order phase transition region. The corresponding points are highlighted with a star in figure 6.5. Essentially, we are moving on a straight line which is almost following the edge between the $\mu_s^2 < 0$ and the SFOPT ($\mu_s^2 > 0$) regions.

The shape and cross-section differences between the standard model and the BSM theories (both the full theory and the EFT) increases as we increase the values of coupling and mass. In particular, we omitted in this analysis smaller mass values as the two frameworks are practically indistinguishable on these sides. The plots are illustrated in figures 6.6 and 6.7.

We summarise the details of the various benchmark points in the table below.

Benchmarks (λ_m, m_s)	\bar{c}_h	\bar{c}_6	σ_{EFT}	σ_{FT}	diff	$\Delta\sigma/\sigma_{\text{tot}}$
B ₁ = (6.5, 450)	0.01332	0.3331	0.0132	0.0131	0.06043	0.0038
B ₂ = (8, 500)	0.01635	0.5031	0.0115	0.0114	0.04673	0.0043
B ₃ = (9, 550)	0.01710	0.5920	0.0107	0.0107	0.0438	0
B ₄ = (11, 600)	0.02240	0.9082	0.00865	0.00848	0.05686	0.0099
B ₅ = (13, 650)	0.02554	1.277	0.00728	0.00718	0.0744	0.0069
B ₆ = (14, 700)	0.02554	1.375	0.00715	0.00711	0.10487	0.0028

From this table we can see how the EFT turns out to be a good approximation of the full theory in all the selected benchmark points. Moreover, we also find the deviation from the SM to be noticeable as the coupling and mass raise up.

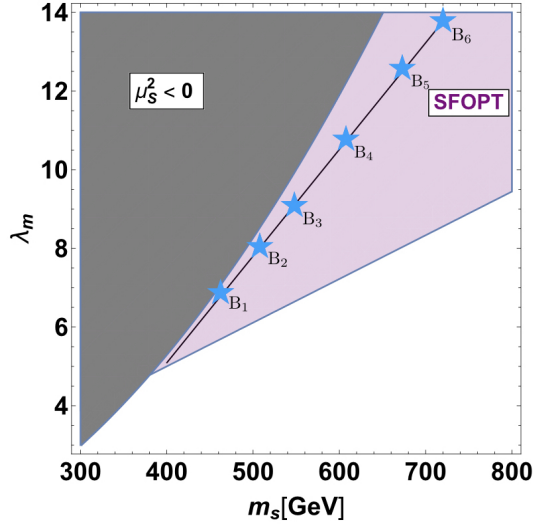


Figure 6.5: Parameter space region where the FOPT is viable. The points highlighted with a star correspond to the benchmark points we choose for this investigation, which are (λ_m, m_s) in B₁ = (6.5, 450) ; B₂ = (8, 500) ; B₃ = (9, 550) ; B₄ = (11, 600) ; B₅ = (13, 650) ; B₆ = (14, 700).

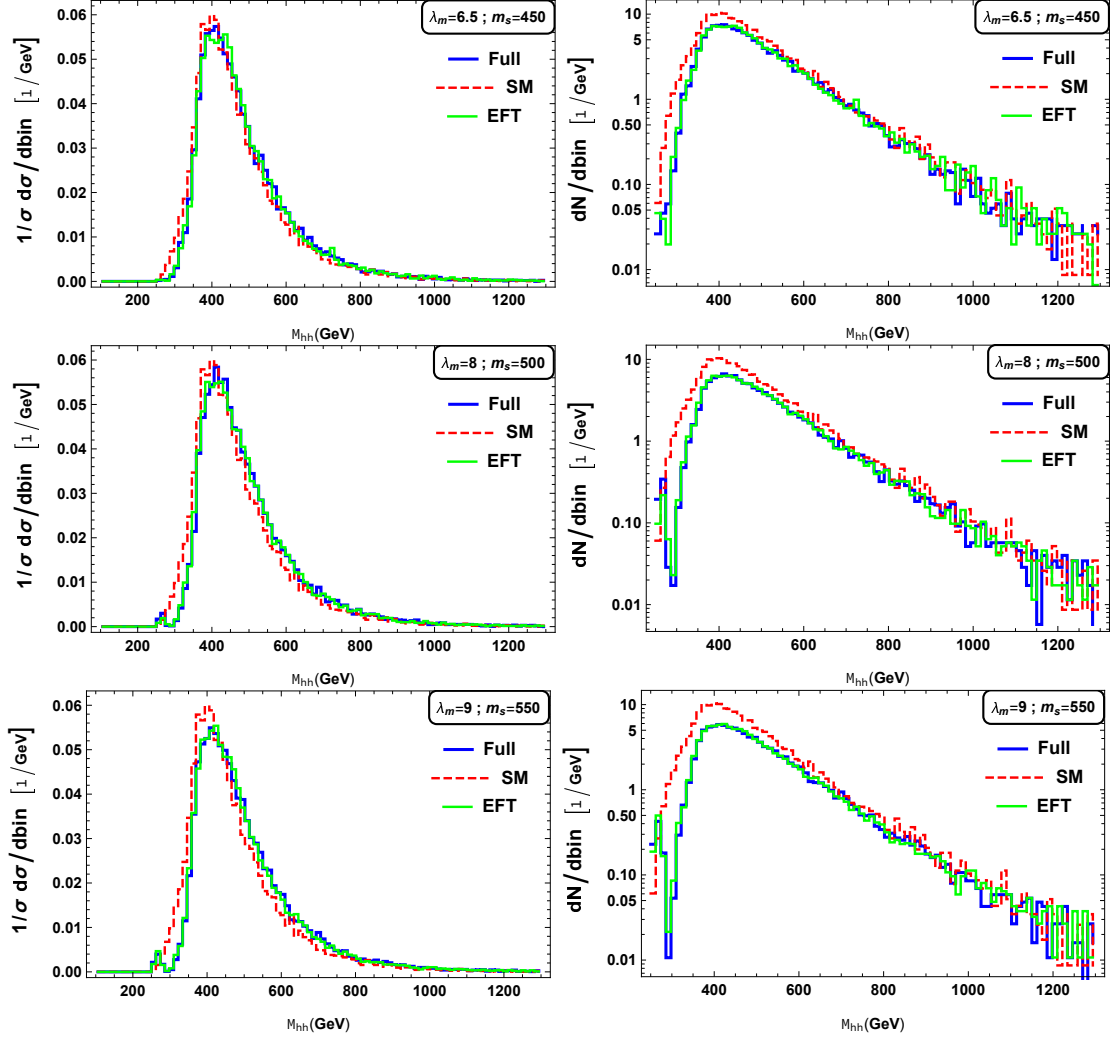


Figure 6.6: Selected benchmarks for the two final state Higgs invariant mass. We follow the point highlighted with a star on the straight line in figure 6.5. The benchmarks in this figure correspond to B_1, B_2, B_3 . We see the **full theory**, **effective theory** and the **standard model** at comparison. The histograms are normalised to one (using a bin size of 12 GeV). The right column features logarithmic scale of the same histograms normalised to the integrated luminosity of 10^{-1} fb.

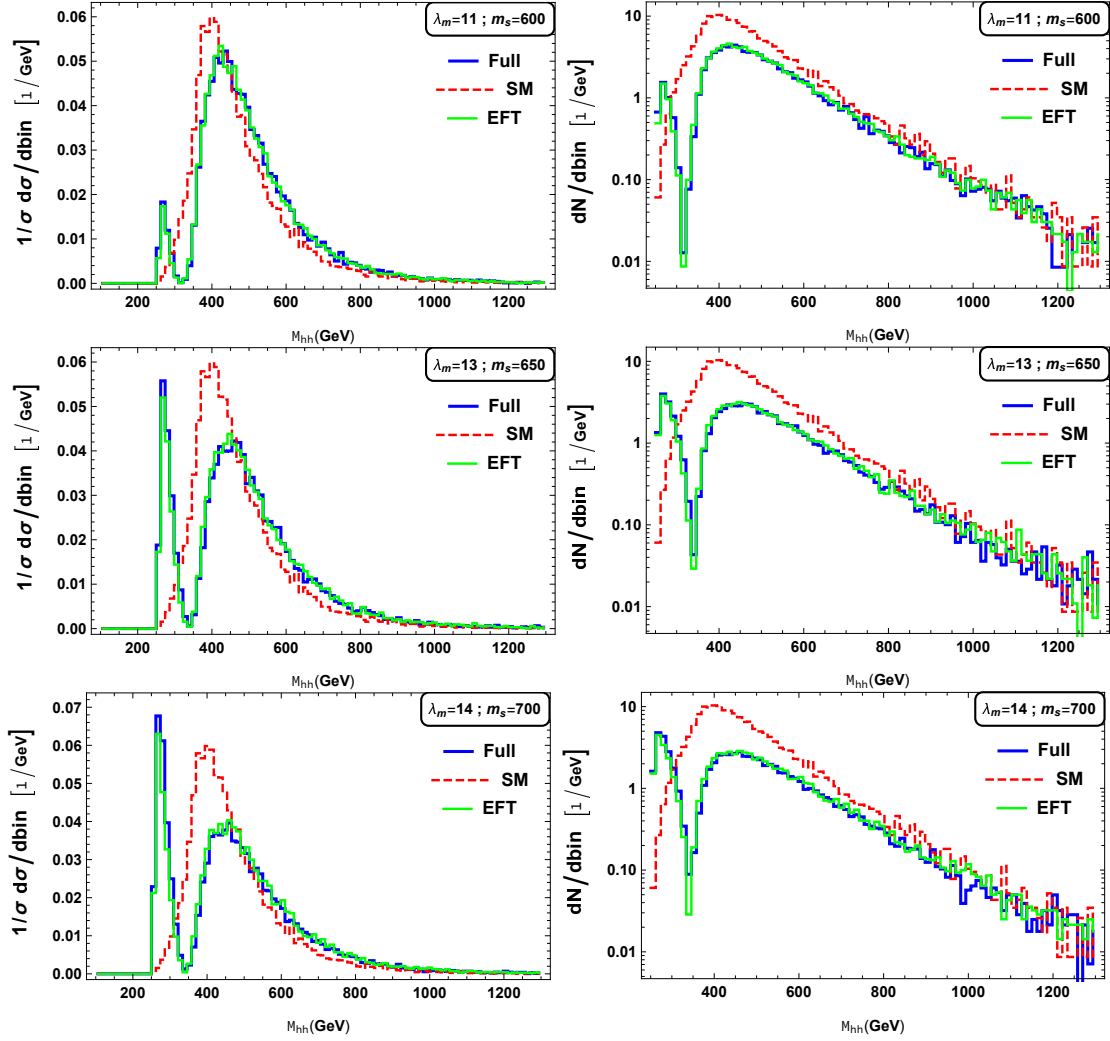


Figure 6.7: More benchmarks following the straight line in figure 6.5. The benchmarks correspond to B_4, B_5, B_6 .

Having analyzed these borderline configurations of (λ_m, m_s) (considering also the benchmarks in section 6.3.1), we can conclude that:

- The effective theory seems to be a reasonable approximation of the full theory in the SFOPT region.
- The singlet extended BSM scenario features interesting and promising signatures, as the singlet effects on the double Higgs production results to be noticeable for sizeable couplings. A more detailed analysis will be needed to estimate the sensitivity of this channel at the HL-LHC.

In this work we have investigated the possibility of achieving the strong first order EW phase transition by minimally extending the SM with a scalar singlet. This is important to achieve the electroweak baryogenesis and to possibly describe the baryon asymmetry of the universe.

We studied many singlet extended scenario taking into account both the full theory and the effective approximation. In particular, we examined the possibility of a \mathbb{Z}_2 symmetric singlet potential or not. Moreover, we considered both the cases in which the singlet takes a vacuum expectation value or not.

Then, we started by reviewing the techniques necessary to evaluate the Wilson coefficients of the effective theory. We independently calculated c_h , c_6 and c_8 in the different scenarios by using two different approaches. In particular, we analyzed the residual effects of the singlet by comparing the scattering amplitudes in the two framework, and we also integrated out the singlet via its equations of motion. In this analysis we have confirmed results existing in the literature as well as extended the investigation to higher dimensional operators.

Then, we focused on the \mathbb{Z}_2 symmetric scenario in which the singlet do not take a VEV, investigating its phenomenological aspects. First we analyzed the possibility of this model to modify the EWPT making it strongly of first order. Moreover we probed the viable parameter space region to achieve this goal. As mentioned this is interesting to analyze electroweak baryogenesis. In this analysis we independently verified some already existing results in the literature.

Finally, we implemented the \mathbb{Z}_2 symmetric minimal extension of the SM with a software for performing LHC phenomenological studies, i.e. MADGRAPH. Using this implementation we made our own phenomenological analysis. We considered several benchmarks for the double Higgs production at LHC. The benchmarks of interest are chosen in the SFOPT region. We show the differential distributions for the invariant mass of

the two Higgses in this process. The plots in figure 6.6 and especially 6.7 show the features due to the interference between the two Feynman diagrams involved. This feature and the difference with respect to the SM case could be promising for a future probe of this scenario at LHC. We implemented both the full model, exploiting the LOOPTOOLS library, and the EFT approximation by modifying the already existing SM model in MADGRAPH. Considering the two Higgs boson invariant mass, we can compare the prediction of the full model and the EFT with respect to the SM. Our preliminary results show that:

1. An EFT approach is reliable for many values of the singlet mass and coupling, possibly compatible with the SFOPT regime. Anyhow, for low masses, the EFT approximation turns out to be (as expected) not valid (in these cases, the full theory analysis has to be considered).
2. The shape and cross section differences between the singlet extended model and the standard model, in the SFOPT region, are noticeable starting from a 500 GeV mass. This means that the effects of the singlet loop in the double Higgs production at LHC can be detectable.

Our implementation of the full model in MADGRAPH and the analysis of the resulting differential distribution constitute an original contribution of this thesis.

It will be also interesting to enrich this analysis by considering, for example, the full \mathbb{Z}_2 breaking potential, and to also introduce a possible \mathcal{CP} -violating sector to achieve all of the three Sakharov conditions. We refer this discussion to future investigations.

Covariant Derivative Expansion

Here we discuss the procedure of integrating out an heavy field from a given Lagrangian. The result will lead us to an effective Lagrangian, which contains the residual effects of a BSM theory in both the renormalisable and non-renormalisable interaction terms involving the light degrees of freedom.

The procedure is explained in detail in [32]. Our aim here is to recall the essential features to treat the models shown in 4. We write the general effective action up to the 1-loop order. Anyhow, all the calculation in this thesis following this procedure are performed at the tree level.

We can set up the problem introducing an Action containing a light field Φ and an heavy field s . Integrating out the heavy field s exactly means to path integrate over it while taking Φ as a background field. This is expressed by

$$e^{iS_{\text{eff}}[\Phi](\mu)} = \int \mathcal{D}s e^{iS[\Phi,s](\mu)}, \quad (\text{A.1})$$

where $\mu \sim m_s$ is the so called matching scale.

Then we can calculate the Effective Action to the 1-Loop order by expanding s around it's minimum $s_{\text{min}}(s)$, *i.e.*

$$e^{iS_{\text{eff}}[\Phi]} = \int \mathcal{D}[s_{\text{min}} + \eta] \exp \left\{ iS[s_{\text{min}}] + \frac{i\eta^2}{2} \frac{\delta^2 S}{\delta s^2} \Big|_{s_{\text{min}}} + \dots \right\} \quad (\text{A.2})$$

$$= e^{iS[s_{\text{min}}]} \int \mathcal{D}\eta \exp \left\{ \frac{i\eta^2}{2} \frac{\delta^2 S}{\delta s^2} \Big|_{s_{\text{min}}} \right\} = e^{iS[s_{\text{min}}]} \det \left(\frac{\eta^2}{2} \frac{\delta^2 S}{\delta s^2} \Big|_{s_{\text{min}}} \right)^{1/2},$$

$$\text{and so : } S_{\text{eff}}[\Phi] = S[s_{\text{min}}] + \frac{i}{2} \text{Tr} \log \left(- \frac{\delta^2 S}{\delta s^2} \Big|_{s_{\text{min}}} \right). \quad (\text{A.3})$$

The terms on the r.h.s. are respectively for the tree and 1-Loop level.

A.1 Exemplifying with the \mathbb{Z}_2 -preserving singlet extension

Without loss of generality we can take as an example the \mathbb{Z}_2 -preserving potential already defined in chapter 4. In this example we do not consider mixing effects arising from the Higgs VEV.

As we expand the singlet over its VEV, i.e. $s \rightarrow s + v_s$, the potential reads

$$\begin{aligned} \mathcal{L} = & \frac{1}{2}(\partial^\mu s)^2 + (D^\mu \Phi)^\dagger (D_\mu \Phi) + \tilde{\mu}_h^2 |\Phi|^2 - \lambda |\Phi|^4 - \frac{m_s^2}{2} s^2 \\ & - \frac{\lambda_s}{4} s^4 - \lambda_s v_s s^3 - \lambda_m v_s |\Phi|^2 s - \frac{\lambda_m}{2} |\Phi|^2 s^2 . \end{aligned} \quad (\text{A.4})$$

The new Higgs mass is defined as $\tilde{\mu}_h^2 = \mu_h^2 - \frac{\lambda_m v_s^2}{2}$.

Then we calculate the equations of motion for the heavy field including up to s^3 terms from \mathcal{L}

$$\frac{\delta \mathcal{L}}{\delta s} = -m_s^2 s - \lambda_m v_s |\Phi|^2 - \lambda_m |\Phi|^2 s \quad (\text{A.5})$$

$$\partial_\mu \frac{\delta \mathcal{L}}{\delta (\partial_\mu s)} = \square s . \quad (\text{A.6})$$

Labelling $\square = \partial^2 = -\mathcal{P}^2$, we have

$$s (|\Phi|^2 \lambda_m + m_s^2 - \mathcal{P}^2) + |\Phi|^2 \lambda_m v_s + 3s^2 \lambda_s v_s = 0 . \quad (\text{A.7})$$

This second order equation provide us with two solutions. We have to choose the solution which vanishes as Φ goes to zero¹.

We have

$$s_{\min} = \frac{-|\Phi|^2 \lambda_m - m_s^2 + \mathcal{P}^2 + \sqrt{(|\Phi|^2 \lambda_m + m_s^2 - \mathcal{P}^2)^2 - 12|\Phi|^2 \lambda_m \lambda_s v_s^2}}{6\lambda_s v_s} . \quad (\text{A.8})$$

Expanding s_{\min} for $m_s \rightarrow \infty$, and substituting the result inside the full Lagrangian in equation (A.4), we are lead to

$$\begin{aligned} \mathcal{L}_{\text{eff}} \supset & \frac{\lambda_m^2 v_s^2}{2m_s^4} D^\mu |\Phi|^2 D_\mu |\Phi|^2 + (D^\mu \Phi)^\dagger (D_\mu \Phi) + \tilde{\mu}_h^2 |\Phi|^2 + \left(-\lambda + \frac{\lambda_m^2 v_s^2}{2m_s^2} \right) |\Phi|^4 \\ & + \left(\frac{\lambda_m^3 \lambda_s v_s^4}{m_s^6} - \frac{\lambda_m^3 v_s^2}{2m_s^4} \right) |\Phi|^6 + \left(\frac{9\lambda_m^4 \lambda_s^2 v_s^6}{2m_s^{10}} - \frac{13\lambda_m^4 \lambda_s v_s^4}{4m_s^8} + \frac{\lambda_m^4 v_s^2}{2m_s^6} \right) |\Phi|^8 , \end{aligned} \quad (\text{A.9})$$

which has been truncated up to the term of interest already introduced in 4.1.1. Thus, by using the fact that $2\lambda_s v_s^2 = m_s^2$, we get $c_6 = c_8 = 0$.

Moreover, considering the full equations of motion for s , it is possible to show that all the c_{2n} 's Wilson coefficients of the (4.5) are null. Nevertheless, we always find $c_h = \lambda_m^2 / 2\lambda_s$.

¹In other words, we have to recover the free equation of motion for s if no interaction term with Φ is present.

Constraints in the Singlet Extension

Here we will discuss various theoretical and experimental bounds concerning the singlet extended models introduced in 4. We start by reviewing the tree level unitarity constraint in B.1. Then, we proceed to review the conditions arising from the vacuum stability requirement in B.2. All the results obtained in this Appendix are already available in the literature (see for example [56]), but are reproduced independently.

B.1 Perturbative unitarity at tree-level

Here we discuss the constraints arising from perturbative unitarity. As we are interested only in $2 \rightarrow 2$ scattering processes, we will just explicitly show the calculations for the singlet model introduced in 4.4. The results are eventually translatable in the other models discussed.

We start by partial-wave expanding the scattering amplitude as

$$\mathcal{M}(s, t, u) = 16\pi \sum_{\mathfrak{J}=0}^{\infty} (2\mathfrak{J} + 1) P_{\mathfrak{J}}(\cos \theta) a_{\mathfrak{J}}(s) , \quad (\text{B.1})$$

where s, t, u are the Mandelstam variables, $a_{\mathfrak{J}}$ is the partial-wave of spin \mathfrak{J} and $P_{\mathfrak{J}}$ are Legendre polynomials.

Then, using the definition of the differential cross section we have

$$\frac{d\sigma}{d\Omega} = \frac{1}{64\pi^2 s} |\mathcal{M}|^2 , \quad (\text{B.2})$$

and so

$$\sigma = \frac{16\pi}{s} \sum_{\mathfrak{J}=0}^{\infty} (2\mathfrak{J} + 1) |a_{\mathfrak{J}}|^2 . \quad (\text{B.3})$$

Using the optical theorem [1], we understand the cross section to be proportional to the imaginary part of the scattering amplitude in the $\theta = 0$ -forward direction:

$$\sigma = \frac{1}{s} \text{Im} |\mathcal{M}(\theta = 0)| . \quad (\text{B.4})$$

This leads us to

$$|a_{\mathfrak{J}}|^2 = \text{Im}(a_{\mathfrak{J}}) . \quad (\text{B.5})$$

This equation gives us the partial-wave amplitude unitarity constraint, namely

$$|a_{\mathfrak{J}}|^2 \leq \frac{1}{2} . \quad (\text{B.6})$$

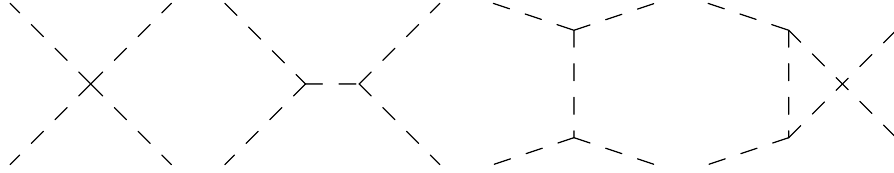
It is sufficient to focus only on the $\mathfrak{J} = 0$ partial wave to obtain the constraint [56]. So, we will just consider [2, 1, 57]

$$a_0 = \frac{1}{32\pi} \sqrt{\frac{4\rho_f^{cm}\rho_i^{cm}}{s}} \int_{-1}^1 d\cos\theta \mathcal{T}_{2\rightarrow 2} , \quad (\text{B.7})$$

where ρ_i^{cm} and ρ_f^{cm} respectively indicate the densities of the initial and final states, and where $\mathcal{T}_{2\rightarrow 2}$ is the transition matrix element for the scattering process.

Then, we analyze all the $2 \rightarrow 2$ scattering processes occurring in the singlet extended model. Since the calculations are very similar we will discuss in more detail only the $hh \rightarrow hh$ scattering, and we will directly extend the procedure to the other cases.

diagrams $hh \rightarrow hh$ The diagrams are shown in figure B.1. A direct calculation gives



$$\mathcal{T} = 4! \cdot \frac{\lambda}{4} + 3!3! \cdot (\lambda v)^2 \left(\frac{1}{s - m_h^2} + \frac{1}{t - m_h^2} + \frac{1}{u - m_h^2} \right) . \quad (\text{B.8})$$

In the present case of elastic scattering we have

$$\cos\theta = 1 + \frac{t}{2|\vec{p}|^2} ,$$

$$|\vec{p}|^2 = \frac{1}{2}(s - 4m_h^2) ,$$

so that (B.7) gives

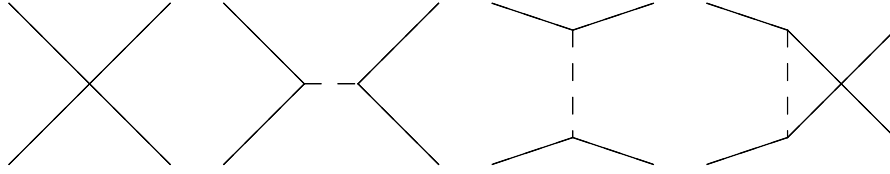
$$\begin{aligned}
a_0(hh \rightarrow hh) &= \\
&= \frac{3m_h^2}{16\pi v^2} \sqrt{1 - \frac{4m_h^2}{s}} \int_{-1}^1 d\cos\theta \left(1 + \frac{3m_h^2}{s - m_h^2} + \frac{3m_h^2}{\frac{s-4m_h^2}{2}(\cos\theta - 1) - m_h^2} \right) \quad (\text{B.9}) \\
&= \frac{3m_h^2}{16\pi v^2} \sqrt{1 - \frac{4m_h^2}{s}} \left(1 + \frac{3m_h^2}{s - m_h^2} - \frac{6m_h^2}{s - 4m_h^2} \ln \left(\frac{s}{m_h^2} - 3 \right) \right).
\end{aligned}$$

Definitely, imposing the unitarity constraint in the high energy limit $s \gg m_h^2, m_s^2$, we have

$$\boxed{m_h \leq \sqrt{\frac{8\pi}{3}} v} \quad (\text{B.10})$$

diagrams $ss \rightarrow ss$

$$\mathcal{T} = 4! \cdot \frac{\lambda_s}{4} + (\lambda_m v)^2 \left(\frac{1}{s - m_h^2} + \frac{1}{t - m_h^2} + \frac{1}{u - m_h^2} \right), \quad (\text{B.11})$$



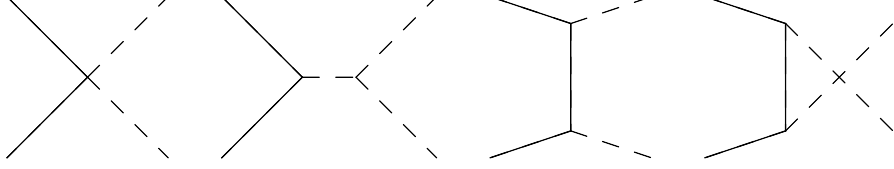
$$\begin{aligned}
a_0(hh \rightarrow hh) &= \\
&= \frac{1}{16\pi} \sqrt{1 - \frac{4m_s^2}{s}} \int_{-1}^1 d\cos\theta \left(6\lambda_s + \frac{\lambda_m^2 v^2}{s - m_h^2} + \frac{\lambda_m^2 v^2}{\frac{s-4m_h^2}{2}(\cos\theta - 1) - m_h^2} \right) \quad (\text{B.12}) \\
&= \frac{1}{16\pi} \sqrt{1 - \frac{4m_s^2}{s}} \left(\lambda_s + \frac{\lambda_m^2 v^2}{s - m_s^2} - \frac{2\lambda_m^2 v^2}{s - 4m_s^2} \ln \left(\frac{s}{m_s^2} - 3 \right) \right).
\end{aligned}$$

The unitarity constraint gives:

$$\boxed{\lambda_s \leq 8\pi}. \quad (\text{B.13})$$

diagrams $ss \rightarrow hh$

$$\mathcal{T}_{ss \rightarrow hh} = \lambda_m \left(1 + \frac{6\lambda v^2}{s - m_h^2} + 3\lambda_m v^2 \left(\frac{1}{t - m_s^2} + \frac{1}{u - m_s^2} \right) \right), \quad (\text{B.14})$$



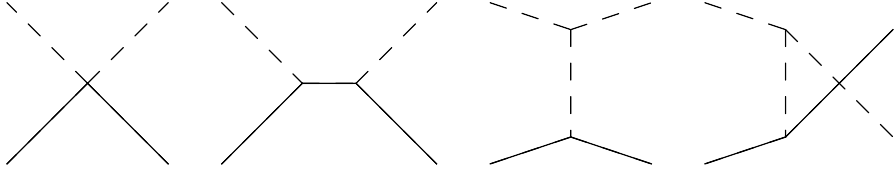
$$a_0(ss \rightarrow hh) = \frac{\lambda_m}{16\pi} \left(1 - \frac{4m_s^2}{s} \right)^{1/4} \left(1 - \frac{4m_h^2}{s} \right)^{1/4} \left[1 + \frac{6\lambda v^2}{s - m_h^2} - \frac{2\lambda_m v^2}{\sqrt{s - 4m_s^2} \sqrt{s - 4m_h^2}} \ln \left(1 + \frac{2\sqrt{s - 4m_s^2} \sqrt{s - 4m_h^2}}{s - \sqrt{s - 4m_s^2} \sqrt{s - 4m_h^2} - 2m_h^2} \right) \right], \quad (\text{B.15})$$

unitarity gives

$$\boxed{\lambda_m \leq 8\pi}. \quad (\text{B.16})$$

diagrams $sh \rightarrow hs$

$$\mathcal{T}_{sh \rightarrow hs} = \lambda_m \left(1 + \frac{3\lambda_m v^2}{s - m_s^2} + 6\lambda v^2 \left(\frac{1}{t - m_s^2} + \frac{1}{u - m_s^2} \right) \right), \quad (\text{B.17})$$



$$a_0(hs \rightarrow sh) = \frac{\lambda_m}{16\pi} \sqrt{\left(1 - \frac{(m_h + m_s)^2}{s} \right) \left(1 - \frac{(m_h - m_s)^2}{s} \right)} \left(1 + \frac{\lambda_m v^2}{s - m_h^2} - \frac{3s}{s^2 - 2s(m_h^2 + m_s^2) + (m_h - m_s)^2} \ln \left(\frac{(s - 3m_s^2)s + (m_h^2 - m_s^2)^2}{s(2m_h^2 - m_s^2)} \right) \right). \quad (\text{B.18})$$

Eventually, here we find the same bound obtained in the $ss \rightarrow hh$ scattering analysis.

B.2 Couplings and boundedness from below

The conditions arising from the request of vacuum stability can be deduced by imposing the determinant of the hessian potential matrix to be greater than zero in the stationary points. This in fact ensures us that these points are minima, and so the potential is bounded from below.

B.2.1 \mathbb{Z}_2 Symmetric Model

Let us recall the \mathbb{Z}_2 symmetric potential introduced in equation (4.10). Then, evaluating the potential for $\Phi = \frac{v}{\sqrt{2}}$ and $s = v_s$, with $v, v_s > 0$, we have

$$\begin{cases} \frac{\partial V}{\partial v}(v, v_s) = v \left(-\mu_h^2 + \lambda v^2 + \frac{\lambda_m v_s^2}{2} \right) = 0 \\ \frac{\partial V}{\partial v_s}(v, v_s) = v_s \left(-\mu_s^2 + \lambda v_s^2 + \frac{\lambda_m v^2}{2} \right) = 0 \end{cases} \rightarrow \begin{cases} \mu_h^2 = \lambda v^2 + \frac{\lambda_m v_s^2}{2} \\ 2\mu_s^2 = \lambda_s v_s^2 + \frac{\lambda_m v^2}{2} \end{cases} . \quad (\text{B.19})$$

Then, moving on to the second derivatives, we obtain

$$\frac{\partial^2 V}{\partial v^2} = -\mu_h^2 + 3\lambda v^2 + \frac{\lambda_m v_s^2}{2} , \quad (\text{B.20})$$

$$\frac{\partial^2 V}{\partial v_s^2} = -2\mu_s^2 + 3\lambda v_s^2 + \frac{\lambda_m v^2}{2} , \quad (\text{B.21})$$

$$\frac{\partial^2 V}{\partial v \partial v_s} = \lambda_m v v_s . \quad (\text{B.22})$$

So, the hessian matrix of the system reads

$$\begin{aligned} \mathbb{V}(v, v_s) &= \begin{pmatrix} -\mu_h^2 + 3\lambda v^2 + \frac{\lambda_m v_s^2}{2} & \lambda_m v v_s \\ \lambda_m v v_s & -\mu_s^2 + 3\lambda v_s^2 + \frac{\lambda_m v^2}{2} \end{pmatrix} \\ &= \begin{pmatrix} 2\lambda v^2 & \lambda_m v v_s \\ \lambda_m v v_s & 2\lambda_s v_s^2 \end{pmatrix} . \end{aligned} \quad (\text{B.23})$$

In the last step we evaluated the matrix in the stationary point obtained.

Definitely, by requiring the determinant of the hessian to be greater than zero, we find

$$4\lambda\lambda_s - \lambda_m^2 > 0 \quad ; \quad \lambda, \lambda_s > 0 . \quad (\text{B.24})$$

B.2.2 The General Case

Lastly, we repeat the calculation for the \mathbb{Z}_2 -breaking potential introduced in (4.3).

The stationary points are given by

$$\begin{cases} \frac{\partial V}{\partial v}(v, v_s) = v(\mu_h^2 + \lambda v^2 + \frac{\lambda_m v_s^2}{2} + \mu_4 v_s) = 0 \\ \frac{\partial V}{\partial v_s}(v, v_s) = v_s(\mu_s^2 + \frac{\lambda_m v^2}{2} + \mu_3 v_s + \lambda v_s^2 + \frac{\mu_4 v^2}{2 v_s}) = 0 \end{cases} , \quad (\text{B.25})$$

$$\mu_h^2 = - \left(\lambda v^2 + \frac{\lambda v_s^2}{2} + \mu_4 v_s \right) ; \mu_s^2 = - \left(\frac{\lambda_m v^2}{2} + \mu_3 v_s + \lambda v_s^2 + \frac{\mu_4 v^2}{2 v_s} \right) . \quad (\text{B.26})$$

Then, the second derivatives are

$$\frac{\partial^2 V}{\partial v^2} = \mu_h^2 + 3\lambda v^2 + \frac{\lambda_m v_s^2}{2} + \mu_4 v_s , \quad (\text{B.27})$$

$$\frac{\partial^2 V}{\partial v_s^2} = \mu_s^2 + 3\lambda v_s^2 + \frac{\lambda_m v^2}{2} + \mu_3 v_s , \quad (\text{B.28})$$

$$\frac{\partial^2 V}{\partial v \partial v_s} = v v_s \left(\lambda_m + 2 \frac{\mu_4}{v_s} \right) . \quad (\text{B.29})$$

The hessian matrix reads

$$\mathbb{V}(v, v_s) = \begin{pmatrix} \mu_h^2 + 3\lambda v^2 + \frac{\lambda_m v_s^2}{2} + \mu_4 v_s & v v_s \left(\lambda_m + \frac{\mu_4}{v_s} \right) \\ v v_s \left(\lambda_m + \frac{\mu_4}{v_s} \right) & \mu_s^2 + 3\lambda_s v_s^2 + \frac{\lambda_m v^2}{2} + \mu_3 v_s \end{pmatrix} \quad (\text{B.30})$$

$$\begin{pmatrix} 2\lambda v^2 & v v_s \left(\lambda_m + \frac{\mu_4}{v_s} \right) \\ v v_s \left(\lambda_m + \frac{\mu_4}{v_s} \right) & 2\lambda_s v_s^2 - \frac{\mu_4 v^2}{2 v_s} - \mu_3 v_s \end{pmatrix} .$$

Definitely, by requiring the determinant of the hessian to be greater than zero, we find

$$4\lambda\lambda_s - \frac{\mu_4 v^2}{2v_s^3} - \frac{\mu_3}{v_s} - \lambda_m^2 - \frac{2\lambda_m \mu_4}{v_s} - \frac{\mu_4^2}{v_s^2} > 0 \quad ; \quad \lambda, \lambda_s > 0 . \quad (\text{B.31})$$

Bibliography

- [1] R. Soldati, “Field Theory 2 - Intermediate Quantum Field Theory.”
- [2] M. E. Peskin and D. V. Schroeder, *An Introduction to quantum field theory*. Reading, USA: Addison-Wesley, 1995.
- [3] Y. Nir, “CP violation in and beyond the standard model,” in *Proceedings, 27th SLAC Summer Institute on Particle Physics: CP Violation in and Beyond the Standard Model (SSI 99): Stanford, USA, July 7-16, 1999*, pp. 165–243, 1999.
- [4] S. Abachi *et al.*, “Observation of the top quark,” *Phys. Rev. Lett.*, vol. 74, pp. 2632–2637, 1995.
- [5] K. Kodama *et al.*, “Observation of tau neutrino interactions,” *Phys. Lett.*, vol. B504, pp. 218–224, 2001.
- [6] G. Aad *et al.*, “Observation of a new particle in the search for the Standard Model Higgs boson with the ATLAS detector at the LHC,” *Phys. Lett.*, vol. B716, pp. 1–29, 2012.
- [7] G. Elgaard-Clausen and M. Trott, “On expansions in neutrino effective field theory,” *JHEP*, vol. 11, p. 088, 2017.
- [8] J. Baglio and C. Weiland, “The triple Higgs coupling: A new probe of low-scale seesaw models,” *JHEP*, vol. 04, p. 038, 2017.
- [9] J. Hisano, “Effective theory approach to direct detection of dark matter,” 2017.
- [10] A. Falkowski, “Effective field theory approach to LHC Higgs data,” *Pramana*, vol. 87, no. 3, p. 39, 2016.
- [11] I. Brivio and M. Trott, “The Standard Model as an Effective Field Theory,” 2017.

- [12] K. Schneck *et al.*, “Dark matter effective field theory scattering in direct detection experiments,” *Phys. Rev.*, vol. D91, no. 9, p. 092004, 2015.
- [13] D. E. Morrissey and M. J. Ramsey-Musolf, “Electroweak baryogenesis,” *New J. Phys.*, vol. 14, p. 125003, 2012.
- [14] F. R. Klinkhamer and N. S. Manton, “A Saddle Point Solution in the Weinberg-Salam Theory,” *Phys. Rev.*, vol. D30, p. 2212, 1984.
- [15] P. Huet and E. Sather, “Electroweak baryogenesis and standard model CP violation,” *Phys. Rev.*, vol. D51, pp. 379–394, 1995.
- [16] M. McCullough, “Lectures on Physics Beyond the Standard Model,” in *6th Tri-Institute Summer School on Elementary Particles (TRISEP 2018) Waterloo, Canada, July 9-20, 2018*.
- [17] W. Skiba, “Effective Field Theory and Precision Electroweak Measurements,” in *Physics of the large and the small, TASI 09, proceedings of the Theoretical Advanced Study Institute in Elementary Particle Physics, Boulder, Colorado, USA, 1-26 June 2009*, pp. 5–70, 2011.
- [18] G. P. Lepage, “What is renormalization?,” in *Boulder ASI 1989:483-508*, pp. 483–508, 1989.
- [19] R. Soldati, “Field Theory 1 - Introduction to Quantum Field Theory.”
- [20] C. N. Leung, S. T. Love, and S. Rao, “Low-Energy Manifestations of a New Interaction Scale: Operator Analysis,” *Z. Phys.*, vol. C31, p. 433, 1986.
- [21] B. Grzadkowski, M. Iskrzynski, M. Misiak, and J. Rosiek, “Dimension-Six Terms in the Standard Model Lagrangian,” *JHEP*, vol. 10, p. 085, 2010.
- [22] G. F. Giudice, C. Grojean, A. Pomarol, and R. Rattazzi, “The Strongly-Interacting Light Higgs,” *JHEP*, vol. 06, p. 045, 2007.
- [23] G. Passarino and M. Trott, “The Standard Model Effective Field Theory and Next to Leading Order,” 2016.
- [24] G. Passarino, “Field reparametrization in effective field theories,” *Eur. Phys. J. Plus*, vol. 132, no. 1, p. 16, 2017.
- [25] R. E. Kallosh and I. V. Tyutin, “The Equivalence theorem and gauge invariance in renormalizable theories,” *Yad. Fiz.*, vol. 17, pp. 190–209, 1973. [Sov. J. Nucl. Phys.17,98(1973)].
- [26] M. Gorbahn, J. M. No, and V. Sanz, “Benchmarks for Higgs Effective Theory: Extended Higgs Sectors,” *JHEP*, vol. 10, p. 036, 2015.

- [27] F. Maltoni, D. Pagani, and X. Zhao, “Constraining the Higgs self-couplings at e+e-colliders,” *JHEP*, vol. 07, p. 087, 2018.
- [28] L. Di Luzio, R. Gröber, and M. Spannowsky, “Maxi-sizing the trilinear Higgs self-coupling: how large could it be?,” *Eur. Phys. J.*, vol. C77, no. 11, p. 788, 2017.
- [29] D. Curtin, P. Meade, and C.-T. Yu, “Testing Electroweak Baryogenesis with Future Colliders,” *JHEP*, vol. 11, p. 127, 2014.
- [30] N. Craig, C. Englert, and M. McCullough, “New probe of naturalness,” *Phys. Rev. Lett.*, vol. 111, p. 121803, Sep 2013.
- [31] S. Kanemura, M. Kikuchi, and K. Yagyu, “One-loop corrections to the Higgs self-couplings in the singlet extension,” *Nucl. Phys.*, vol. B917, pp. 154–177, 2017.
- [32] B. Henning, X. Lu, and H. Murayama, “How to use the Standard Model effective field theory,” *JHEP*, vol. 01, p. 023, 2016.
- [33] J. M. Cline, “Baryogenesis,” in *Les Houches Summer School - Session 86: Particle Physics and Cosmology: The Fabric of Spacetime Les Houches, France, July 31-August 25, 2006*, 2006.
- [34] M. Quiros, “Finite temperature field theory and phase transitions,” in *Proceedings, Summer School in High-energy physics and cosmology: Trieste, Italy, June 29-July 17, 1998*, pp. 187–259, 1999.
- [35] J. Zinn-Justin, “Quantum field theory at finite temperature: An Introduction,” 2000.
- [36] A. M. Polyakov, “Quark Confinement and Topology of Gauge Groups,” *Nucl. Phys.*, vol. B120, pp. 429–458, 1977.
- [37] H. P. Nilles, M. Ratz, A. Trautner, and P. K. S. Vaudrevange, “ \mathcal{CP} Violation from String Theory,” 2018.
- [38] S. Kraml, “CP violation in SUSY,” in *SUSY 2007 Proceedings, 15th International Conference on Supersymmetry and Unification of Fundamental Interactions, July 26 - August 1, 2007, Karlsruhe, Germany*, pp. 132–139, 2007.
- [39] A. D. Linde, “Vacuum Structure In Gauge Theories: The Problem of Strong CP violation and Cosmology,” *Phys. Lett.*, vol. 93B, pp. 327–330, 1980.
- [40] A. A. Belavin, A. M. Polyakov, A. S. Schwartz, and Yu. S. Tyupkin, “Pseudoparticle Solutions of the Yang-Mills Equations,” *Phys. Lett.*, vol. B59, pp. 85–87, 1975. [350(1975)].
- [41] G. V. Dunne, “Aspects of Chern-Simons theory,” in *Topological Aspects of Low-dimensional Systems: Proceedings, Les Houches Summer School of Theoretical Physics, Session 69: Les Houches, France, July 7-31 1998*, 1998.

- [42] V. A. Kuzmin, V. A. Rubakov, and M. E. Shaposhnikov, “On the Anomalous Electroweak Baryon Number Nonconservation in the Early Universe,” *Phys. Lett.*, vol. 155B, p. 36, 1985.
- [43] D. Bodeker, G. D. Moore, and K. Rummukainen, “Chern-Simons number diffusion and hard thermal loops on the lattice,” *Phys. Rev.*, vol. D61, p. 056003, 2000.
- [44] C. Jarlskog, “Commutator of the Quark Mass Matrices in the Standard Electroweak Model and a Measure of Maximal CP Violation,” *Phys. Rev. Lett.*, vol. 55, p. 1039, 1985.
- [45] G. R. Farrar and M. E. Shaposhnikov, “Baryon asymmetry of the universe in the minimal Standard Model,” *Phys. Rev. Lett.*, vol. 70, pp. 2833–2836, 1993. [Erratum: *Phys. Rev. Lett.* 71,210(1993)].
- [46] M. B. Gavela, P. Hernandez, J. Orloff, and O. Pene, “Standard model CP violation and baryon asymmetry,” *Mod. Phys. Lett.*, vol. A9, pp. 795–810, 1994.
- [47] E. J. Weinberg, *Radiative corrections as the origin of spontaneous symmetry breaking*. PhD thesis, Harvard U., 1973.
- [48] A. Katz and M. Perelstein, “Higgs Couplings and Electroweak Phase Transition,” *JHEP*, vol. 07, p. 108, 2014.
- [49] M. Quiros, “On daisy and superdaisy resummation of the effective potential at finite temperature,” in *Elementary particle physics. Proceedings, 4th Hellenic School, Corfu, Greece, September 2-20, 1992. 1&2*, pp. 502–511, 1992.
- [50] J. M. Cline, K. Kainulainen, P. Scott, and C. Weniger, “Update on scalar singlet dark matter,” *Phys. Rev.*, vol. D88, p. 055025, 2013. [Erratum: *Phys. Rev.* D92,no.3,039906(2015)].
- [51] H. H. Patel and M. J. Ramsey-Musolf, “Baryon Washout, Electroweak Phase Transition, and Perturbation Theory,” *JHEP*, vol. 07, p. 029, 2011.
- [52] P. H. Damgaard, A. Haarr, D. O’Connell, and A. Tranberg, “Effective Field Theory and Electroweak Baryogenesis in the Singlet-Extended Standard Model,” *JHEP*, vol. 02, p. 107, 2016.
- [53] D. Buttazzo, D. Redigolo, F. Sala, and A. Tesi, “Fusing Vectors into Scalars at High Energy Lepton Colliders,” 2018.
- [54] C. Grojean, G. Servant, and J. D. Wells, “First-order electroweak phase transition in the standard model with a low cutoff,” *Phys. Rev.*, vol. D71, p. 036001, 2005.
- [55] J. Alwall, R. Frederix, S. Frixione, V. Hirschi, F. Maltoni, O. Mattelaer, H. S. Shao, T. Stelzer, P. Torrielli, and M. Zaro, “The automated computation of tree-level and next-to-leading order differential cross sections, and their matching to parton shower simulations,” *JHEP*, vol. 07, p. 079, 2014.

- [56] S. K. Kang and J. Park, “Unitarity Constraints in the standard model with a singlet scalar field,” *JHEP*, vol. 04, p. 009, 2015.
- [57] B. W. Lee, C. Quigg, and H. B. Thacker, “Weak interactions at very high energies: The role of the higgs-boson mass,” *Phys. Rev. D*, vol. 16, pp. 1519–1531, Sep 1977.